The water cycle with climate change

A study on atmospheric moisture transport using GFDL climate forecasts

Umbriël Post
4226720

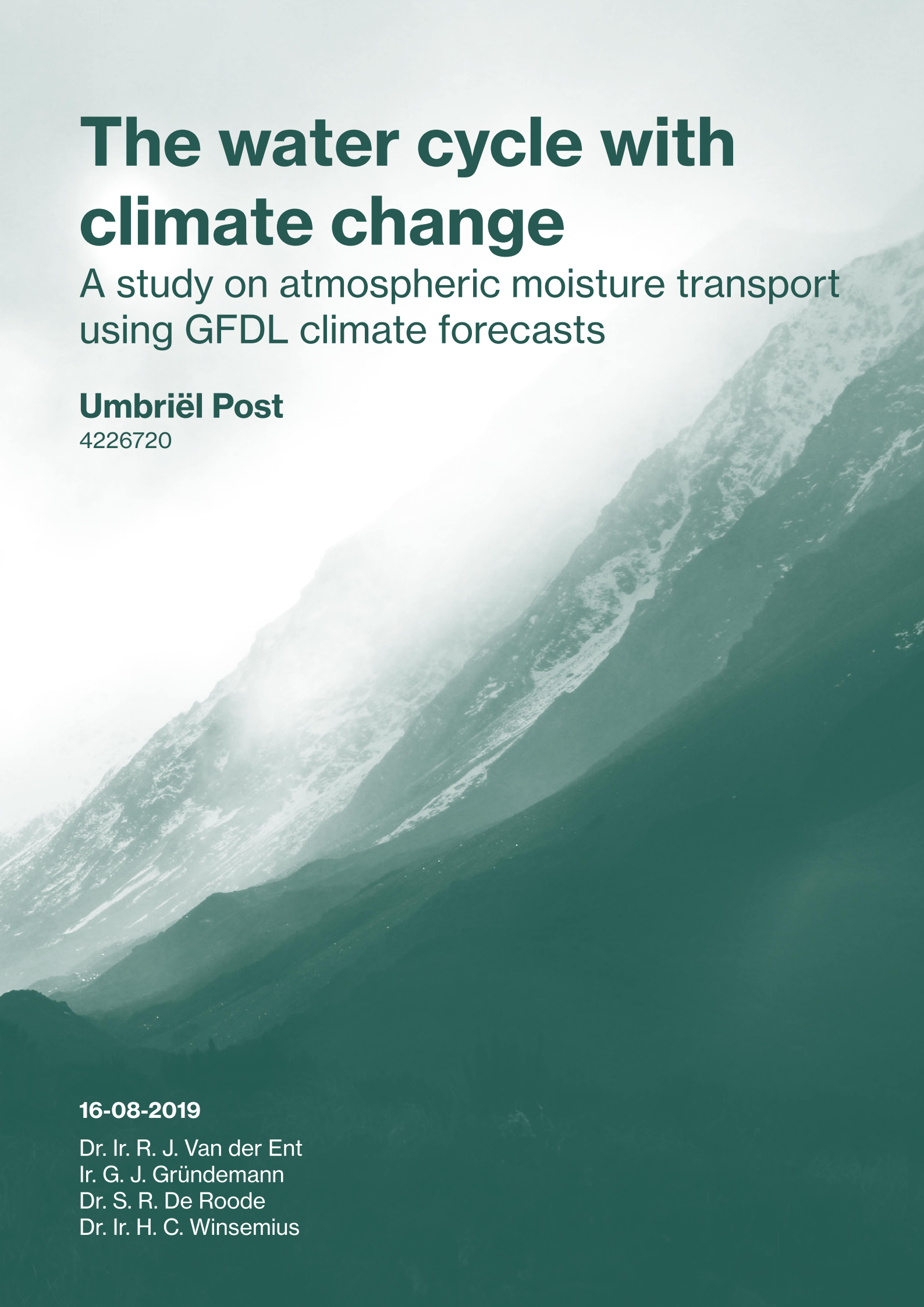

16-08-2019

Dr. Ir. R. J. Van der Ent
Ir. G. J. Gründemann
Dr. S. R. De Roode
Dr. Ir. H. C. Winsemius

The water cycle with climate change

A study on atmospheric moisture transport using GFDL climate forecasts

by

Umbriël Post

to obtain the degree of Master of Science
at Delft University of Technology,
to be defended publicly on August 28th, 2019 at 11:00 AM.

Student number: 4226720

Thesis committee:	Dr. Ir. R.J. Van der Ent	TU Delft, chairman
	Dr. Ir. H.C. Winsemius	TU Delft
	Dr. S.R. De Roode	TU Delft
	Ir. G.J. Gründemann	TU Delft

TU Delft

Preface

During my entire study career at Delft University of Technology, I have been wanting to learn more about climate change and greenhouse gases in order to change people's behaviour and greenhouse gas emissions. In my application for the Honours Programme in my first year at the Bachelor in Systems Engineering, Policy Analysis and Management I expressed my belief in a more sustainable world by wanting to answer the question: "Why don't we just switch over to green energy sources, since everyone knows by now it is better for the world?". Back then, in my eyes this was a small question. However, it was not possible to answer this simply by taking a few extracurricular courses. My drive to find out more about Earth sciences, led me to switching to Water management. My specialisation in hydrology gave me the possibility to do some elective courses in the scientific world behind climate change, the atmospheric sciences. The subject of my Master's thesis is a wonderful combination between what I have been studying for the past two years and my passion of wanting to understand climate change and changing people's ways by showing what will happen if we do not 'just switch over to green energy sources'. This thesis has been the cherry on top of my entire Master's degree. One and a half year of Water management courses in Delft and half a year of extracurricular courses in Environmental Sciences at the University of Melbourne have been a good basis to start this thesis. The thesis has definitely taught me a lot, mostly in Python programming and atmospheric sciences. Using climate forecasts from a widely recognised research institute and seeing what this institute forecasts to happen in the future if humans do not change their behavior has been eye-opening. In this thesis I have been trying to explain why changes in precipitation due to climate change happen as clearly as possible. I hope the reader will have as much fun reading it as I had figuring it all out during this past year.

I would like to thank my thesis committee for their great support during this full year of work. My first supervisors Ruud van der Ent and Gaby Gründemann, thank you so much for all the support and mostly with answering all my questions about the model and modelling in general. I have always felt very free to contact you whenever I needed to, even while finishing this thesis in the USA. To Stephan de Roode and Hessel Winsemius, I would like to express my gratitude for being sharp and critical during the progress meetings with the entire committee, especially Stephan, thank you for helping me understand the physics behind some of the equations I had been using in the modelling phase. All in all I believe this thesis committee was the right combination between different fields of study and even personalities in order to be a perfect fit for me as a graduating student.

Umbriël Post
Missoula, MT, USA, August 2019

Abstract

Climate change causes temperatures to rise worldwide. Up until now it is unclear what effect this has on the global water cycle. In this study the output of two GFDL model experiments were thoroughly investigated and used in the moisture tracking model WAM-2layers, accounting for model runs in a past case in the end-20th century and future case in the end-21st century, based on RCP8.5. This is done in order to acquire knowledge on what will happen to the global as well as regional water cycle in the future and to find out what processes provide climate change to have an effect on the water cycle. Changes in precipitation and evaporation rates are spatially highly dissimilar, therefore regional differences can be distinguished. Past studies have suggested that a DDWW paradigm - where dry regions dry out further and wet regions get wetter - will take place with climate change. Even though in some regions this might happen, results show that on land this is not necessarily the case - at least, if precipitation rate is the benchmark for a region to get drier or wetter. Processed GFDL data concludes that dry region Western Sahara gets wetter while dry region Middle East gets drier and wet region Indonesia gets wetter while wet region Amazonia gets drier. The DDWW paradigm covers another aspect as well, that there will be a larger spatial variability for variables characterising a region to be wet or dry. However, while everywhere on the globe the temperatures will rise according to the GFDL data, the spread of the yearly mean temperatures over the globe will actually decrease, meaning that mean yearly temperature in the coldest place will lie closer to the mean yearly temperature in the warmest place. This is also the case for mean yearly precipitation and evaporation rates. The mean yearly precipitation and evaporation rate in the driest place will lie closer to the mean yearly precipitation and evaporation rate in the wettest place in the future case. Continents show divergent effects in water cycle due to climate change. The continents with relatively larger sources of terrestrial moisture - North America, Europe and Asia - have an increased water cycle with higher precipitation and evaporation rates in the future. The increases in precipitation rates on these continents will originate from terrestrial evaporation and a higher percentage of evaporation will return as precipitation on land. South America shows a distinct effect, different than all other continents. This continent shows a decreased water cycle with lower precipitation and evaporation rates in the future. Of this precipitation a lower percentage comes from land and the evaporated moisture will return less on land. Africa and Oceania show another pattern. Both these continents will experience more precipitation in the future case, but this moisture will come from oceanic evaporation. Two case study areas are examined in more depth by looking at seasonality effects. A case study in the Amazon forest shows a distinct dry season in the future case, the effect of possible land use change in the Amazon forest. Less evaporation that is an effect of deforestation of the rain forest gives less moisture for clouds to form and precipitate. Moisture evaporates from the oceans on the East of Amazon region but moves over the region before it can precipitate. A case study in Western Africa shows a magnified rain season. The analyses show that during the wet season in the future case there in an increased amount of moisture coming from the oceans West and South of Western Africa and meanwhile there was still moisture coming in from the tropical rain forest East of the area.

Contents

1 Introduction

Droughts and floods are points of interest in current news, because they can be disastrous for large groups of people. These events are caused by a deficiency or an abundance of precipitation. Weather conditions seem to change globally and several studies have indicated that climate change is in fact likely the cause of the increase in the frequency as well as the magnitude of floods and droughts in many regions (N. Diffenbaugh, 2013; IPCC, 2007; Chang et al., 2018; Marengo and Espinoza, 2016).

Since the industrial revolution, people have used up more and more fossil fuels, such as coal and gas (Smil, 2016). Ancient sources of CO_2 that have slowly been compressed into oil and gas over centuries have been mined to provide for the growing energy need for the present-day human society up until today. The burning of fossil fuels that is needed for the increasing energy consumption causes an increase in CO_2 in the atmosphere. CO_2 together with other greenhouse gases, such as NO_x and CH_4, have an heat-absorbing effect in the atmosphere (Huber and Knutti, 2011). These gases can hold heat, which causes the temperatures in the atmosphere to rise. Higher temperatures makes it more favorable for the air to hold water vapor. Water vapor in turn can absorb more heat, leading to a feedback effect. The human interactions with the Earth caused a warming of the atmosphere (IPCC, 2014b). This is called athropogenic climate change.

It is necessary to investigate future climate change and its potential impacts on the natural environment in order to reduce risks and increase resilience for future water resource planning and management (Vano and Lettenmaier, 2014). This takes into account not only the warming air temperatures but also the global water cycle, more specifically precipitation and evaporation patterns.

1.1. Global changes in precipitation with climate change

Trenberth (2011) looked into what would happen with global precipitation because of climate change. Higher temperatures lead to more energy available for water to evaporate. Only taking this factor into account would lead to a drying surface, which increases the intensity and duration of droughts. Yet, another factor is that the water holding capacity of air increases with 7% per degree Kelvin, leading to more water vapor in the atmosphere. As opposed to the drying effect of more evaporation, more water in the atmosphere results in precipitation events of higher intensity and duration (Trenberth, 2011). Because of the increase in water holding capacity of air however, more evaporation does not necessarily mean that there will be more intense rainfall events. Moisture could also accumulate in the atmosphere, leading to an increase in residence time. Research from Van Der Ent and Tuinenburg (2017) shows that currently the residence time over the ocean is about 2 days less than over land, as over land there is fewer supply from evaporation. Next to this, in winter the residence time tends to be much lower than in summer (Van Der Ent and Tuinenburg, 2017). This might be because of the higher temperatures in summer, causing more evaporation. A study from Bosilovich et al. (2005) concluded that the amount of water vapor in the atmosphere increases with increasing temperatures and so does the residence time of the water vapor in the atmosphere. With increasing surface temperatures, the experiments show increase in precipitation, evaporation and water vapor in the atmosphere and an increase of residence time. Even though the total precipitation will increase, the increasing residence time suggests that the global atmospheric water cycle slows down. Regional deviations from the global trends are detected and the study advises to study this in more depth in the future.

1.2. Regional changes in precipitation with climate change

Zooming into regions specifically, the study of Kumar et al. (2004) points out that an increase in precipitation and associated upward vertical mass transport due to convection over one geographical region has to be balanced by an increased descending motion in another region, where precipitation then would decrease. Even though this implies that overall global changes in precipitation would stay small, specific regions could still get drier or wetter. This is supported by a study from Held and Soden (2006), which suggests that - in terms of precipitation rates - Dry regions get Drier and Wet regions get Wetter (DDWW). According to the study, water vapor in the atmosphere will increase as climate warms, but the relative humidity and flow will remain unchanged. This would imply that the poleward water vapor transport and the pattern of evaporation minus precipitation increases proportionally to the water vapor in the atmosphere, which leads to higher evaporation minus precipitation in dry regions and lower evaporation minus precipitation in wet regions (Held and Soden, 2006). This 'DDWW paradigm' however is contradicted by the findings of another study. Greve et al. (2014) found that only 10.8% of the global land area shows a 'dry gets drier, wet gets wetter' pattern, compared to 9.5% of global land area with the opposite pattern, that is, dry gets wetter, and wet gets drier. In order to understand changes in precipitation both globally and regionally, a new generation of climate modelling experiments is needed (Allen and Ingram, 2002). For this it is needed that the overall climate response to increasing atmospheric concentrations of greenhouse gases is studied.

1.3. Climate modelling

To study climate change and the effects of it, many climate models have been made over the last decades. The Intergovernmental Panel on Climate Change (IPCC) is an organisation of governments that are members of the United Nations or World Meteorological Organisation. Thousands of people from all over the world contribute to the work of the IPCC. For their assessment reports, IPCC scientists volunteer to assess thousands of scientific papers published each year in order to provide a comprehensive summary of what is known about the drivers of climate change, its impacts and future risks, and how adaptation and mitigation can reduce those risks. The IPCC does not conduct its own research. For each of the assessment reports the IPCC collects research based on the questions risen from the previous assessment report. The most recent assessment report was based on the Coupled Model Intercomparison Project Phase 5 (CMIP5). CMIP5 experiments were undertaken by several research institutes, such as by the Geophysical Fluid Dynamics Laboratory (GFDL). The GFDL is a research institute collaborating with Princeton University and funded by the National Oceanic and Atmospheric Administration (NOAA), an American scientific agency within the United States Department of Commerce.

The uncertainty of human actions makes it difficult to determine what the future greenhouse gas concentrations and consecutive global air temperature will be as a result of antropogenic climate change. Therefore, the IPCC has distinguished four different scenarios. These Representative Concentration Pathways (RCPs), describe outcomes of four different human behavioural paths (Meinshausen et al., 2011). Included in the RCPs are data of land use and cover, greenhouse gas emissions and aerosol, ozone and greenhouse gas concentrations (Vuuren et al., 2011; Hurtt et al., 2011). In the best case scenario humans will alter their behaviour and lower the greenhouse gas emissions and in the worst case scenario humans will increase their energy demand and drastic climate change will occur. The scenarios cause a warming of 2.6, 4.5, 6.7 and 8.5 Wm^{-2} in comparison to pre-industrial radiation (Vuuren et al., 2011). At this moment in time, the current situation is worse than this moment in time in the worst case pathway.

Numerous models that have ran CMIP5 experiments with the RCPs have predicted certain changes for a wide range of atmospheric variables, such as precipitation, evaporation and temperature. The IPCC has combined these experiments in their assessment report. Figure 1.1 shows the combined forecast for the change in precipitation rate with RCP8.5. It shows that while some regions will experience a relative increase in precipitation, other regions will experience a decrease. The IPCC partly endorses the DDWW paradigm, since their report suggests that many mid-latitude and subtropical dry regions will experience a decrease in mean precipitation, while many mid-latitude wet regions will experience an increase in mean precipitation under RCP8.5 (IPCC, 2014a). The changes in precipitation, evaporation and temperature can happen in two ways. The mean annual value can change. This would indicate a region to get drier, wetter, warmer or colder. However, looking at a region specifically, there can also be seasonal shifts. Seasonal changes could for example happen in intensity, duration and timing of a rain season.

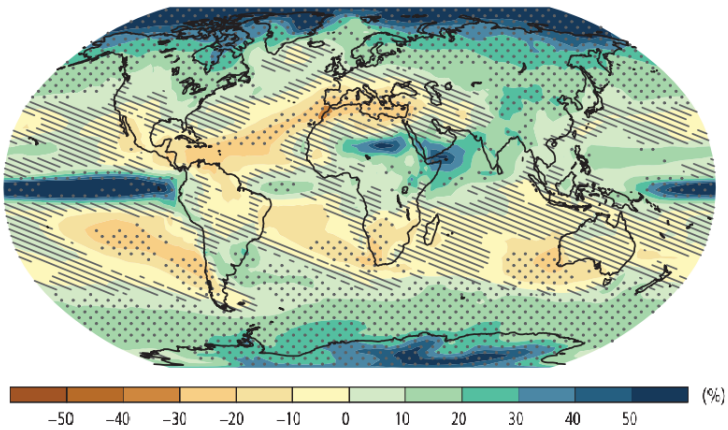

Figure 1.1: Change in average precipitation (1986-2005 to 2081-2100) RCP8.5 (IPCC, 2014a). Dots indicate where the estimated precipitation change is larger than one standard deviation in comparison to natural interannual variability and where at least 90% of models agree on the sign of change. Hatching indicates where the estimated change is less than one standard deviation.

1.4. Moisture recycling

Precipitation at a certain location on Earth is evaporated from another location, either from land or from the ocean. The process of water evaporating from land and precipitating on land again, is called moisture recycling (van der Ent, 2014). This principle can be used in moisture tracking models, from which can be learned how moisture travels through the atmosphere. Several studies looked in more depth into the regional specific influence of upwind regions on downwind regions in terms of moisture availability, such as Weng et al. (2018). In this study, research has been conducted regarding the influence of land-use scenarios upwind on rainfall and runoff downwind. Influential source areas were identified, where land use change might reduce the water reception in the sink area. Parts of the Peruvian Amazon and western Bolivia are identified as the sink areas most sensitive to land use change in the Amazon. Sensitive sinks and influential sources are therefore suggested as hot spots for achieving sustainable land–water management (Weng et al., 2018). Research from Tuinenburg et al. (2012) also explored where evaporation travels to. The study suggested that evaporation might precipitate in the same basin, which for instance happened in the Ganges basin in India. In contrast to this, a study by Wang-Erlandsson et al. (2018) found that in some of the world's largest basins, precipitation was influenced stronger by land-use change occurring outside than inside the basin. An example of land-use change is the replacement of forests by pasture or crops. Climate models predict that large-scale tropical deforestation causes reduced regional precipitation (Spracklen et al., 2012). The study from Spracklen et al. (2012) also found that, based on observations, for more than 60 per cent of the tropical land surface (latitudes 30 degrees south to 30 degrees north), air that has passed over extensive vegetation in the preceding few days produces at least twice as much rain as air that has passed over little vegetation.

Bosilovich et al. (2005) looked at differences between precipitation that originated from land versus precipitation that originated from oceans. Even though the total continental precipitation will increase with a global increase of sea surface temperatures, the study suggests that the amount of precipitation coming from land will decrease, which means that the amount of precipitation from oceanic origin will increase significantly. On the contrary, zooming into regional scale shows an increasing trend of continental precipitation coming from land. In order to find out why these differences a regional scale occur, the precipitationshed can provide a part of the explanation. For every location on Earth specifically it was studied that there is a core precipitationshed (Keys et al., 2014). The precipitationshed provides a boundary of from where water was evaporated in order to precipitate at that specific location. Van Der Ent et al. (2010) looked at two variables specifically in order to determine where precipitation originates from and where evaporation goes to. The continental evaporation ratio (ϵ_c) is the land evaporation that returns as precipitation on land as a percentage of the total land evaporation. The continental precipitation ratio (ρ_c) is the land precipitation that has an origin as land evaporation as a percentage of the total land precipitation. These variables can provide the information about what the moisture giving areas (upwind) and the moisture receiving areas (downwind) are.

1.5. Research objective

Until now, research has been conducted on what would happen to precipitation with climate change and other research has been conducted about the influence of upwind evaporation on downwind precipitation. However, these two research areas are yet to be combined. Therefore, the objective of this research is to examine the changes in the water cycle with climate change and to use a moisture tracking model to explain these changes of the water cycle. In this way it is aimed to acquire knowledge about what will happen to the global and regional water cycle in the future and why this happens to eventually answer the question: To what extent can atmospheric moisture transport explain changes in precipitation with climate change?

The hypothesis is that with increasing temperatures, evaporation will increase which will lead to higher precipitation rates. However, there is a moisture constraint to increasing evaporation rates on land. With rising temperatures, the evaporation would increase as long as there is enough water to be evaporated. In the oceans there is no limit to water availability and on land water is limited, so the expectation is that the percentage of precipitation coming from land would decrease.

More information on the IPCC and its forecasts, research on changing precipitation patterns, research on moisture recycling and modelling moisture recycling can be found in Appendix A. Here a brief problem analysis that led to the main research question has been described as well.

2

Methodology

In this chapter the methodology is formulated. It provides the explanation of the phases that are followed together with an explanation of the model, the data needed to run the model and the definition of the output metrics.

2.1. Method

This research consists of three phases. The first phase includes the definition of the model requirements and the selection of a suitable model that conducted experiments for the Coupled Model Intercomparison Project Phase 5 (CMIP5). In the second as well as the third phase the goal is to derive important hydrological variables as well as modelling moisture recycling. The second phase focuses on the global scale and the third phase focuses on the regional scale. The conclusion and interpretation of the second phase gives input to the choice of regions for the third phase. In the third phase, where the focus lies on specific regions, the analysis is expanded by also doing an impact analysis.

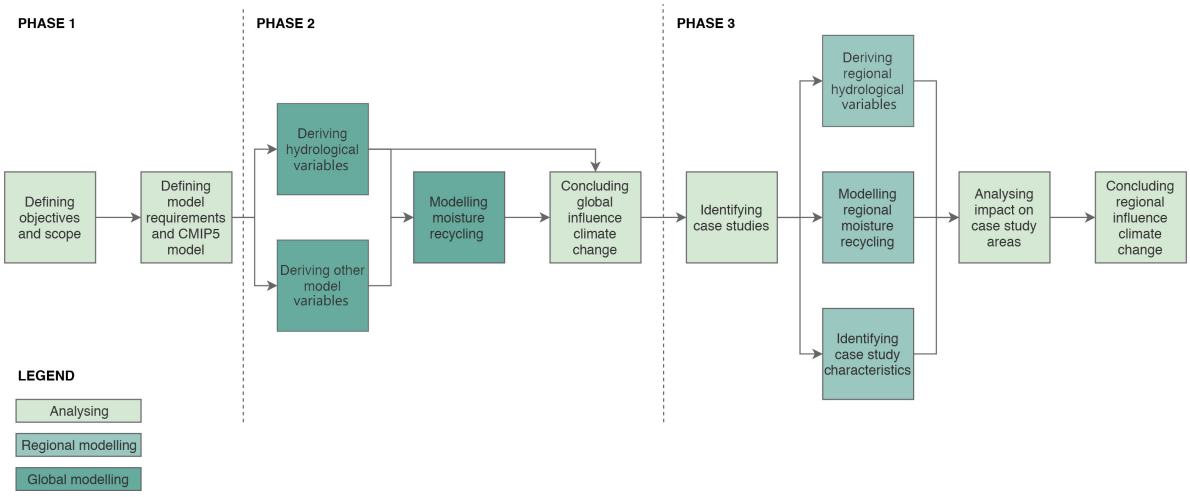

Figure 2.1: Methodology flow chart. The boxes illustrate the different steps of the research, with light green representing analysing steps, middle green representing regional modelling and dark green representing global modelling. Steps flow towards other steps with arrows and phases are divided by dotted lines.

2.2. WAM-2layers

This research uses the Water Accounting Model-2layers (WAM-2layers) to determine the origin and destination of moisture globally as well as regionally (van der Ent, 2014). The model is originally written for ERA-Interim data. However, in this study the model is rewritten to make it compatible with data from the Geophysical Fluid Dynamics Laboratory (GFDL). The model consists of a number of grid cells spread out over

a region of interest. Any grid cell is either labelled as land or as ocean and contains a top and bottom layer, divided by a boundary. Specific humidity, pressure and wind in the horizontal directions are interpolated in both the top and the bottom layer. Moisture is travelling though the model with the following principle: in both layers of each grid cell there is evaporation entering and precipitation exiting vertically and a moisture flux entering and exiting horizontally in all four directions (North, East, South and West). WAM-2layers is an offline Eulerian atmospheric moisture tracking model, that uses the water balance as underlying principle, as presented in Equation 2.1 (van der Ent, 2014).

$$\frac{\partial S_k}{\partial t} = \frac{\partial (S_k u)}{\partial x} + \frac{\partial (S_k v)}{\partial y} + E_k - P_k + \xi_k \pm F_z \tag{2.1}$$

The water balance represents the atmospheric storage of water (S_k) in a layer k, either the top or bottom layer. In Equation 2.1 t represents time, u and v represent the horizontal wind patterns in respectively the x (East-West) or y (North-South) direction. E_k is the evaporation entering layer k, P_k is the precipitation exiting the layer k, ξ_k represents the residual and F_z is the vertical moisture transport between the bottom and top layer.

WAM-2layers calculates the moisture transport between the grid cells. This is computed by the use of moisture fluxes in both horizontal directions (East-West and North-South). In any direction the moisture flux can be calculated by using Equation 2.2 (van der Ent, 2014).

$$F_k = \frac{L}{g\rho_w} \int_{p_{top}}^{p_{bottom}} q u_h dp \tag{2.2}$$

Where F_k stands for the moisture flux in either East-West or North-South direction in layer k, L represents the length of the grid cell perpendicular to the direction of the flux, g is the gravitational acceleration, ρ_w is the density of liquid water, p represents pressure, q is the specific humidity and u_h is the horizontal wind in either East-West or North-South direction. For the top layer, p_{top} is equal to the pressure at the top of the atmosphere, thus equal to 0 and p_{bottom} is equal to the pressure at the boundary layer. For the bottom layer, p_{top} is equal to the pressure at the boundary layer and p_{bottom} is equal to the surface pressure. In each grid cell the surface pressure is calculated using the geopotential height and the temperature. With the surface pressure the pressure at the boundary layer can be calculated. The explanation of these calculations can be found in Appendix B (Equation B.4 and Equation B.5).

2.3. GFDL Data

Before using the GFDL data as input for WAM-2layers, the data is analysed to understand the hydrological cycle in the future due to climate change. The GFDL has completed several model runs within the CMIP5 project. For comparisons of future situations, past situations need to be mapped as well. Two time series are used, a past scenario, running from 1986 to 2005 called the 'end-20th century scenario' and a future scenario, running from 2081 to 2100, called the 'end-21st century scenario'. First, the data for the end-20th century scenario are collected. This experiment, called AMIP, has ran for a time frame from 1979-2008 in the GFDL-HIRAM-C180 model. The end-21st century scenario is collected from the GFDL-ESM2M model, for the RCP8.5 experiment. This data is avaiable from 2006 to 2100. The variables that are used in this study, are from two time series and have multiple dimensions. Although many different variables were calculated by the GFDL, only a few dynamic variables and static parameters are required. The variables are either three or four dimensional. This means that all variables have values in all these dimensions. The dimensions are the following:

- Latitude
  The latitude dimension divides the globe over the full length in several fragments. All fragments have the same length in kilometres. For the end-20th century scenario the size of the latitude dimension is 360. In the end-21st century scenario its size is one fourth, namely 90. Of these 90 latitude fragments, the top 5 and bottom 15 are excluded from the model. This is done because the poles are excluded from this research. Towards the poles the grid cells get insignificantly small in actual surface area, which is not of interest in this study.

- Longitude
  In contrast to the latitude dimension, the fragments of longitude dimension differ in width in kilometres. The width decreases towards the poles and increases towards the equator. The size of the longitude

dimension of the end-20th century scenario is also four times as large as the end-21st century scenario, 576 versus 144. No longitude fragments are excluded.

- Time
  Since the GFDL data has daily time steps, the size of the time dimension for each year is 365. In the end-20th century scenario leap years are taken into account, thus for these years the time step is 366. In the end-21st century scenario leap years are not taken into account.

- Pressure levels
  Several dynamic variables have values over the entire atmosphere, at a certain pressure level instead of a static height.

WAM-2layers variables and parameters
The dynamic variables are the variables that have daily values for every grid cell within the model. Variables with 3 dimensions have dimensions time, latitude and longitude and variables with 4 dimensions also the dimension pressure level. The static parameters are time independent and have values for every grid cell in the model, thus these have two dimensions, namely latitude and longitude. All of the equations for deriving variables with the desired units can be found in Appendix B.

Variable in WAM-2layers	**Data from GFDL**	**Number of dimensions**
Precipitation [m^3d^{-1}]	Precipitation [kgm^2s^{-1}], Surface area grid cell [m^2]	3
Evaporation [m^3d^{-1}]	Evaporation [kgm^2s^{-1}], Surface area grid cell [m^2]	3
Surface pressure [Pa]	Pressure levels [Pa], Surface height [m], Air temperature at pressure levels [K], Geopotential height [m]	3
Eastward wind [ms^{-1}]	Eastward wind [ms^{-1}] at pressure levels, Eastward wind at the surface [ms^{-1}]	4
Northward wind [ms^{-1}]	Northward wind [ms^{-1}], Northward wind at the surface [m^{-1}]	4
Specific humidity [$kgkg^{-1}$]	Specific humidity at pressure levels [$kgkg^{-1}$], Specific humidity at the surface [$kgkg^{-1}$]	4

Table 2.1: Dynamic variables in WAM-2layers model and data needed

Parameter in WAM-2layers	**Data from GFDL**
Land sea mask [0 or 1]	Land sea mask [fraction]
Surface height [m]	Surface height [m]

Table 2.2: Static parameters in WAM-2layers model and data needed

2.4. Definition output metrics

Hydrological variables analysis
For the analysis of the hydrological variables, GFDL data of the precipitation, evaporation and air temperature at the surface are used. For both time series, precipitation and evaporation data are averaged over the twenty years and rewritten to mm d^{-1}. The temperature values are also averaged over the twenty years and rewritten to °C. On all three variables (precipitation, evaporation and surface air temperature) two analyses are done. First, plots are made of the averages in mm d^{-1} or °C that show the spatial variability over all grid cells. This includes a plot for the past scenario, future scenario and a difference plot. The difference plots of the precipitation and evaporation data are defined as the percentage change relative to the past scenario, the difference plot of the surface air temperature is the absolute change in °C. The second analysis includes statistical calculations. The grid cells do not cover uniform surface areas, grid cells around the equator cover the largest surface areas and grid cells at the poles cover the smallest surface areas. Because of these differences, statistical analyses - including spatial averages - can only be done with a correction of the surface area. The statistical analyses are conducted with histograms and the calculations of the mean, standard deviation, 25th, 50th (median) and 75th percentile.
Moisture recycling
Globally the moisture recycling is calculated using the WAM-2layers model as described in Section 2.2. The

WAM-2layers is used to track whether moisture originates from land or from ocean until the moment it precipitates, by tagging whether moisture evaporated from a land grid cell. In this thesis two main terms are used to determine the amount of recycling of land precipitation, ρ_c and ϵ_c.

$$\rho_c = \frac{P_{land}}{P_{total}} \tag{2.3}$$

In Equation 2.3 ρ_c represents the continental precipitation recycling ratio, defined as the ratio between the amount of precipitation that originates as evaporation from land, (P_{land}) over the total amount of precipitation (P_{total}). P_{land} is also defined as the amount of recycled precipitation.

$$\epsilon_c = \frac{E_{land}}{E_{total}} \tag{2.4}$$

Equation 2.4 presents ϵ_c, the continental evaporation recycling ratio. This is defined as the ratio of the amount of evaporation that will precipitate on land (E_{land}) over the total amount of evaporation (E_{total}). E_{land} is also defined as the amount of recycled evaporation.

Plots are made of the continental precipitation recycling ratio and continental evaporation recycling ratio for both scenarios for the entire globe, highlighting only the land regions used in the model and including the moisture fluxes as arrows. The globally averaged ratios are also calculated in one number per ratio per scenario, defined in Equation 2.3 and Equation 2.4. These numbers are also calculated per continent. Firstly, the amount of total precipitation and evaporation are calculated for each continent specifically, corrected for the surface area. Secondly, the amount of recycled land precipitation and evaporation per continent are calculated, also corrected for the surface area. These two outputs result in an averaged ratio for both ρ_c and ϵ_c for six continents: North America, South America, Africa, Europe, Asia and Oceania. Maps are used as well to display the differences in recycled precipitation and evaporation in each continent.

Case studies

Two case studies are determined, the specifics of the case studies are displayed in Table 2.3. The choice of these case studies is based on multiple arguments. The precipitation or the evaporation rate should show a significant change in the future scenario relative to the past scenario. This change or these changes should contrast the changes in the other case study area. The two case study areas should be similar in terms of surface area and number of grid cells. For both case studies only land grid cells are part of the actual case study area.

Case study area	**Amazonia** (**1**)	**Western Africa** (**2**)
Longitudes	-73.75, -48.75	-18.75, 16.25
Latitudes	-9.10, 9.10	3.03, 17.19
Surface area	510667 km^2	482570 km^2
Number of grid cells	82	79

Table 2.3: Specifics of case study areas

The analysis of the case studies consists of three parts: the background information, the analysis of seasonality in the water cycle, the moisture tracking for a full year and the moisture tracking for a specific season. Land cover, elevation and population density are provided as background information with the use of QGIS. The analysis of the seasonality is accomplished by finding the mean precipitation or evaporation of each day during the two twenty-year time series and by plotting these daily means from the 1st of January until the 31st of December. To show the (un)centainty of the mean precipitation and evaporation, boxplots of the monthly output are produced as well. The third part, moisture tracking, is performed by using the WAM-2layers model again. Instead of tracking whether moisture evaporates from or precipitates on land worldwide, with the case studies the WAM-2layers tracks whether moisture evaporates from or precipitates on land within the chosen case study area. The moisture tracking uses the same principles as the global continental moisture tracking. However, tracking moisture towards and from the case study area introduces new variables and their definitions.

$$\rho_A = \frac{P_{fromAmazonia}}{P_{total}} \tag{2.5}$$

$$\rho_{WA} = \frac{P_{fromWesternAfrica}}{P_{total}} \tag{2.6}$$

$$\epsilon_A = \frac{E_{towardsAmazonia}}{E_{total}} \tag{2.7}$$

$$\epsilon_{WA} = \frac{E_{towardsWesternAfrica}}{E_{total}} \tag{2.8}$$

The Amazonian precipitation recycling ratio (Equation 2.5, ρ_A) and the West-African precipitation recycling ratio (Equation 2.6, ρ_{WA}) are ratios at any grid cell in the model - both inside the case study area as well as outside - between total precipitation (P_{total}) and precipitation originating from land grid cells within the case study area ($P_{fromAmazonia}$ and $P_{fromWesternAfrica}$). The Amazonian evaporation recycling ratio (Equation 2.7, ϵ_A) and the West-African evaporation recycling ratio (Equation 2.8, ϵ_{WA}) are ratios at any grid cell in the model - both inside and outside the case study area - between total evaporation (E_{total}) and the amount of evaporation that will precipitate on land within the case study area ($E_{towardsAmazonia}$ and $E_{towardsWesternAfrica}$). However, for both the precipitation recycling ratios (ρ_A and ρ_{WA}) and the evaporation recycling ratios (ϵ_A and ϵ_{WA}) count that there is a certain amount of moisture that recycles within the case study area itself - moisture that evaporates at one location within the case study area and precipitates in another location within the case study area. While the produced plots show the recycling ratios for inside as well as outside the case study area, the numbers for the recycling ratios show the ratio between the amount of precipitation or evaporation and the amount of recycled moisture only within the case study area.

Besides numbers for precipitation rate, evaporation rate, recycled moisture rate and the case study's recycling ratios, plots are made to explain the changing patterns. These are the plots for precipitation rate, evaporation rate, recycled precipitation rate, recycled evaporation rate, the case study's precipitation and evaporation recycling ratios and Eastward, Northward and combined moisture fluxes. All the moisture tracking output mentioned above for the data of both case study areas will be repeated for only the months with specific seasonal changes in the end-21st century scenario.

3

Changes in the global water cycle

This chapter consists of the results of processing hydrological data. In Section 3.1 the plots of three hydrological variables are shown, averaged in time and spatially variable. Statistical analyses are performed on these variables in Section 3.2.

3.1. Visualisation of hydrological variables

The hydrological cycle is examined by analysing the precipitation, evaporation and surface air temperature data. Averaged over the two twenty-year time series these variables vary spatially. Per variable three plots have been produced, first the end-20th century scenario, then the end-21st century scenario and finally the difference between the two scenarios.

Precipitation
In Figure 3.1a the averaged daily precipitation rate is given for the end-20th century scenario. Figure 3.1b shows the averaged daily precipitation rate for the end-21st century scenario. The precipitation plot of the end-20th century scenario (Figure 3.1a) follows the expected patterns. Regions with higher precipitation rates are around the equatorial rain forests in South America, Central Africa and Indonesia. Lower precipitation rates are in the worlds' drier regions such as the Sahara, Australia and Central Asia. In some regions the rates are close to zero, such as in Egypt or North of the Himalayas. The precipitation plot of the end-21st century scenario (Figure 3.1b) shows a similar pattern as the end-20th century. In relation to other parts of the world, the same regions with the highest rates are high and the same regions with the lowest rates are low. However, the rates in the rain forest in South America has shifted from black to red, indicating a decrease. On the contrary, rates in Indonesia have increased, indicated by darker colors. To fully understand the differences, the change in precipitation rate is shown in Figure 3.2. The difference plot in shows a few changes that are worth mentioning. What stands out at first is that there are more areas with increasing precipitation rates than areas with decreasing rates. Increasing precipitation rates are especially visible in parts of Africa, North America and the North of Eurasia. In contrast to this there are regions where the precipitation rate will decrease, such as South America, parts of Australia and the Middle East.

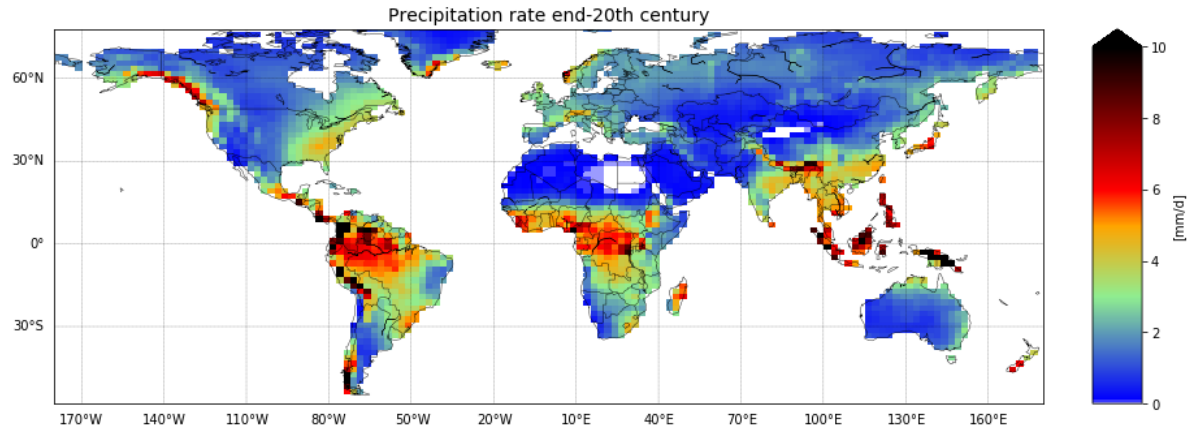

(a)

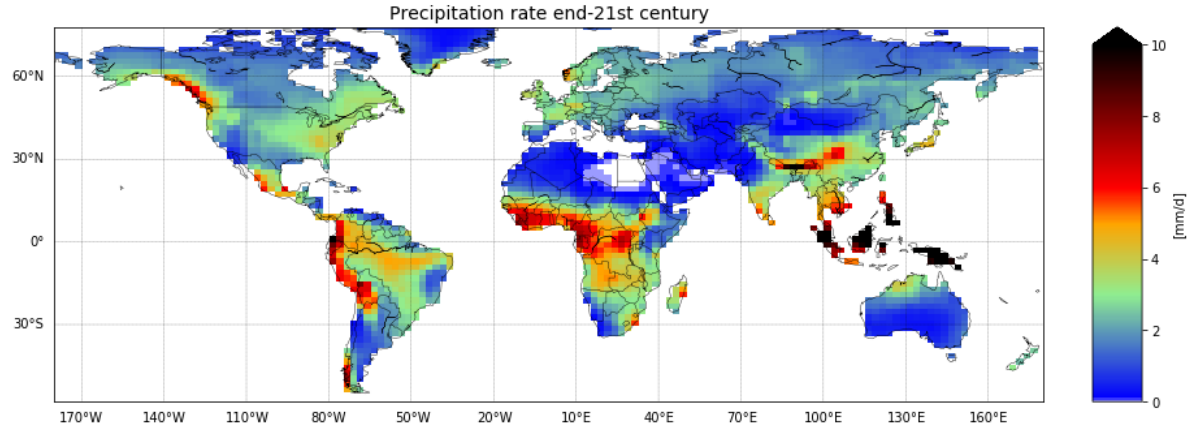

(b)

Figure 3.1: Precipitation rates for end-20th century (a) and end-21st century (b) in mm d^{-1}. The plots show areas with low rates as blue, areas with moderate rates as green to yellow and areas with high rates as red to black. White areas represent regions with precipitation rates close to zero.

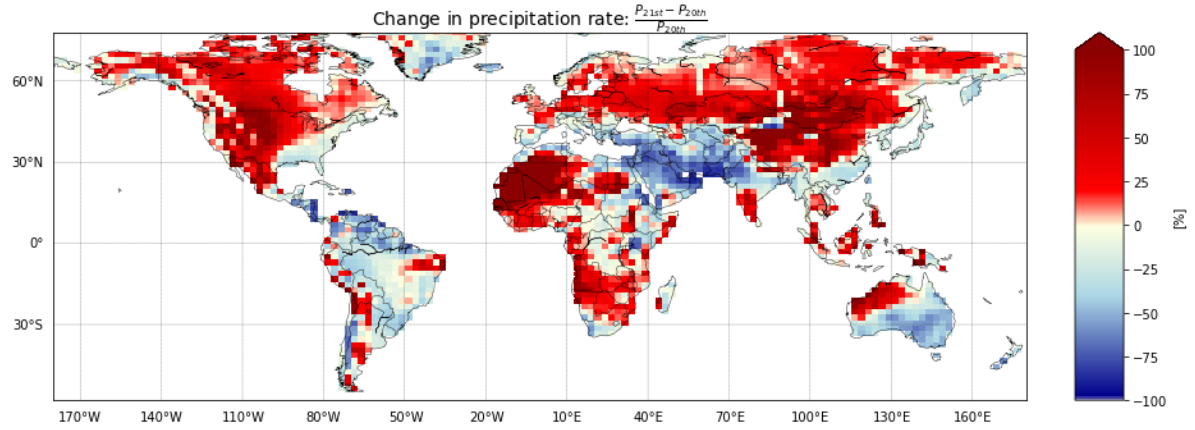

Figure 3.2: Average change in daily precipitation in percentage change relative to the past scenario. Red regions refer to an increase in precipitation and blue regions refer to a decrease in precipitation.

Evaporation

The plot of the averaged daily evaporation rate for the end-20th century scenario is shown in Figure 3.3a. Figure 3.3b shows the averaged daily evaporation rate for the end-21st century scenario. Similarly to the precipitation plot, the evaporation plot for the end-20th century follows the expected patterns. The tropical rain forests in South America, Central Africa and Indonesia experience high evaporation rates and the Sahara and Central Asia experience lower evaporation rates. The plot of the daily evaporation in the end-21st century shows overall the same regions to be high or low as in the end-20th century. The magnitude of the rates however has changed. For example in the Americas. Where in the past scenario there is a clear dissimilarity between North and South America in terms of evaporation rates, in the future scenario the rates in these two continents seem to get more similar. To indicate how severe the change in evaporation rates is for any specific region, the percentage change relative to the past scenario is shown in Figure 3.4. Broadly and in terms of sign of change, this figure is spatially similar to Figure 3.2, the percentage change in precipitation rate. Most of South America shows a decrease in evaporation. The Middle East is the most noticeable, where the largest decrease in evaporation is expected. Decreasing evaporation rates in a region indicate lower moisture availability and could potentially indicate that a region is getting drier. In the Northern hemisphere, in specific in North America and Russia, many regions have increased evaporation.

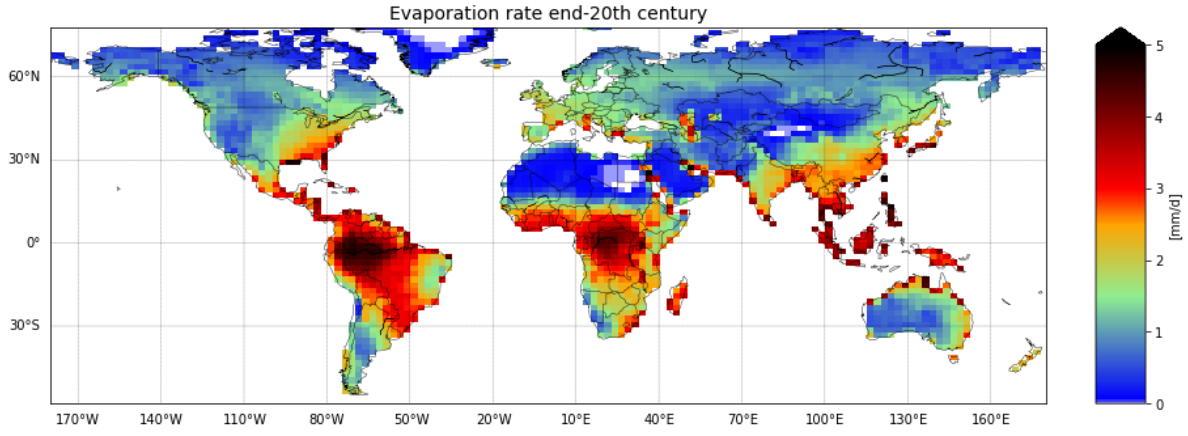

(a)

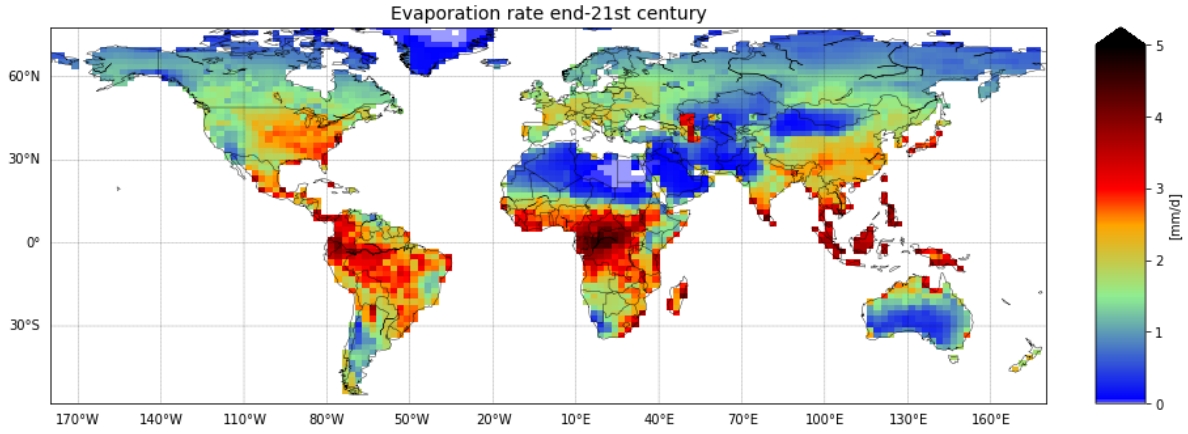

(b)

Figure 3.3: Evaporation rates for end-20th century (a) and end-21st century (b) in mm d^{-1}. The plots show areas with low rates as blue, areas with moderate rates as green to yellow and areas with high rates as red to black. White areas represent regions with evaporation rates close to zero.

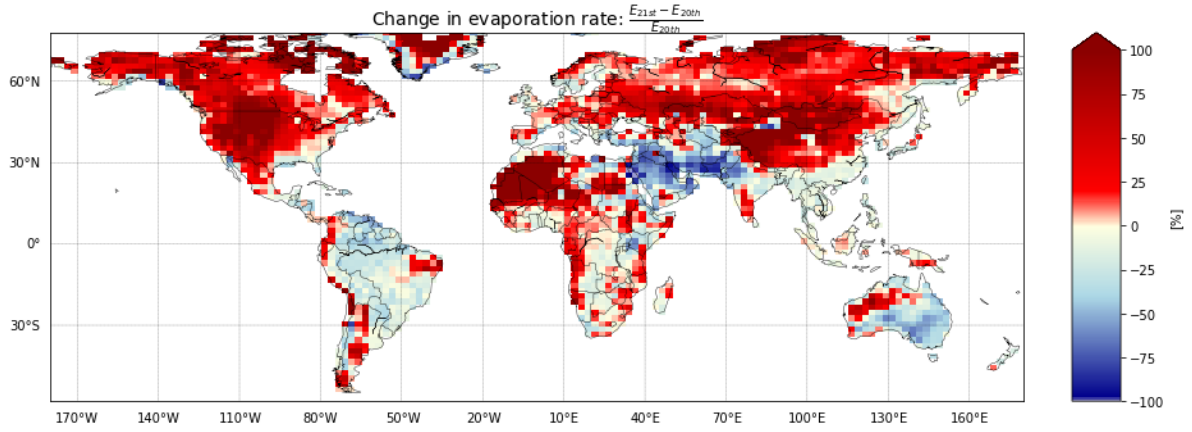

Figure 3.4: Average change in daily evaporation in percentage change relative to the past scenario. Red regions refer to an increase in evaporation and blue regions refer to a decrease in evaporation.

Surface air temperature

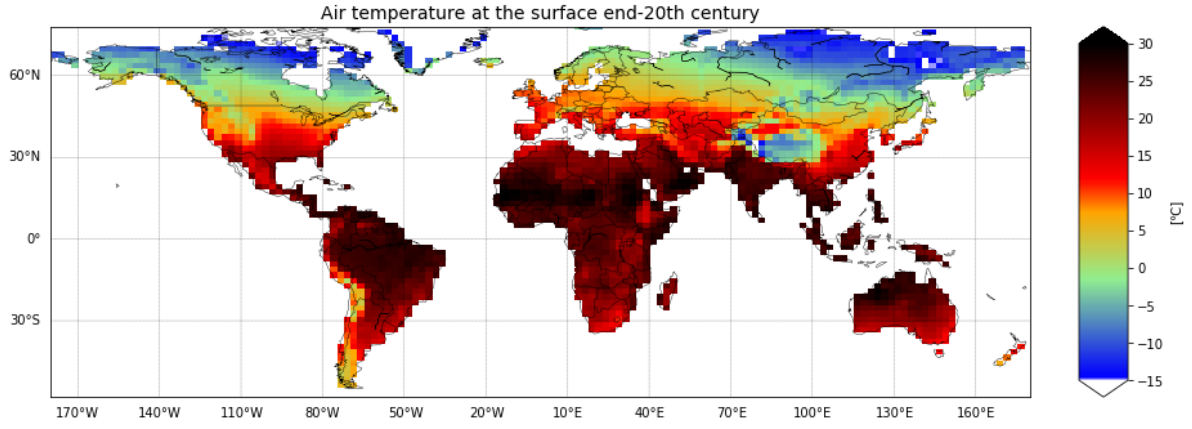

(a)

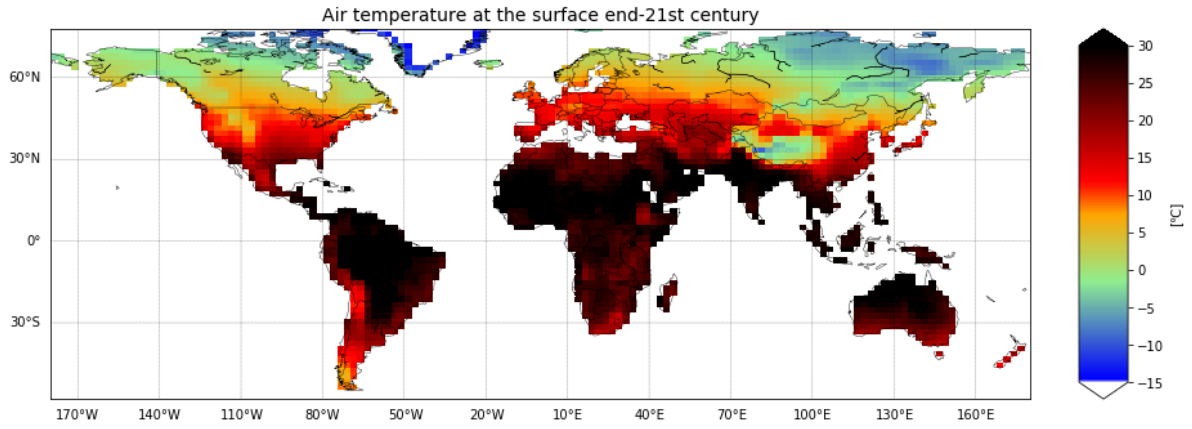

(b)

Figure 3.5: Surface air temperature for end-20th century (a) and end-21st century (b) in °C. Blue colors indicate the lowest temperatures, green to yellow colors indicate moderate temperatures and red to black indicate the highest temperatures.

Figure 3.5a shows the averaged daily surface air temperature in the end-20th century scenario and Figure 3.5b shows the averaged surface air temperature in the end-21st century scenario. The plot of the surface air temperature in the end-20th century scenario shows the expected patterns, that regions around the equator

have the highest temperatures, steadily decreasing towards the poles. The plot of the surface air temperature in the end-21st century scenario shows less blue regions than in the end-20th century, indicating higher temperatures, for example towards the North Pole. Around the equator the areas with high temperatures only seems to get higher, indicated by darker colors. In order to see the change in temperature more clearly, a difference map can be seen in Figure 3.6. Even though there are a few places on Earth that will experience no change (indicated with green), overall the entire land surface seems to experience higher temperatures in the future.

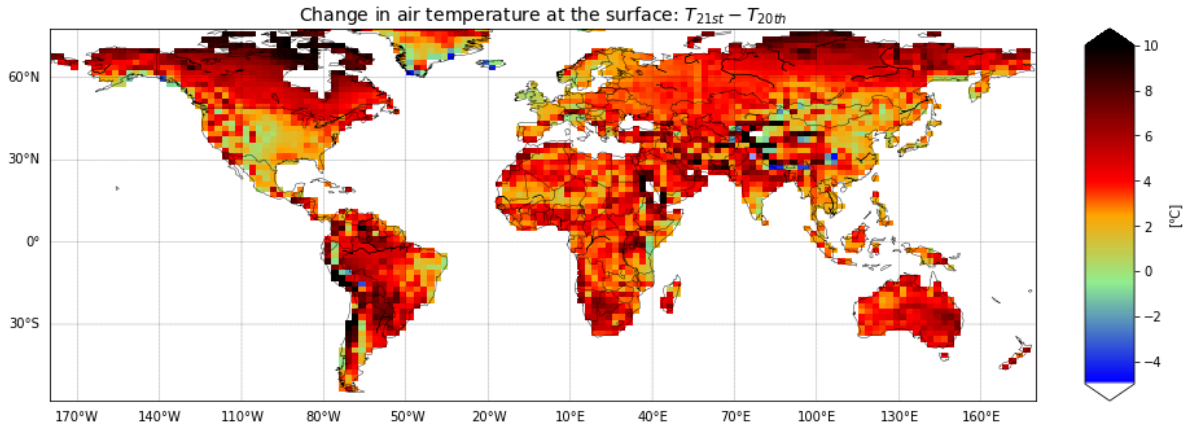

Figure 3.6: Absolute change in daily surface air temperature of the future scenario as respect to the past scenario (end-21st century minus end-20th century) in °C, with green indicating no change, blue indicating lower temperatures in the future and yellow to red to black indicating an increase in temperature in the future.

Since this research focuses on changes on land, the oceans are excluded in the plots of hydrological variables. Appendix C contains all plots from this Section for the entire globe, including the oceans (Figure C.1, C.2, C.3, C.4, C.5 and C.6), giving background information about hydrological variables on the oceans.

3.2. Statistical analyses

A distinction is made between the averaged yearly values of the variables solely over land, solely over the oceans and over the entire globe, including both land and ocean. Table 3.1 shows the mean changes on land, over the oceans and over both land and ocean, for precipitation, evaporation and surface air temperature. This is done by averaging values for all three variables for only land, only ocean or all grid cells, correcting for the changing grid cell size with latitude, since around the equator the grid cell sizes are much larger than toward the poles.

Variable	**Averaged over**	**end-20th**	**end-21st**	**difference**
Precipitation [mm d^{-1}]	Land	2.51	2.48	-0.03
	Ocean	3.26	3.39	+0.13
	Land and ocean	3.06	3.15	+0.09
Evaporation [mm d^{-1}]	Land	1.65	1.67	+0.02
	Ocean	3.55	3.63	+0.08
	Land and ocean	3.04	3.11	+0.07
Surface air temperature [°C]	Land	13.24	17.16	+3.92
	Ocean	16.21	18.45	+2.24
	Land and ocean	15.42	18.10	+2.68

Table 3.1: Averaged values for hydrological variables for land, ocean and total global (land and ocean) surface area. The Table shows mean precipitation and evaporation rates (in mm d^{-1}) and mean surface air temperature (in °C), for end-20th century, end-21st century and the difference between the two.

Surface air temperature increases almost 4 °C on land and a little over 2 °C over the oceans, so relatively speaking there is more increase in temperature on land than on the ocean. Interestingly, there is just a slight decrease in land precipitation and a slight increase in land evaporation rates. However, over the oceans as well as globally these two variables seem to increase in a more significant matter. Even with rising land surface air temperature the spatially and yearly averaged precipitation and evaporation rates do not seem to rise significantly. Therefore a more in-depth analysis on this is done in order to understand the spatial variability of the precipitation, evaporation and surface air temperature data. The histograms have slightly different mean values than the mean values presented in Table 3.1, because of small errors made when calculating the frequency as the amount of squared kilometres. Because the data is averaged over time, the histograms do not take into account seasonal or yearly fluctuations.

Precipitation

The histograms of the precipitation data are displayed in Figure 3.7a (end-20th century) and Figure 3.7b (end-21st century) and the corresponding statistics can be found in Table 3.2.

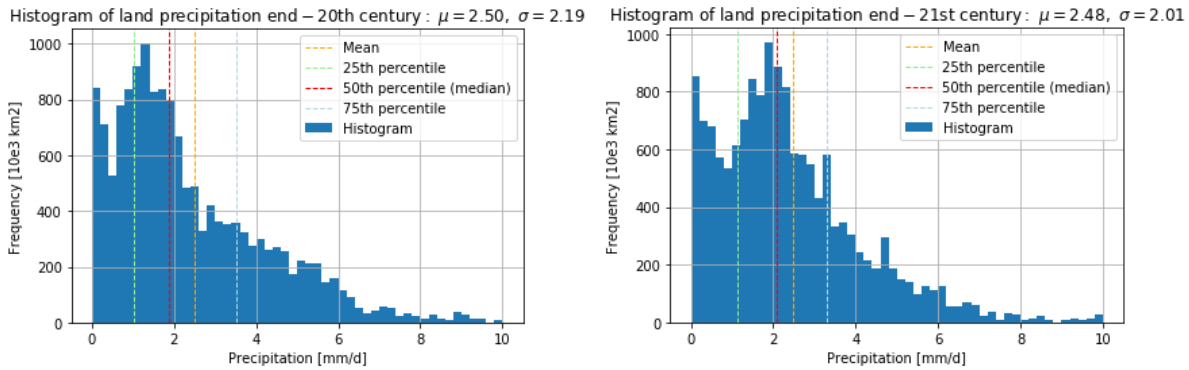

(a) (b)

Figure 3.7: Histogram of land precipitation for end-20th century (a) and end-21st century (b). The precipitation is calculated in mm d^{-1} and the frequency refers to the amount of squared kilometres that have a certain amount of volume of precipitation.

	AMIP	**RCP8.5**	**Difference** (RCP8.5 - AMIP)
Mean	2.5	2.48	-0.02
Standard deviation	2.19	2.01	-0.18
25th percentile	1.03	1.14	+0.11
50th percentile (median)	1.88	2.08	+0.20
75th percentile	3.51	3.30	-0.21
25-75 inter-percentile range	2.48	2.16	-0.32

Table 3.2: Statistical parameters histograms precipitation, all units are mm d^{-1}.

From Table 3.2 can be seen that the inter-percentile range (IPR) between the 25th and 75th percentile of the precipitation data has decreased from 2.48 to 2.16. The inter-percentile range is a stable measure of spread, so a decrease demonstrates that the data scatters less. This is supported by the decrease in standard deviation from 2.19 to 2.01. This means that in the future scenario there is less spatial variability than in the past case, meaning that the precipitation rate in the driest region is closer to the precipitation rate in the wettest region in the end-21st century scenario than in the end-20th century scenario.

Evaporation

Histograms of the evaporation data are computed and displayed in Figure 3.8a for the end-20th century scenario and in Figure 3.8b for the end-21st century scenario. The corresponding statistics can be found in Table 3.3.

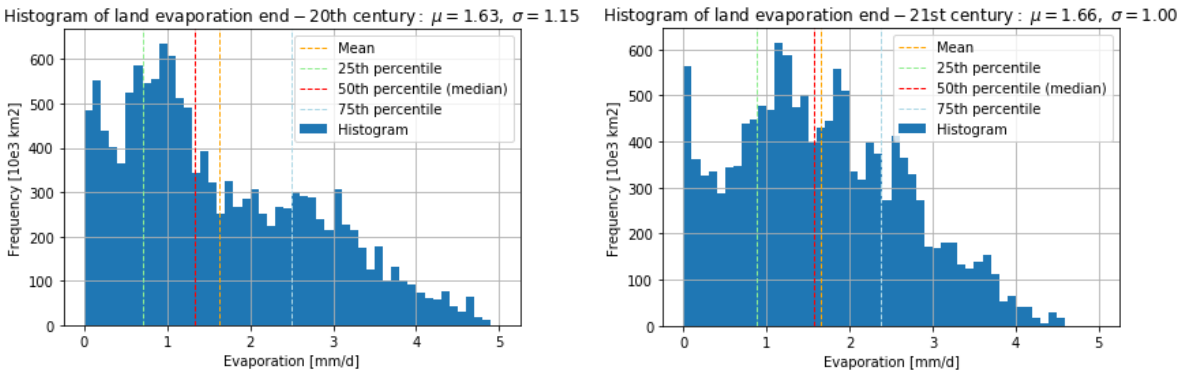

(a) (b)

Figure 3.8: Histogram of land evaporation for end-20th century (a) and end-21st century (b). The evaporation is calculated in mm d^{-1} and the frequency refers to the amount of squared kilometres that have a certain evaporation intensity.

	AMIP	**RCP8.5**	**Difference** (RCP8.5 - AMIP)
Mean	1.63	1.66	+0.03
Standard deviation	1.15	1.00	-0.15
25th percentile	0.70	0.89	+0.19
50th percentile (median)	1.33	1.57	+0.24
75th percentile	2.50	2.38	-0.12
25-75 inter-percentile range	1.80	1.49	-0.31

Table 3.3: Statistical parameters histograms evaporation, all units are mm d^{-1}.

Similarly to the mean precipitation rates, mean evaporation rates in the future scenario is also less scattered spatially. This can firstly be seen by the inter-percentile range from the 25th to 75th percentile, which decreases from 1.80 to 1.49. Secondly the standard deviation decreases from 1.15 to 1.00. This indicates that in the future scenario, the evaporation rate of the region with lowest rate lies closer to the region with the highest rate than in the past scenario.

Surface air temperature

The data of the surface air temperature data is statistically analysed with histograms, which are shown in Figure 3.9a (for the end-20th century) and Figure 3.9b (for the end-21st century). The corresponding statistics can be found in Table 3.4.

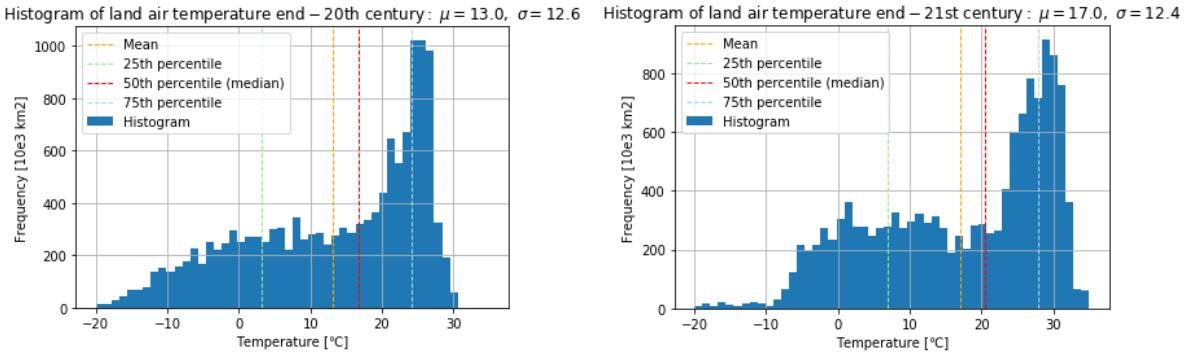

(a) (b)

Figure 3.9: Histogram of land surface air temperature for end-20th century (a) and end-21st century (b). The temperature is in degrees Celcius and the frequency refers to the amount of squared kilometres that have a certain surface air temperature.

	AMIP	**RCP8.5**	**Difference** (RCP8.5 - AMIP)
Mean	13.05	16.98	+3.93
Standard deviation	12.62	12.40	-0.22
25th percentile	3.26	6.93	+3.67
50th percentile (median)	16.74	20.48	+3.74
75th percentile	24.17	27.82	+3.65
25-75 inter-percentile range	20.91	20.89	-0.02

Table 3.4: Statistical parameters histograms surface air temperature, all units are °C.

Similarly to the increasing inter-percentile range between the 25th and 75th percentile of the precipitation and evaporation data, the 25 to 75 inter-percentile range of the temperature data changes from 20.91 to 20.89, thus decreases, which indicates slightly less scatter. Additionally, the standard deviation decreases, which indicates less scatter as well, which is similar to the other two hydrological variables. The histogram itself does not show a normal distribution. The end-21st century has a distribution with two peaks, which is typically a bimodal distribution, indicating that the temperature data has two modals.

From analysing the hydrological variables two main conclusions can be drawn. From the precipitation plots can be concluded that the DDWW paradigm (Bosilovich et al., 2005), mentioned in Section 1.2, suggesting that with climate change dry regions will get dryer and wet regions will get wetter can now be invalidated - at least, when using precipitation rates as an indication whether a region is dry or wet and using the data of this research. Some dry regions indeed dry out further, such as the Middle East and parts of Australia. Other dry regions however will experience more precipitation and will in this sense actually get wetter, such as Western part of the Sahara and Central Asia. Similar changes are visible for wet regions. Some regions will indeed get wetter, such as Indonesia, however other wet regions will get dryer, such as Northern South America. These findings align with the previously found results of Greve et al. (2014).

The second conclusion is based on the statistical analysis. A DDWW paradigm suggests that the driest place in the past will become drier and the wettest place on Earth will become wetter. This implies that the yearly mean precipitation and evaporation rate over the globe would increase, that in the future the mean precipitation rate in the wettest place will lie further away from the mean precipitation rate in the driest place. But, in fact, the opposite of this was found with the statistical analyses. Based on decreasing standard deviations and 25 to 75 inter-percentile range for all three hydrological variables, conclusions can be drawn that GFDL data suggests the mean precipitation and evaporation rate in the driest place lie closer to the mean precipitation and evaporation rate in the wettest place and that the mean temperature in the warmest place lies closer to the mean temperature in the coldest place in the end-21st century.

4

Moisture recycling

Globally the moisture recycling is defined by the use of two ratios, the continental precipitation recycling ratio (in Section 4.1) and the continental evaporation recycling ratio (in Section 4.2). After this the more zoomed in plots of all continents together with continent specific recyled moisture give a more in-depth understanding of moisture recycling (in Section 4.3).

4.1. Global continental precipitation recycling ratio

Figure 4.1a shows the map of the global continental precipitation recycling ratio ρ_c in the end-20th century scenario. Red areas are more dependent on moisture recycling. Thus, changes in water availability in the source area, where the precipitation evaporated, could be crucial. Which areas are more dependent on moisture recycling is determined by among others the geographical location in relation to the location of the ocean and the wind directions. For instance in North America - where the main wind direction is Eastward and thus the moisture fluxes are from West to East - the ρ_c is lower on the West coast and gets higher when moving Eastward. As the moisture travels inland from the West, it first mostly contains water evaporated from the ocean, leading to precipitation of oceanic origin near the coast. As the wind moves more inland where new moisture evaporates, it now contains more moisture of continental origin. Areas in which a large fraction of the precipitation originates from land (the red areas in Figure 4.1a) are Central South America, Central Africa and Eastern Asia.

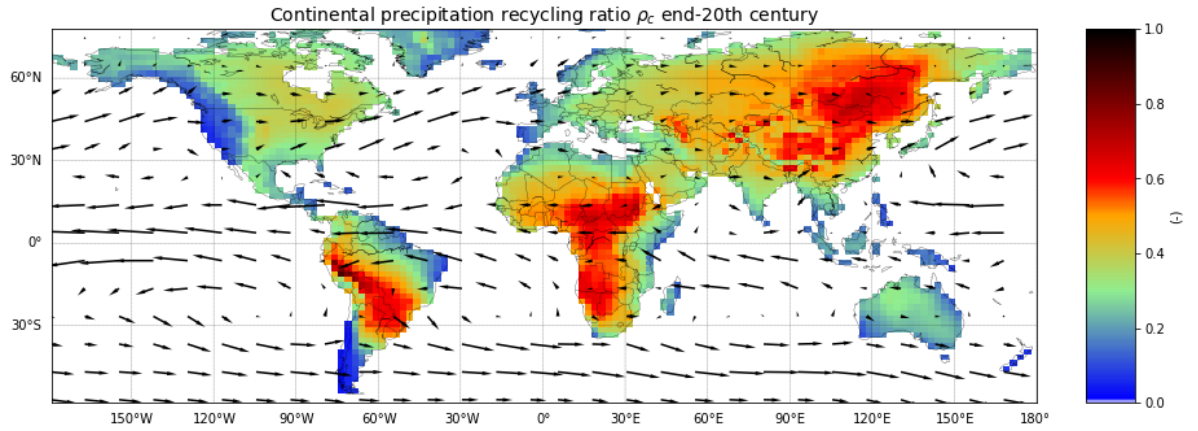

(a)

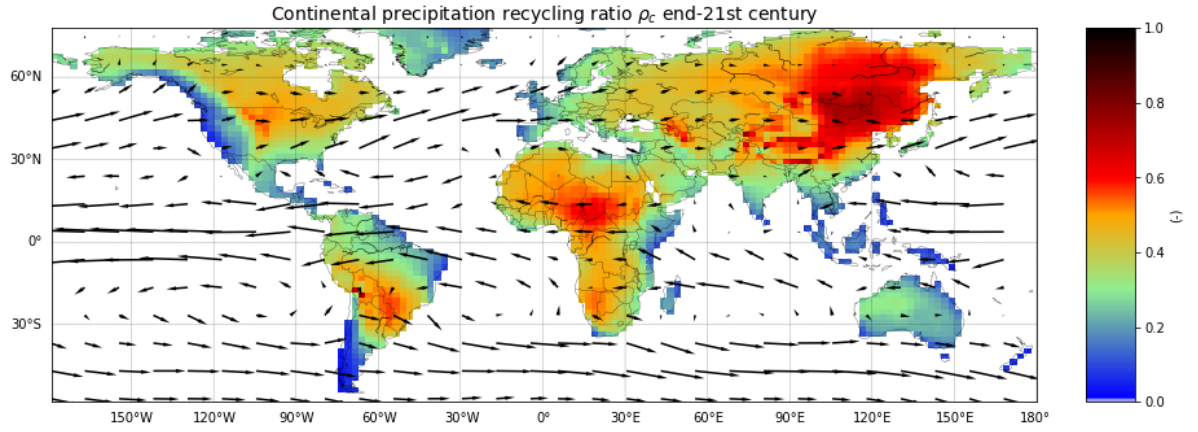

(b)

Figure 4.1: Continental precipitation recycling ratio for end-20th century (a) and end-21st century (b), defined as the ratio between the precipitation in a specific grid cell that originated as evaporation from land surface and the total precipitation in that grid cell. Red colors indicate that a relatively large amount of the precipitation originates from land and blue colors indicate that a relatively small amount of precipitation originates from land, thus in blue areas most precipitation originates from the ocean. Arrows represent the direction and magnitude of the moisture fluxes.

The continental precipitation recycling ratio ρ_c of the end-21st century scenario is displayed in Figure 4.1b. Comparing the two scenarios, the end-21st century scenario shows changes in red areas. The ratios in central North America and Eastern Asia get higher, indicating an increase in the fraction of precipitation from continental origin in these areas. On the contrary, the ratios in the end-20th century scenario in Central South America and Central Africa decrease in the end-21st century scenario, indicating a decrease in fraction of precipitation coming from land evaporation and hence a larger percentage originating from oceanic evaporation.

4.2. Global continental evaporation recycling ratio

In Figure 4.2a the global map of the continental evaporation recycling ratio ϵ_c in the end-20th century is displayed. The continental evaporation recycling ratio in a region depends on the geographical location in relation to the oceans and wind directions. For instance in North America: where the ρ_c (Figure 4.1a) shows a lower percentage near the West coast, ϵ_c actually shows a higher percentage at these locations, moving to lower percentages inland Eastward. Starting at the West coast, when water evaporates it moves towards the East and as it moves it precipitates. The further to the East coast, the lower the fraction of evaporation that will return as precipitation on land. Regions that have high ϵ_c are sources of precipitation for other regions. Changes in water availability in the source regions could lead to changes in the water availability in the receiving regions. Source regions (red areas in Figure 4.2a) are the Amazon rain forest, Eastern North America, Eastern Africa and Europe stretching to Central Asia. Combining this with the continental precipitation recy-

cling ratio from Figure 4.1a and keeping the moisture flux directions in mind, conclusions can be drawn that the Amazon rain forest is a source for the sink region of Central South America, Eastern North America is a source for sink region Western North America, Eastern Africa is a source region for sink region Central Africa and Europe to Central Asia is a source for sink region Eastern Asia.

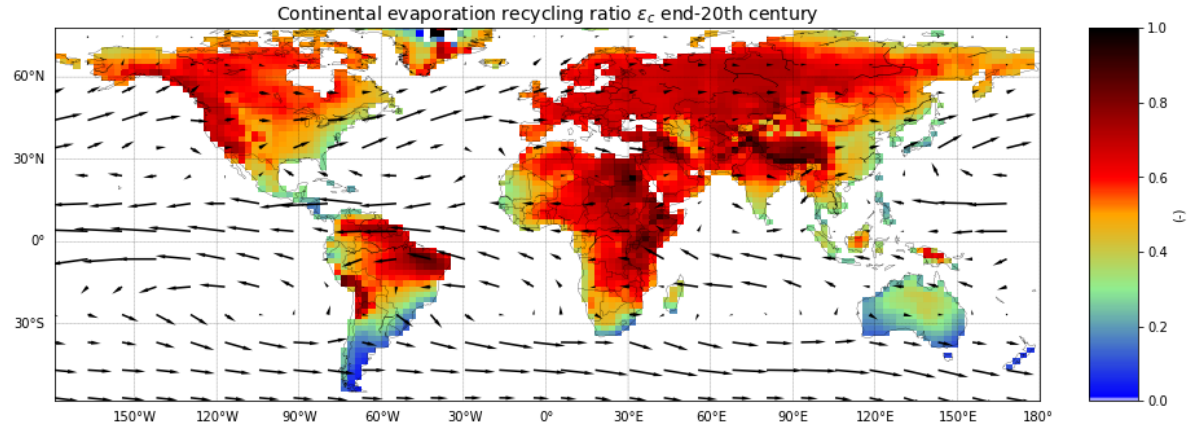

(a)

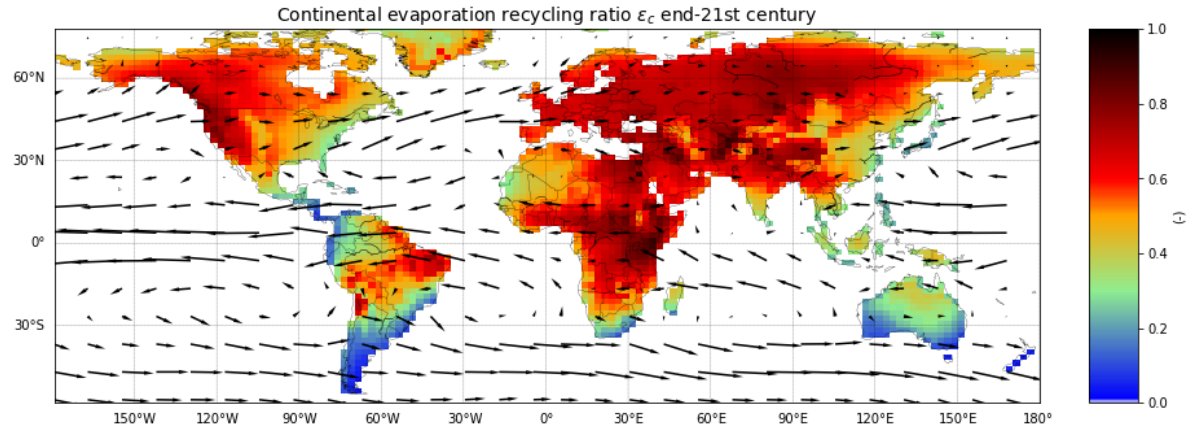

(b)

Figure 4.2: Continental evaporation recycling ratio for end-20th century (a) and end-21st century (b), defined as the ratio between the evaporation in a specific grid cell that will return as precipitation on land and the total evaporation in that grid cell. Red colors indicate that a relatively large amount of the evaporation will precipitate on land and blue colors indicate that a relatively small amount of evaporation will precipitate on land, thus in blue areas most evaporation will precipitate on the oceans. Arrows represent the direction and magnitude of the moisture fluxes.

Figure 4.2b displays the map of the continental evaporation recycling ratio ϵ_c in the end-21st century. Generally the same regions count as source regions for the same sink regions. Yet, shifts are present in the region outlines and the how large the ratios are. In order to see these changes in more detail, Section 4.3 shows the changes between the time periods for the recycled moisture per continent. Appendix C contains plots for the continental precipitation and evaporation recycling ratios worldwide, including the oceans (Figure C.7 and Figure C.8). Corresponding to these worldwide moisture recycling plots, the eastward and northward fluxes are included in Appendix C too, in Figure C.9 and Figure C.10.

4.3. Processes per continent

Each RCP consists of certain assumptions of greenhouse gas concentrations, air pollutant emissions and land use (IPCC, 2014a). Table 4.1 shows the total amount of transitioned land according to the RCP8.5 scenario per year between 2000 and 2100. Proportionally to their total surface area, the continents South America and Africa seem to be most affected by land use transitions according to RCP8.5.

	Total land change per year [10^5 km^2]	Total surface area [10^5 km^2]	Ratio per year
World	50.41	135,725,039	3.71e-7
North America	4.49	21,611,637	2.08e-7
South America	8.81	18,315,721	4.81e-7
Africa	15.90	33,237,930	4,78e-7
Eurasia	19.35	54,073,043	3.58e-7
Oceania	1.82	10,091,622	1.80e-7

Table 4.1: Total yearly land transitions between 2000 and 2100 per continent for RCP8.5 (Hurtt et al., 2011). The Table includes the total surface area of the continents (from GFDL data) and the ratio between the transitioned land per year and the total surface area.

Table 4.2 shows the precipitation and evaporation rates on land for both scenarios for each continent and globally. Antarctica is not taken into account. South America is the only continent that shows a decrease in precipitation rate, all other continents show an increase. However, the decrease in precipitation rate in South America is large enough to provoke a globally averaged decrease in precipitation rate as well. The evaporation rate however increases globally. South America shows a large decrease in evaporation rate as well, as does Oceania. All other continents however show an increase in evaporation rate.

	P (end-20th century)	P (end-21st century)	E (end-20th century)	E (end-21st century)
World	2.51	2.48	1.65	1.67
North America	2.20	2.46	1.30	1.65
South America	4.43	3.32	2.82	2.41
Africa	2.27	2.46	1.71	1.75
Europe	2.39	2.41	1.57	1.62
Asia	1.83	1.91	1.27	1.33
Oceania	3.12	3.31	1.89	1.68

Table 4.2: Precipitation (P) and evaporation (E) rates for land regions per continent, averaged over land grid cells. Both rates are shown for the end-20th century scenario and the end-21st century scenario. All rates are in mm d^{-1}.

In Table 4.3 the continental precipitation ρ_c and evaporation ϵ_c recycling ratios are displayed worldwide and for six continents specifically. Lower ρ_c indicates a lower percentage of land precipitation originating as evaporation from land and a higher percentage from the ocean. Lower ϵ_c indicates that a smaller fraction of the evaporated land moisture is going to land again and more going to the ocean. Three continents show that a larger fraction of precipitation is coming from land in the end-21st century scenario: North America, Europe and Asia. The other three continents - South America, Africa and Oceania - show the opposite, where a smaller fraction of precipitation in the end-21st century will come from land and thus a larger fraction of precipitation will come from oceans. Interestingly, Africa and South America are the two continents with the largest fraction of transitioned land per year (see Table 4.1). Land transitions can lead to less moisture available on land for evaporation, by for example deforestation. This could be a reason why Africa and South America get a smaller fraction of their precipitation rates from land. The two different patterns worldwide lead to a small decrease in fraction of global precipitation coming from land as evaporation. There is also a small decrease in fraction of evaporation going towards land globally. North America, Europe, Asia and Africa show an increase in fraction of evaporation going towards land. South America and Oceania show a decrease in fraction of evaporation going towards land.

	ρ_c (end-20th century)	ρ_c (end-21st century)	ϵ_c (end-20th century)	ϵ_c (end-21st century)
World	0.371	0.365	0.520	0.517
North America	0.28	0.34	0.49	0.51
South America	0.38	0.34	0.50	0.39
Africa	0.48	0.43	0.60	0.62
Europe	0.27	0.31	0.63	0.65
Asia	0.41	0.42	0.55	0.57
Oceania	0.20	0.16	0.32	0.30

Table 4.3: Continental precipitation (ρ_c) and evaporation (ϵ_c) recycling ratios for land regions worldwide and per continent. Ratios are given for the end-20th century scenario and the end-21st century scenario in values ranging from 0 to 1.

North America

Table 4.4 shows that North America will have an increase in precipitation, evaporation and recycled precipitation and evaporation rates. On top of that, the amount of recycled precipitation and evaporation increase more than proportionally to how much the precipitation and evaporation increase, so both ρ_c and ϵ_c increase as well. This indicates an increase in moisture recycling. In the future scenario there will be more precipitation coming from land and more evaporation going towards land. Increasing precipitation rates combined with increasing ρ_c means that the addition in precipitation originates from land, supported by the increased recycled precipitation. Increasing evaporation rates combined with increasing ϵ_c shows that the addition in evaporation will return on land, supported by the increase in recycled evaporation. Figure 4.3 shows the recycled precipitation (4.3a and 4.3b) and evaporation (4.3c and 4.3d). In the end-21st century scenario more of the precipitation near the East coast will be recycled from land (Figure 4.3b). This is supported by the fact that North America will experience an increase in evaporation and the Eastern direction of the wind in this continents, which makes evaporation in the West be a source for precipitation in the East. In line with this, the end-21st century scenario shows a higher recycled evaporation rate near the West coast (Figure 4.3d).

	P [mm d^{-1}]	$P_{recycled}$ [mm d^{-1}]	ρ_c	E [mm d^{-1}]	$E_{recycled}$ [mm d^{-1}]	ϵ_c
end-20th century	2.29	0.62	0.281	1.30	0.63	0.486
end-21st century	2.46	0.83	0.338	1.65	0.83	0.506

Table 4.4: Precipitation rate (P), recycled precipitation, continental precipitation recycling ratio (ρ_c), evaporation rate (E), recycled evaporation and continental evaporation recycling ratio (ϵ_c) of land regions in North America, for both end-20th century and end-21st century.

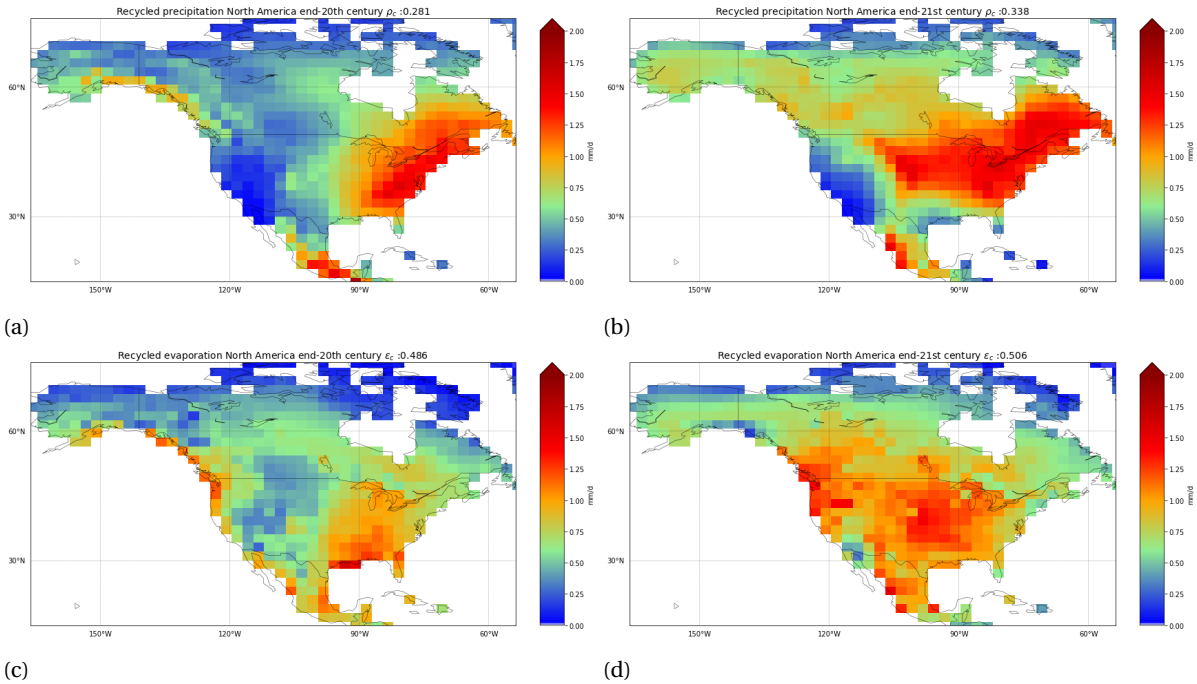

Figure 4.3: Recycling rates in North America: recycled precipitation rate end-20th century (a), recycled precipitation rate end-21st century (b), recycled evaporation rate end-20th century (c) and recycled evaporation rate end-21st century (d). Blue colors correspond to lower rates and red colors to higher rates. All rates are in mm d^{-1}.

South America

The largest differences between the end-20th century and end-21st century scenarios can be seen in South America. In contrast to other continents, Table 4.5 shows that South America will have less precipitation, evaporation and recycling rates. On top of that, there is a decrease in ρ_c and ϵ_c, indicating that of the lower precipitation rate proportionally even less came from land and of the lower evaporation rate proportionally even less will precipitate on land. The lower ρ_c is supported by the decrease in both precipitation and evaporation rates, because less evaporation from the continent causes less precipitation on this continent, lowering the moisture recycling rate ρ_c. However, while decreasing ρ_c, precipitation and evaporation rates are interlinked, an explanation for the lower ϵ_c is more difficult to find. Lower ϵ_c means an increase of land evaporation going towards the ocean. Yet, decreasing evaporation rates already indicate less moisture available to precipitate on the continent and it is not clear why of that smaller amount of evaporation, also less will return on land. Figure 4.4 shows the recycling rates for South America. In South America the dominant direction of the moisture fluxes is Westward. Comparing Figure 4.4a to 4.4b makes clear that the West coast will get less precipitation recycled from continental moisture. Figure 4.4c and Figure 4.4d show that this is mostly because the amount of recycled evaporation on the East will decrease significantly, mostly around the Amazon forest. South America is one of the two continents with the highest transitions in land use rates (see Table 4.1), this could be the cause of this decrease in evaporation from this region. For example the change of land use from forests to meadows lowers the moisture available for evaporation.

	P [mm d^{-1}]	$P_{recycled}$ [mm d^{-1}]	ρ_c	E [mm d^{-1}]	$E_{recycled}$ [mm d^{-1}]	ϵ_c
end-20th century	4.43	1.70	0.384	2.82	1.42	0.503
end-21st century	3.32	1.14	0.344	2.41	0.95	0.393

Table 4.5: Precipitation rate (P), recycled precipitation, continental precipitation recycling ratio (ρ_c), evaporation rate (E), recycled evaporation and continental evaporation recycling ratio (ϵ_c) of land regions in South America, for both end-20th century and end-21st century.

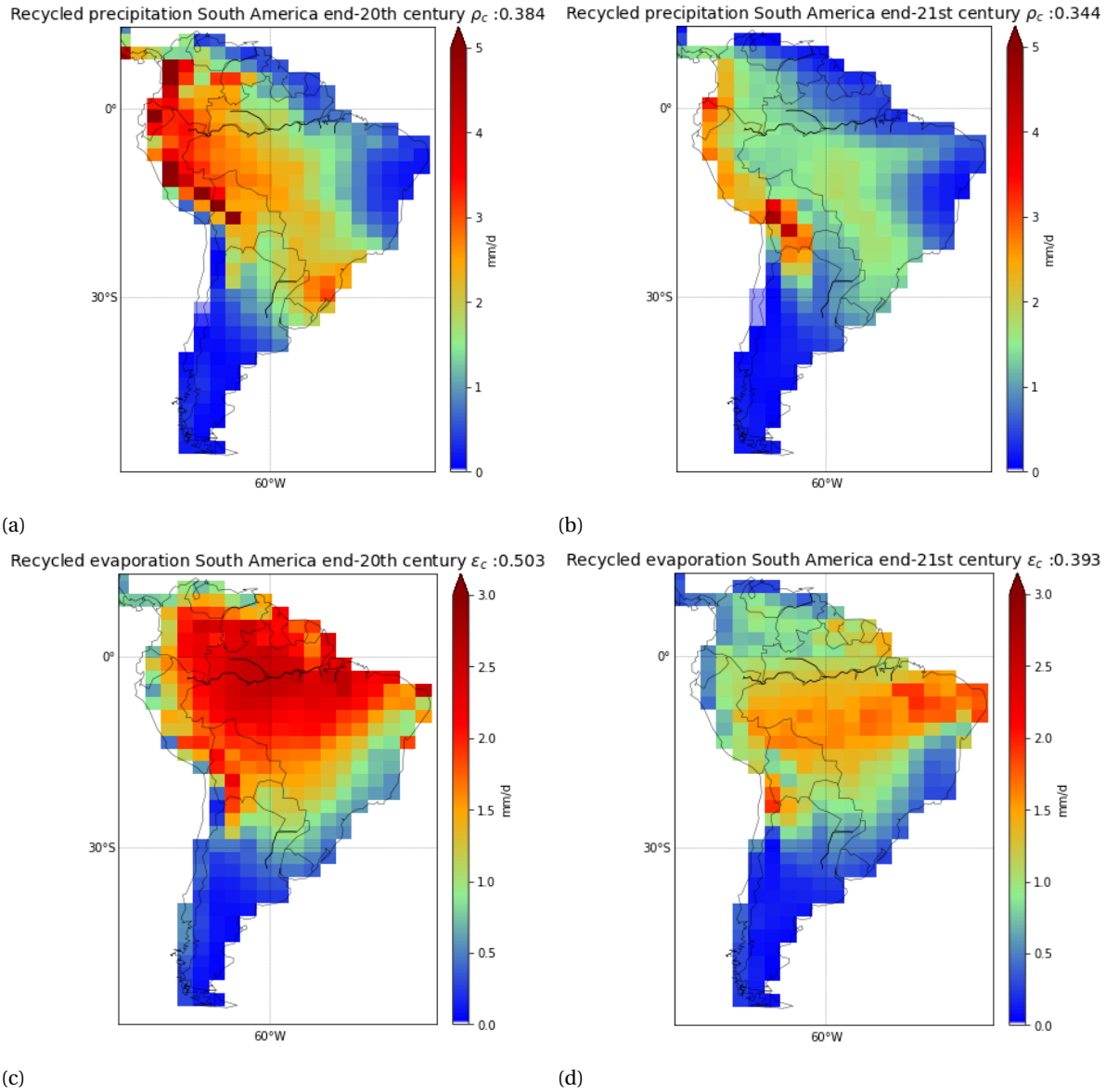

Figure 4.4: Recycling rates in South America: recycled precipitation rate end-20th century (a), recycled precipitation rate end-21st century (b), recycled evaporation rate end-20th century (c) and recycled evaporation rate end-21st century (d). Blue colors correspond to lower rates and red colors to higher rates. All rates are in mm d^{-1}.

Africa

Table 4.6 shows that Africa will experience an increase in precipitation, evaporation and the recycled evaporation. However, in the end-21st century scenario Africa will have less ρ_c compared to the past scenario. This means that in this continent a higher percentage of the precipitation will originate from the ocean. Combined with the fact that Africa will experience higher precipitation rates and the decrease in recycled precipitation, this means that this addition in precipitation will all originate from the oceans. On the other hand, ϵ_c is increasing, meaning that of the higher evaporation rates, proportionally more will go towards land regions. Looking at the recycled rates in Figure 4.5, the decrease in recycled precipitation can be seen by comparing central Africa in Figure 4.5b to Figure 4.5a and the increase in recycled evaporation by comparing Figure 4.5d to Figure 4.5c.

	P [mm d^{-1}]	P$_{recycled}$ [mm d^{-1}]	ρ_c	E [mm d^{-1}]	E$_{recycled}$ [mm d^{-1}]	ϵ_c
end-20th century	2.27	1.10	0.483	1.71	1.02	0.595
end-21st century	2.46	1.07	0.434	1.75	1.08	0.617

Table 4.6: Precipitation rate (P), recycled precipitation, continental precipitation recycling ratio (ρ_c), evaporation rate (E), recycled evaporation and continental evaporation recycling ratio (ϵ_c) of land regions in Africa, for both end-20th century and end-21st century.

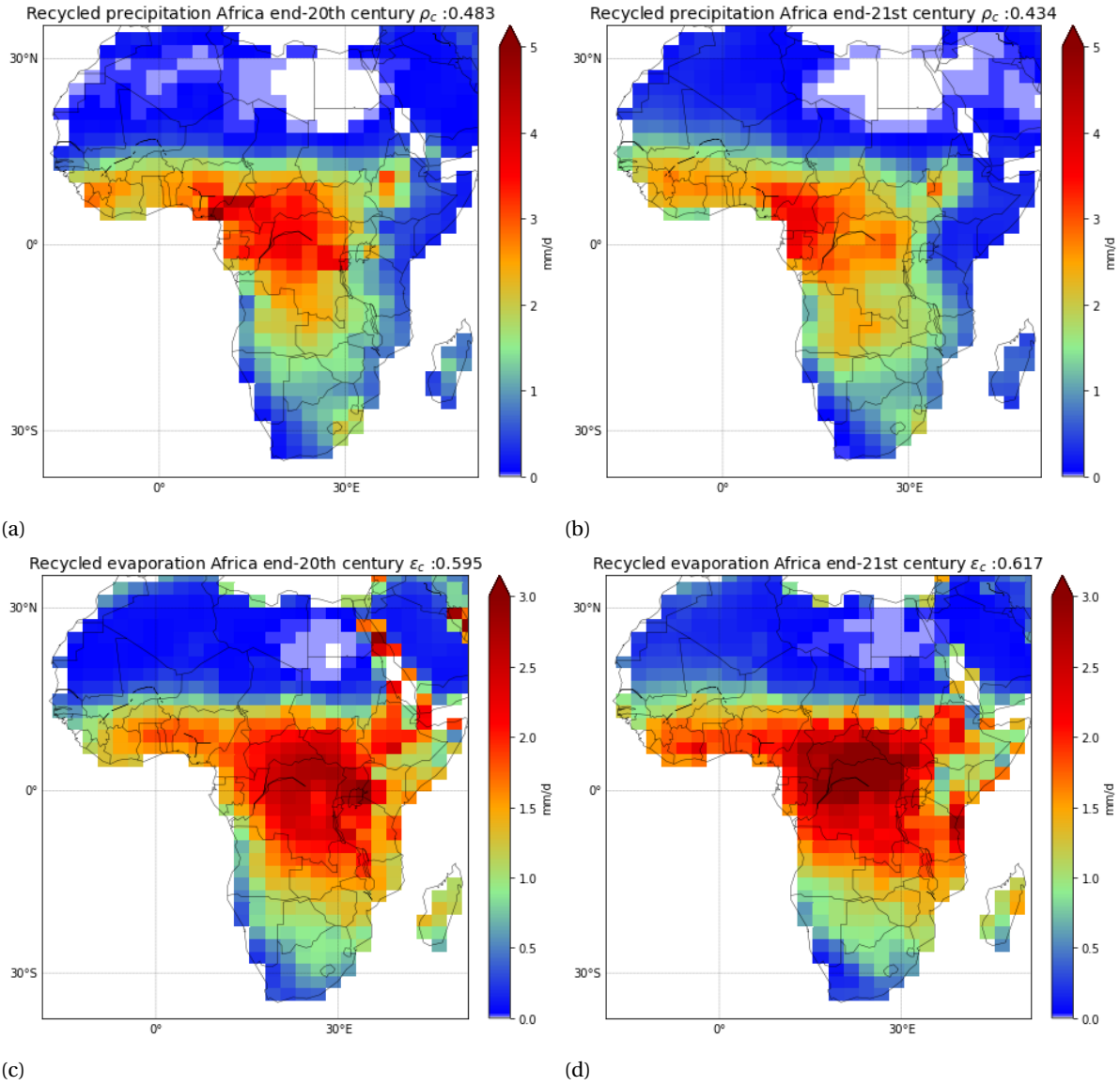

Figure 4.5: Recycling rates in Africa: recycled precipitation rate end-20th century (a), recycled precipitation rate end-21st century (b), recycled evaporation rate end-20th century (c) and recycled evaporation rate end-21st century (d). Blue colors correspond to lower rates and red colors to higher rates. All rates are in mm d^{-1}.

Europe

From Table 4.7 can be seen that Europe shows an increase in precipitation, evaporation, recycled rates and both ρ_c and ϵ_c in the future scenario. The continent receives moisture from the West and the moisture evaporated from the continent moves towards the East, where Asia is located. While more ϵ_c can be explained by the increasing evaporation rates locally and geographical location of the continent moving moisture towards Asia, an increase in ρ_c is harder to understand because of the geographical location. More precipitation originating from land could be from the continent itself, recycling at a relatively short length. However, comparing Figure 4.6a to Figure 4.6b shows that the coastal regions also seem to receive more precipitation from land origin. This might be explained by an increase in moisture fluxes coming over the ocean from North America, this is however not yet looked into. Two different patterns can be seen by looking at Figure 4.6c and Figure 4.6d, displaying the the recycled evaporation, the amount of evaporation that will precipitate on land again, there are . In the South of Europe, near the Mediterranean sea, the evaporation rate that will recycle decreases, however, in Central Europe and Northern Europe, this rate seems to increase.

	P [mm d^{-1}]	P$_{recycled}$ [mm d^{-1}]	ρ_c	E [mm d^{-1}]	E$_{recycled}$ [mm d^{-1}]	ϵ_c
end-20th century	2.39	0.64	0.267	1.57	0.99	0.631
end-21st century	2.41	0.74	0.306	1.62	1.05	0.650

Table 4.7: Precipitation rate (P), recycled precipitation, continental precipitation recycling ratio (ρ_c), evaporation rate (E), recycled evaporation and continental evaporation recycling ratio (ϵ_c) of land regions in Europe, for both end-20th century and end-21st century.

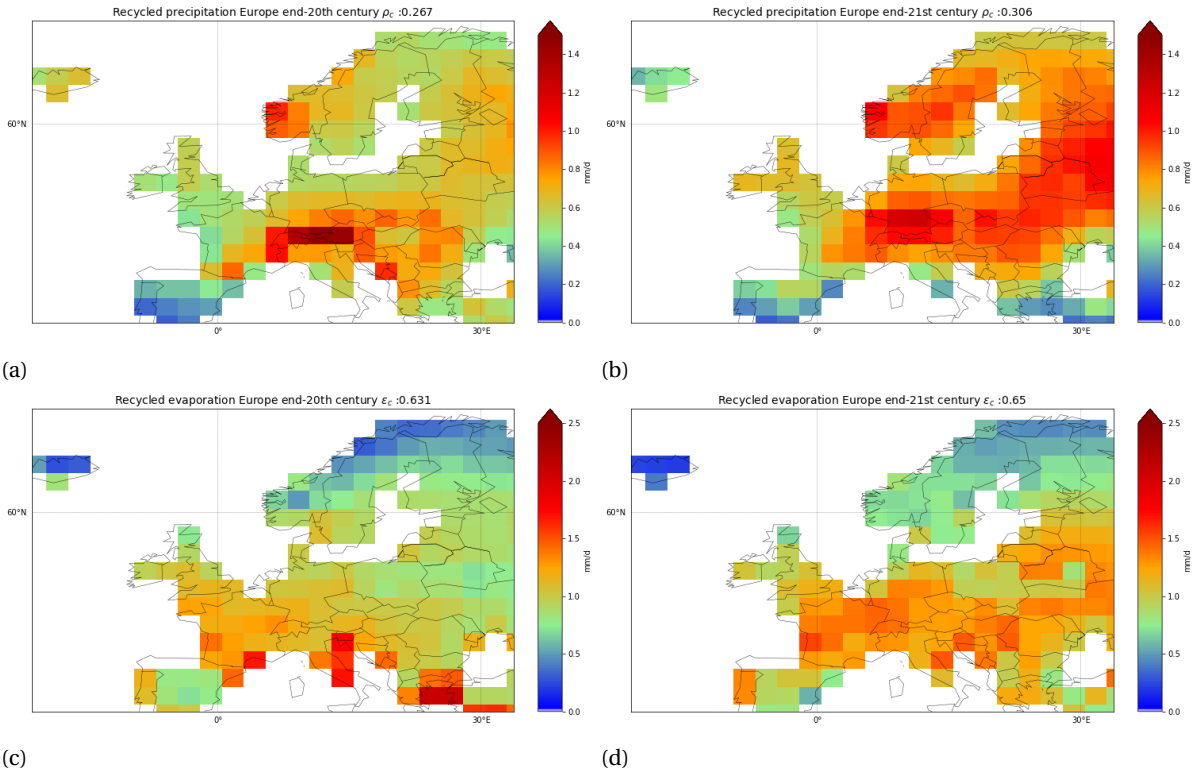

Figure 4.6: Recycling rates in Europe: recycled precipitation rate end-20th century (a), recycled precipitation rate end-21st century (b), recycled evaporation rate end-20th century (c) and recycled evaporation rate end-21st century (d). Blue colors correspond to lower rates and red colors to higher rates. All rates are in mm d^{-1}.

Asia

Table 4.8 shows an increase in precipitation, evaporation, recycled rates and both ρ_c and ϵ_c in Asia. Possibly partly because of the increase in recycled evaporation in Europe, Asia will experience an increase in recycled precipitation. A higher percentage of evaporation from Europe will return as land precipitation and a higher percentage of precipitation in Asia originates from land evaporation. However, Asia will also experience an increase in ϵ_c. Because of the scale of Asia, most of the evaporation can also return on the continent itself as precipitation. Figure 4.7 shows the recycled precipitation and evaporation rates in Asia. Comparing Figure 4.7b to Figure 4.7a shows the increase in recycled precipitation in Asia in the Central Northern area. However, the region around Burma, Thailand and Laos shows a decrease in recycled precipitation. Figure 4.7d compared to Figure 4.7c shows that Northern Asia will have higher recycled evaporation rates, this could be because of increased recycling within the continent itself, supported by the higher ϵ_c.

	P [mm d^{-1}]	$P_{recycled}$ [mm d^{-1}]	ρ_c	E [mm d^{-1}]	$E_{recycled}$ [mm d^{-1}]	ϵ_c
end-20th century	1.83	0.75	0.408	1.27	0.70	0.548
end-21st century	1.91	0.81	0.423	1.33	0.76	0.570

Table 4.8: Precipitation rate (P), recycled precipitation, continental precipitation recycling ratio (ρ_c), evaporation rate (E), recycled evaporation and continental evaporation recycling ratio (ϵ_c) of land regions in Asia, for both end-20th century and end-21st century.

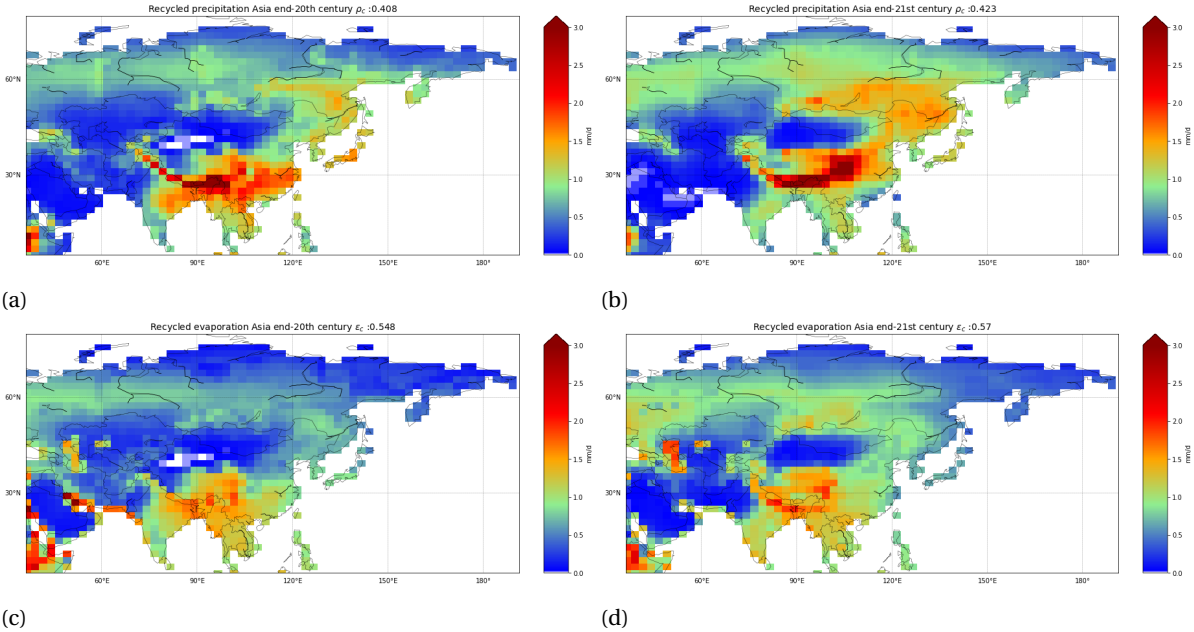

(a) (b)

(c) (d)

Figure 4.7: Recycling rates in Asia: recycled precipitation rate end-20th century (a), recycled precipitation rate end-21st century (b), recycled evaporation rate end-20th century (c) and recycled evaporation rate end-21st century (d). Blue colors correspond to lower rates and red colors to higher rates. All rates are in mm d^{-1}.

Oceania

Oceania shows contrasting precipitation and evaporation rates in the future compared to the past scenario. Table 4.9 shows that while precipitation increases, evaporation, recycled rates and both ρ_c and ϵ_c will decrease. This can be seen in Figure 3.4 and Figure 3.2 in Section 3.1, that show the percentage change in evaporation and precipitation. The largest changes in precipitation and evaporation are in the region of Indonesia, where precipitation increases and evaporation decreases. Looking at the maps in Figure 4.8a, Figure 4.8b, Figure 4.8c and Figure 4.8d, it is also clear that most changes appear in the region of the islands, in the North. However, these Figures show that Indonesia will get lower recycled precipitation and recycled evaporation rates. Relatively less precipitation originates from land - indicated by a decrease in ρ_c. Moreover, of the lower evaporation rates, a lower percentage will return as precipitation on land, indicated by lower ϵ_c.

	P [mm d^{-1}]	$P_{recycled}$ [mm d^{-1}]	ρ_c	E [mm d^{-1}]	$E_{recycled}$ [mm d^{-1}]	ϵ_c
end-20th century	3.12	0.61	0.195	1.89	0.60	0.319
end-21st century	3.31	0.54	0.163	1.68	0.51	0.303

Table 4.9: Precipitation rate (P), recycled precipitation, continental precipitation recycling ratio (ρ_c), evaporation rate (E), recycled evaporation and continental evaporation recycling ratio (ϵ_c) of land regions in Oceania, for both end-20th century and end-21st century.

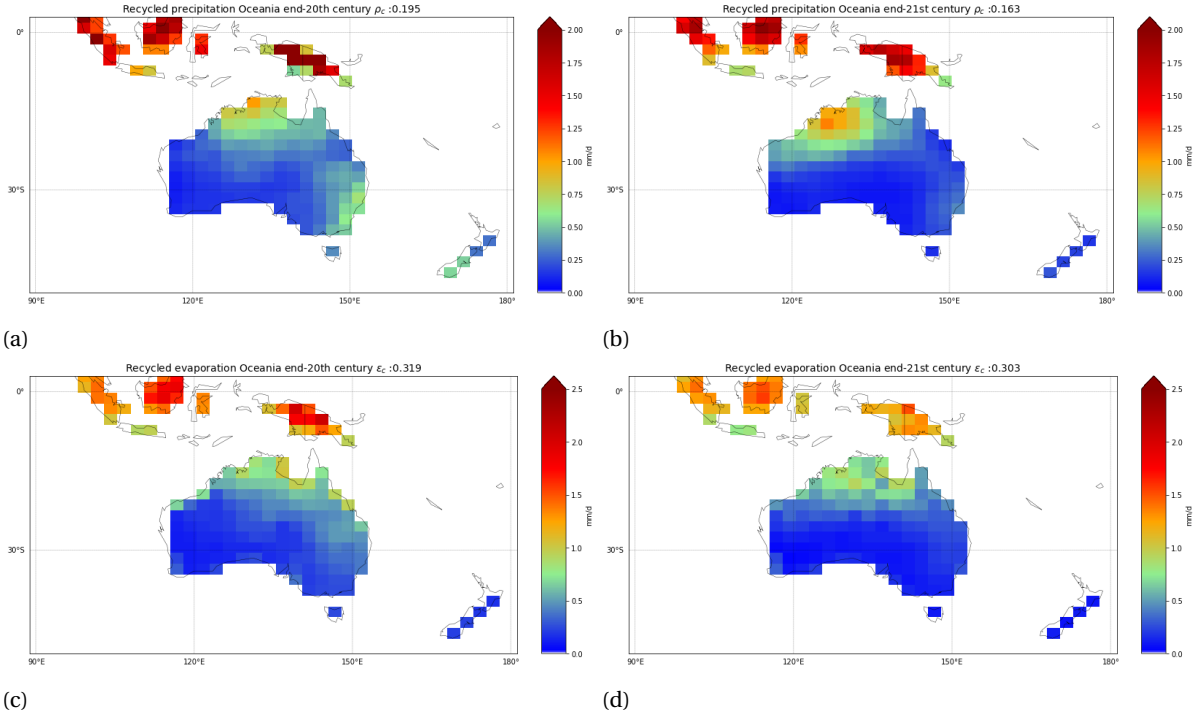

Figure 4.8: Recycling rates in Oceania: recycled precipitation rate end-20th century (a), recycled precipitation rate end-21st century (b), recycled evaporation rate end-20th century (c) and recycled evaporation rate end-21st century (d). Blue colors correspond to lower rates and red colors to higher rates. All rates are in mm d^{-1}.

Three different groups in behaviour between the continents can be distinguished. First, there is the group of North America, Europe and Asia, all three continents of the Northern Hemisphere. This group of continents all show increases in precipitation and evaporation rates, as well as recycled evaporation towards other land regions and recycled precipitation from other land regions. These recycled moisture rates increase in such a manner, that even proportionally to the increased precipitation and evaporation rates, the continental precipitation and evaporation rates increase as well. In these three continents there is an increase in the water cycle and an increase in moisture recycling. The second group consists of only South America. In this continent the opposite effect takes place from what happens in the first group. South America experiences lower precipitation and evaporation rates, as well as lower recycled precipitation and evaporation rates. The recycling is such, that proportionally to the lower precipitation and evaporation, the recycled rates are even lower in the future. This leads to lower continental precipitation and evaporation recycling ratios for the second group. The third group consists of the last two remaining continents, Africa and Oceania. These two do not show exactly the same changes, however, they do have some resemblances. Both continents show increase in precipitation rate, but slightly higher African and lower Oceanian recycled precipitation, leading to much more of precipitation coming from evaporation from oceans (lower ρ_c). Africa shows an increase in evaporation rate, increase in recycled evaporation on land and proportionally an increase in continental evaporation recycling ratio, thus proportionally more of the evaporation will return as precipitation on land. This is the same effect as the first group. Oceania however shows a decrease in evaporation, a decrease in recycled evaporation towards land and proportionally to the decreased evaporation this is even less than it was in the end-20th century.

5

Regional impact analysis

Because of the fact that seasonality could not be studied in larger regions and moisture recycling patterns are clearer when looking at smaller regions, in this Chapter the studied regions will be even more detailed, defined as the case study areas. The two case study areas that are chosen are in Northern South America (Amazonia) and in Western Africa. The specifics of the case study areas are declared in Table 2.3 in Chapter 2.

5.1. Definition case studies

The case study area located in the Amazon forest (Amazonia), stretches from the Amazon river mouth in the East to the Peruvian border in the West and the Bolivian border in the South to the Northern Guyanian border in the North (see Figure 5.1a). This area contains three countries completely - Guyana, Suriname and French Guiana - and four countries partly - Colombia, Venezuela, Peru and Brazil. Even though Brazil is only covered partly, most of the surface area of this case study is covered by this country. Amazonia is a region with relatively high precipitation and evaporation rates compared to other areas worldwide (see Section 2.4). Both rates however decrease in the future scenario (see Figure 3.2 and Figure 3.4).

The case study area in Western Africa is specifically located South of the Sahara desert and West of the Central African Republic. The area stretches from the Eastern border of Cameroon in the East to the Atlantic Ocean in the West and the Southern border of Nigeria in the South to the Northern border of Senegal in the North (see Figure 5.1b). Western Africa includes twelve countries completely - Senegal, The Gambia, Guinea-Bissau, Guinea, Sierra Leone, Liberia, Côte d'Ivoire, Burkina Faso, Ghana, Togo, Benin and Nigeria - and five countries partly - Mali, Mauritania, Niger, Chad and Cameroon. Looking at the plots of the change in precipitation rates in the Western Africa case study region reveals more precipitation in the future scenario (Figure 3.2). However, the evaporation rate shows differences within the case study area, with more evaporation towards the North and less evaporation towards the South (Figure 3.4).

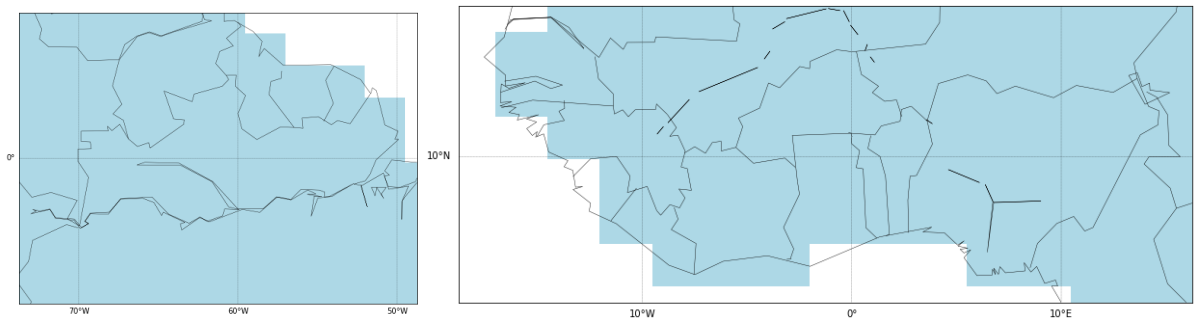

(a) (b)

Figure 5.1: Case study areas Amazonia (a) and Western Africa (b) as used in WAM-2layers. Regions are shown as land-sea masks from GFDL data, with blue grid cells as land and white grid cells as sea. Coast lines, country borders and water bodies are drawn in black.

5.2. Case study area 1: Amazonia

Background information
In Figure 5.2 the land cover map of Amazonia is shown. The most striking about this map is the amount of dark green area, actually representing 40% of the global tropical forest area (Weng et al., 2018). This tropical forest is the extensive rain forest of the Amazon, with a total surface area of about 5.3 million km^2. The Amazon catchment covers the rain forest with an area of about 7 million km^2, which makes it the largest river basin in the world (Weng et al., 2018). The Amazon catchment is shown in the elevation map of Amazonia in Figure 5.3 with the blue outline. There are some regions with relatively higher altitudes within the case study area. Most notable however is the large green area with low altitude (around 0.1 m), where the branches of the Amazon river can be seen that flow through the Amazon forest. The population density in the case study area is low (see Figure 5.29). The choice of this case study area however is not based on population density, but on the importance of the Amazon rain forest itself. The rain forest of the Amazon transpires moisture into the atmosphere abundantly, which makes the forests an important component of the hydrological cycle, both regionally and globally. When regulating the water cycle in the region, the Amazon forest is a key component of the regional but also global climate system (Anderson-Teixeira et al., 2012). Since the last century, deforestation and expanding agricultural activities have been changing the land cover and the ecosystem's provision of moisture to the atmosphere (Weng et al., 2018). The deforestation and land cover changes in the Amazon are also indicated by the large area of land in South America that will transition each year (see Table 4.1).

Figure 5.2: Land cover map for case study area 1: Amazonia. The map shows different land cover types, indicated with the colors on the left. The case study area is demarcated with the black outline (UCL, 2009; GADM, 2018).

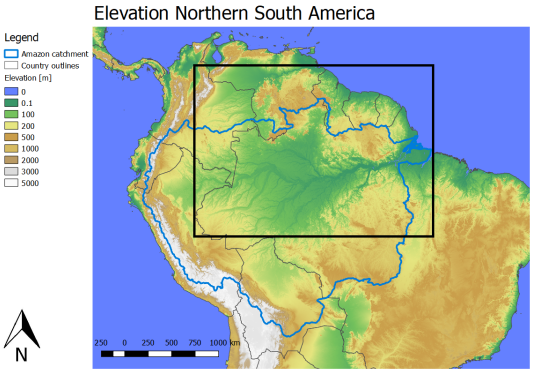

Figure 5.3: Elevation map for case study area 1: Amazonia. The map shows the elevation of the surface and the outline of the Amazon catchment, indicated with the colors on the left. The case study area is demarcated with the black outline (FAO, 2009; USGS, 2010; GADM, 2018).

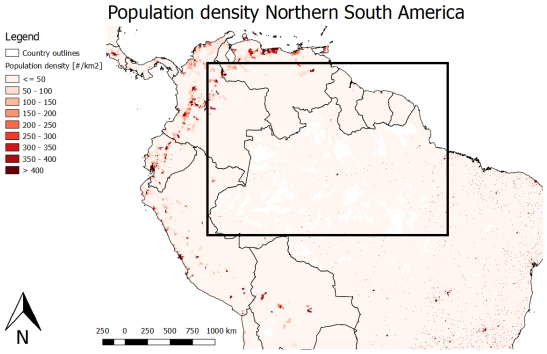

Figure 5.4: Population density map for case study area 1: Amazonia. The map shows the population density in inhabitants per km^2, scaled with the colors on the left. The case study area is demarcated with the black outline (SEDAC, 2015; GADM, 2018).

Seasonality

Figure 5.5 shows the mean daily precipitation in Amazonia as a plot over the year for the end-20th century scenario and the end-21st century scenario. Amazonia experiences a mean precipitation rate of 5.58 mm d^{-1} in the past scenario and 3.52 mm d^{-1} in the future scenario. While the precipitation rates are relatively constant in the past scenario, in the future scenario Amazonia will experience much more effects of seasonality. Even though the mean precipitation rate will decrease, there will be a peak in precipitation in April and May and a long dry period with almost no precipitation, with rates close to 0 mm d^{-1} in August to November.

Figure 5.6 presents the mean daily evaporation in Amazonia as a plot over the year for the end-20th century scenario and the end-21st century scenario. The mean evaporation rate in the past scenario is 3.69 mm d^{-1}, in the future scenario the rate decreases to 2.65 mm d^{-1}. Again, from the graphs can be seen that there is going to be more seasonal variability within the year in the case study area of Amazonia. The dry period in the future scenario, where the precipitation rates are low, has an effect on the evaporation rates in the same months. The effect might be the other way around, that the decrease in evaporation causes a decrease in precipitation. The lower evaporation rate is an indication of a decrease in moisture availability. Given the fact that the case study area is currently covered by mostly broad leaved forest, which provides transpiration as a contribution to the total evaporation, this might mean that this the land cover type broad leaved forest has decreased significantly in the end-21st century. This could be true since land transitions with RCP8.5 in South America are proportionally to surface area the highest of all continents, as shown in Table 4.1. Whether the precipitation in the case study area is dependent on the evaporation in the case study area will be determined with the moisture tracking model, which will be explained in Section 5.2.1.

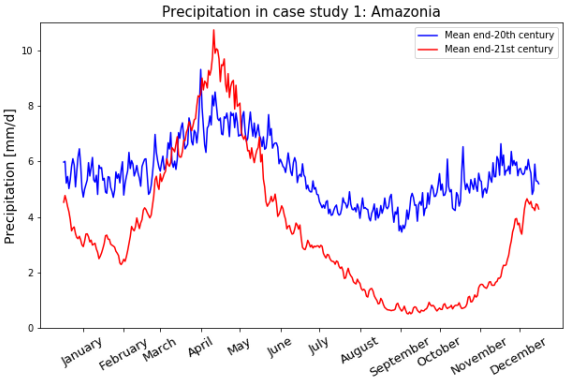

Figure 5.5: Mean land precipitation in the case study area of Amazonia. The blue line represents the end-20th century scenario and the red line represents the end-21st century scenario. The graph displays the rate in mm d^{-1}.

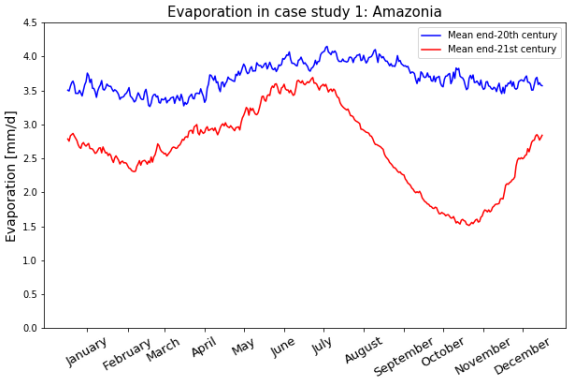

Figure 5.6: Mean land evaporation in the case study area of Amazonia. The blue line represents the end-20th century scenario and the red line represents the end-21st century scenario. The graph displays the rate in mm d^{-1}.

The distribution of the precipitation and evaporation data in Amazonia is determined with the use of box

plots. For the precipitation rates, Figure 5.7a shows the box plot of the past scenario and Figure 5.7b shows the box plot of the future scenario, both corresponding to Figure 5.5. Even though the higher precipitation rates that are predicted in April are relatively uncertain, the lower precipitation rates in the dry period from August to November seems to be fairly certain, because of the lower spread.

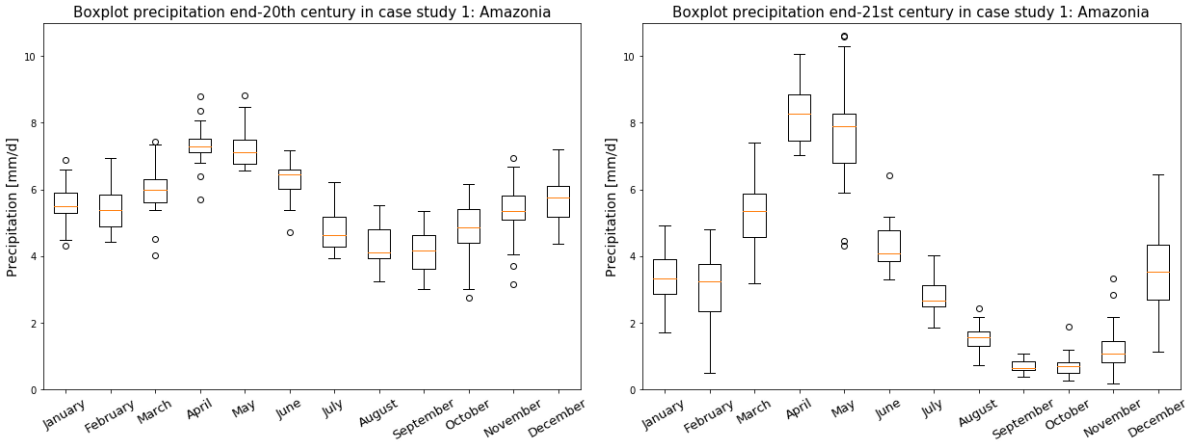

(a) (b)

Figure 5.7: Box plots of land precipitation in the case study area of Amazonia for the end-20th century scenario (a) and end-21st century scenario (b). The box plots represent the statistical spread for each month within the year by using quartiles to show the distribution of the used data. The median precipitation rate per month is shown as the orange line (second quartile), the box represents the data from the first quartile until the third quartile and the two whiskers have maximum and minimum of 1.5 times the interquartile range (from Q1 to Q3). The dots are the outliers.

The distribution of the evaporation data is shown in the box plots in Figure 5.8a for the past scenario and Figure 5.8b for the future scenario, corresponding to Figure 5.6. In the future scenario in the months of May to July the spread is lower than during the sharp decrease of evaporation in the months of August to October. So, the months with the lowest evaporation rates seems to be relatively uncertain in comparison to the months with the highest evaporation rates in the future.

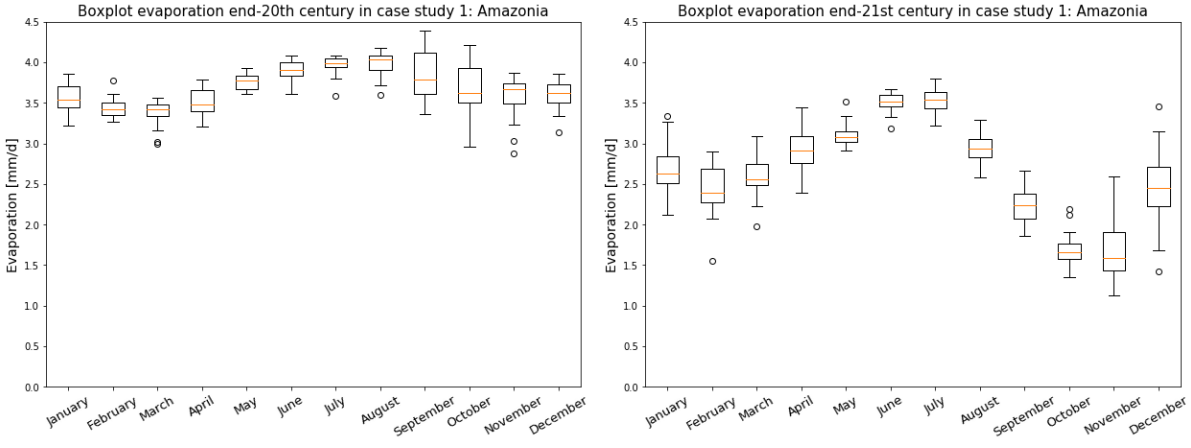

(a) (b)

Figure 5.8: Box plots of land evaporation in the case study area of Amazonia for the end-20th century scenario (a) and end-21st century scenario (b). The box plots represent the statistical spread for each month within the year by using quartiles to show the distribution of the used data. The median evaporation rate per month is shown as the orange line (second quartile), the box represents the data from the first quartile until the third quartile and the two whiskers have maximum and minimum of 1.5 times the interquartile range (from Q1 to Q3). The dots are the outliers.

5.2.1. Moisture tracking for full year

	Precipitation [mm d^{-1}]	Evaporation [mm d^{-1}]	Recycled moisture [mm d^{-1}]	ρ_A	ϵ_A
end-20th century	5.58	3.69	1.31	0.24	0.36
end-21st century	3.52	2.65	0.61	0.17	0.23

Table 5.1: Precipitation (P), evaporation (E) and recycled moisture rates (in mm d^{-1}) within the case study area of Amazonia. The Amazonian precipitation (ρ_A) and evaporation (ϵ_A) recycling ratios are the ratios between either the precipitation or the evaporation rate and the recycled moisture rate, thus within the case study area as well.

Table 5.1 shows that the together with the precipitation and evaporation rates, the amount of recycled moisture within the case study of Amazonia will decrease as well. On top of the fact that there will be less precipitation, a smaller fraction of that precipitation will originate from land in the end-21st century scenario. Spatially - in each grid cell over the study area - Figure 5.9 shows that the precipitation rates decrease and Figure 5.10 shows that the evaporation rates decrease. Figure 5.11 and Figure 5.12 show a decrease all over the case study area in recycled moisture from as well as towards the case study area. The Amazonian precipitation recycling ratio (Figure 5.13) and the Amazonian evaporation recycling ratio (Figure 5.14) show lower ratios in the end-21st century scenario. This means of the lower precipitation and evaporation rates, even less will come from the case study area or go towards the case study area. Interestingly, Figure 5.12a demonstrates that in the end-20th century scenario large amounts of moisture that precipitate in Amazonia originate from the ocean. In the end-21st century (Figure 5.12b) - where evaporation rates on the same ocean grid cells stay the same (see Figure 5.10b) - the amount of evaporation from these ocean grid cells that will be a source for Amazonian precipitation decreases significantly. Looking at the moisture flux directions in Figure 5.15 conclusions can be drawn that the direction is still Westward. The magnitude however seems to have increased slightly. It might be the case that the moisture that evaporates from the oceans on the East side of the Amazon forest travels over the Amazon forest in the future scenario instead of precipitating in this region. This could be explained by the fact that the Amazonian forest will provide less moisture to fill up the clouds and make them precipitate. Too little moisture coming from the surface will then lead to a longer duration before clouds precipitate and by that time the clouds have already moved Westward, over Amazonia. This idea can be supported by the plots of the Eastward moisture flux in Figure 5.16, where on the West side of the case study area there is a stronger Westward moisture flux in the end-21st century (Figure 5.16b) than in the end-20th century (Figure 5.16a). This can however be the effect of two different causes. First being the clouds moving Westward over the case study area as mentioned before, second being the effect of stronger Westward wind, which is supported by the data. The less strong Northward moisture fluxes (in Figure 5.17) on the other hand show a more Southward moving moisture flux at the West side of Amazonia. This means that there is an increase in moisture entering the case study area from the North. This Southward moisture flux however does not lead to increase in precipitation in the case study area, as can be seen by the recycled evaporation in Figure 5.12b.

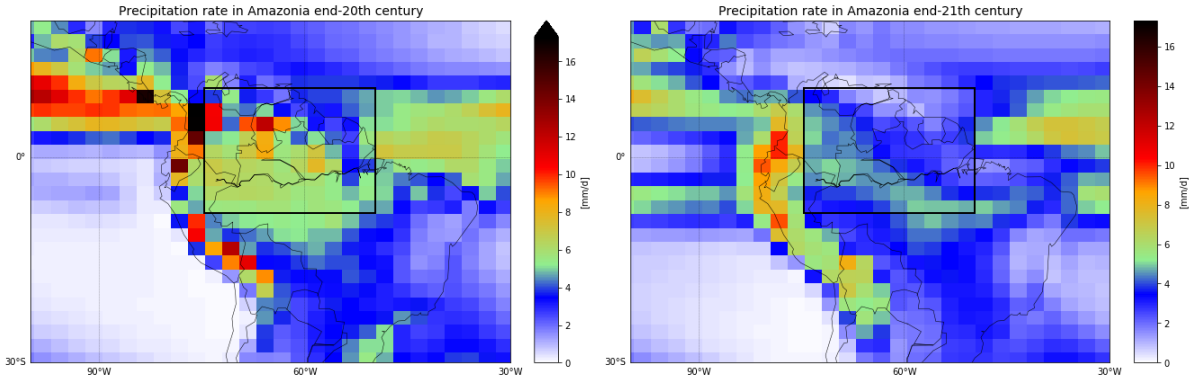

(a) (b)

Figure 5.9: The averaged daily precipitation rates in Amazonia for end-20th century (a) and end-21st century (b). The colors indicate the precipitation rate in mm d^{-1}, with red color indicating a higher rates and blue lower rates. The case study area is demarcated by the black rectangle.

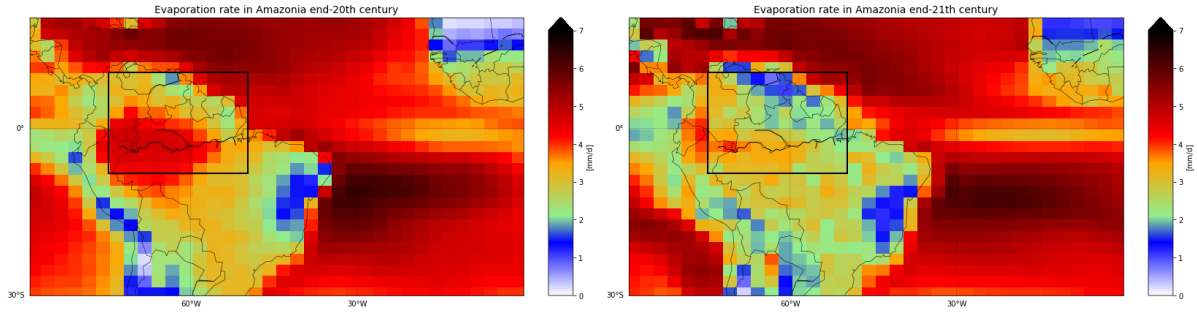

(a) (b)

Figure 5.10: The averaged daily evaporation rates in Amazonia for end-20th century (a) and end-21st century (b). The colors indicate the evaporation rate in mm d^{-1}, with red color indicating a higher rates and blue lower rates. The case study area is demarcated by the black rectangle.

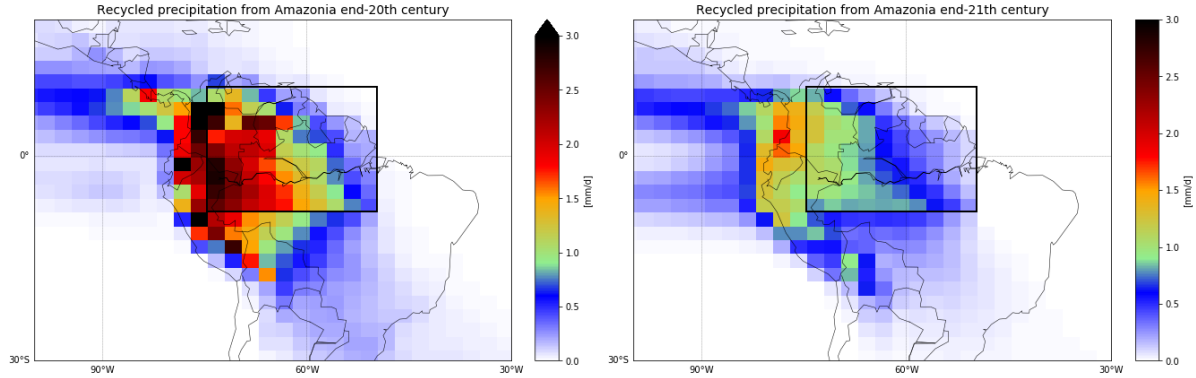

(a) (b)

Figure 5.11: The averaged daily rates that have recycled from Amazonian land for end-20th century (a) and end-21st century (b). The colors indicate the recycled precipitation rate in mm d^{-1}, with red color indicating a higher rates and blue lower rates. The case study area is demarcated by the black rectangle.

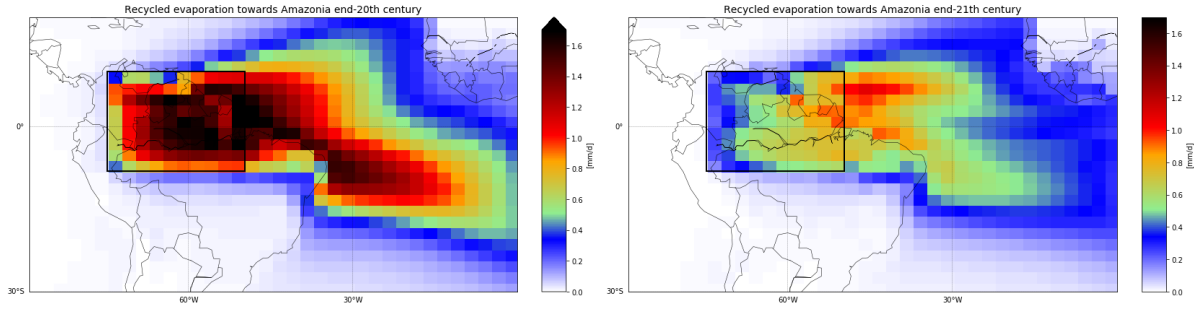

(a) (b)

Figure 5.12: The averaged daily rates of evaporation that will precipitate on Amazonian land for end-20th century (a) and end-21st century (b). The colors indicate the recyclable evaporation rate in mm d^{-1}, with red color indicating a higher rates and blue lower rates. The case study area is demarcated by the black rectangle.

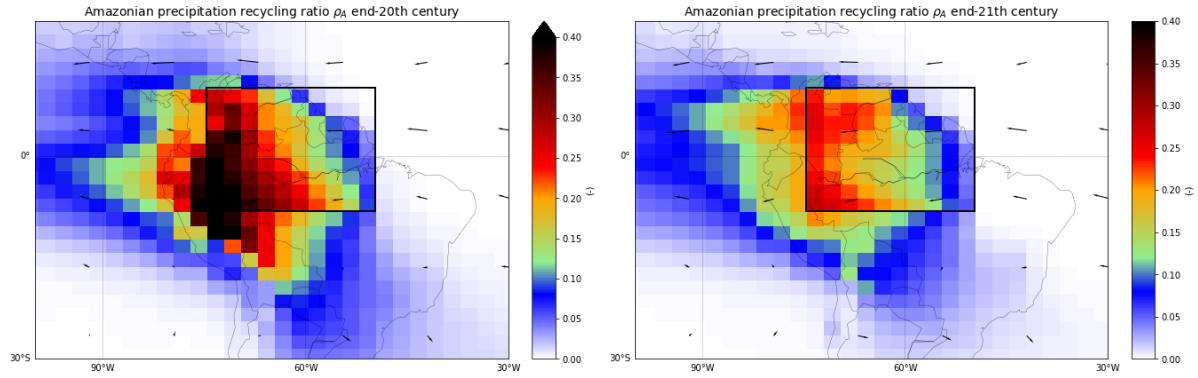

(a) (b)

Figure 5.13: The Amazonian precipitation recycling ratio for end-20th century (a) and end-21st century (b). The colors indicate the percentage of local precipitation in a specific grid cell that originates from the case study area (demarcated by the black rectangle), with red areas indicating a high percentage and blue low percentage. Arrows represent the direction and magnitude of the moisture fluxes.

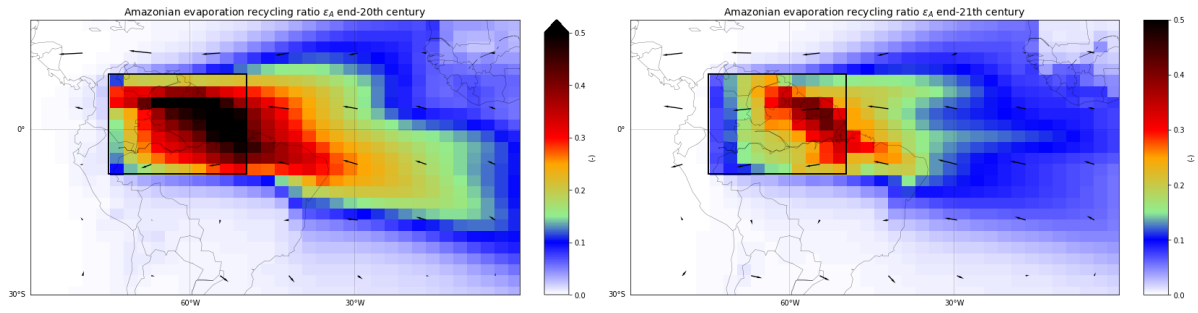

(a) (b)

Figure 5.14: The Amazonian evaporation recycling ratio for end-20th century (a) and end-21st century (b). The colors indicate the percentage of local evaporation in a specific grid cell that will return as precipitation in the case study area (demarcated by the black rectangle), with red areas indicating a high percentage and blue low percentage. Arrows represent the direction and magnitude of the moisture fluxes.

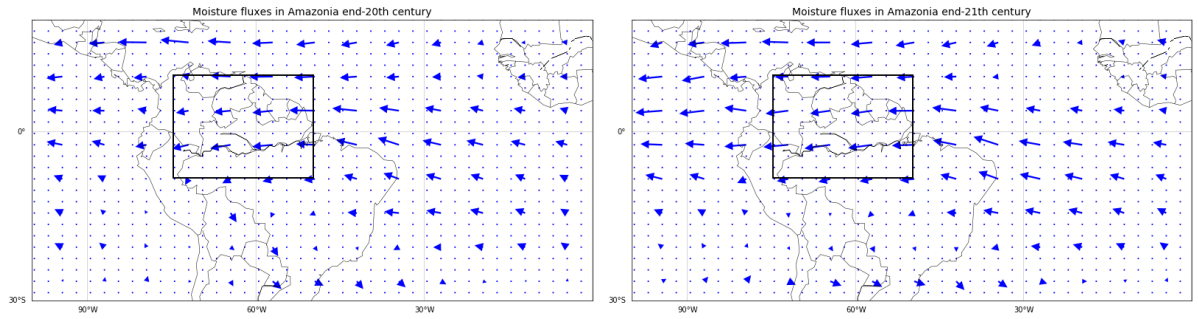

(a) (b)

Figure 5.15: The moisture fluxes for end-20th century (a) and end-21st century (b). The arrows indicate the direction and magnitude of the moisture flux in the the horizontal directions. The case study area is demarcated by the black rectangle.

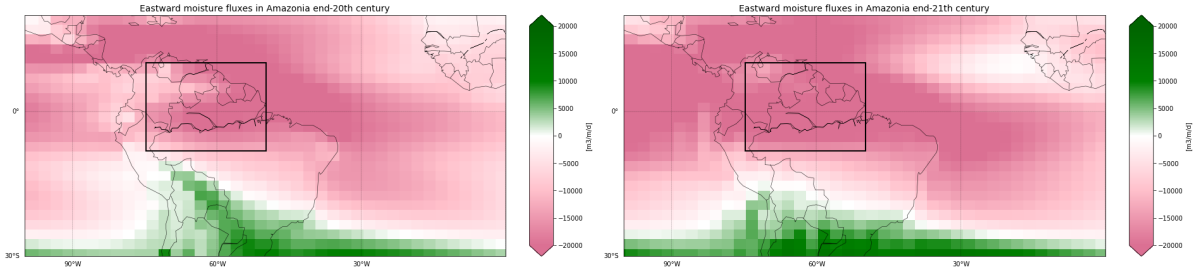

(a) (b)

Figure 5.16: The Eastward moisture flux for end-20th century (a) and end-21st century (b). The colors indicate the direction and magnitude of the moisture flux in the East-West plane. Green colors indicate an Eastward movement of moisture and pink colors indicate a Westward movement of moisture. The case study area is demarcated by the black rectangle.

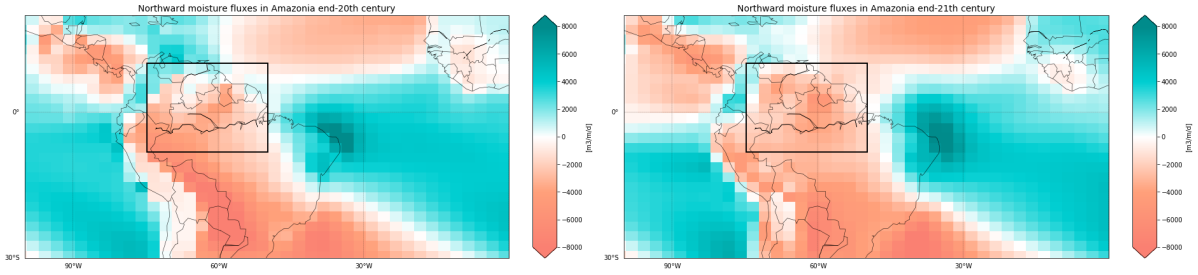

(a) (b)

Figure 5.17: The Northward moisture flux for end-20th century (a) and end-21st century (b). The colors indicate the direction and magnitude of the moisture flux in the North-South plane. Blue colors indicate an Northward movement of moisture and orange colors indicate a Southward movement of moisture. The case study area is demarcated by the black rectangle.

5.2.2. Moisture tracking during dry season (August - November)

	Precipitation [mm d^{-1}]	Evaporation [mm d^{-1}]	Recycled moisture [mm d^{-1}]	ρ_A	ϵ_A
end-20th century	4.65	3.77	1.27	0.27	0.34
end-21st century	1.03	2.11	0.24	0.23	0.11

Table 5.2: Precipitation (P), evaporation (E) and recycled moisture rates (in mm d^{-1}) within the case study area of Amazonia during the dry season (August until November). The Amazonian precipitation (ρ_A) and evaporation (ϵ_A) recycling ratios are the ratios between either the precipitation or the evaporation rate and the recycled moisture rate, thus within the case study area as well.

The dry season in Amazonia is from August until November: in both scenarios the precipitation rates are lower than during the rest of the year, in the end-21st century precipitation rates during these months are significantly lower than in the end-20th century scenario (see Figure 5.5). The analysis of the dry months in Amazonia (Table 5.2) shows that during these months the effects in the end-21st century are the most severe. Precipitation rates drop from 4.65 to 1.01 mm d^{-1} and evaporation rates from 3.77 to 2.11 mm d^{-1}. The amount of recycled moisture within the case study area has decreased to as little as 0.24 mm d^{-1} which means that on top of the decreases in both precipitation and evaporation rates proportionally even less will recycle and a larger fraction of the scarce moisture that is left will leave Amazonia before it precipitates - since the ϵ_A drops from 34 to 11 percent. The effects that were seen in the analysis of the full year water cycle in Section 5.2.1 are enlarged by looking at solely the dry months. Spatially too, the precipitation (Figure 5.18) and evaporation rates (Figure 5.19) decrease significantly in Amazonia, while evaporation rates on the oceans stay relatively more constant. The amount of recycled precipitation decreases as well, as can be seen in Figure 5.20, where it is clear that almost no moisture that evaporated from the case study area precipitates in the case study area again. The largest difference can be seen in the recycled evaporation plots (Figure 5.21), where rates in the end-21st century (Figure 5.21b) have gotten lower than 1 mm d^{-1} everywhere on the map. This means that in the end-21st century scenario nowhere more than 1 mm d^{-1} of local evaporation will go towards Amazonia, while in the dry season evaporation rates on the ocean East of the area easily go up to 7 mm d^{-1} and in the dry season in the end-20th century the highest recycled evaporation rates used to be around 2 mm d^{-1}. Similarly to the analysis of the full year, on top of the lower precipitation and evaporation rates, the Amazonian precipitation (Figure 5.22) and evaporation (Figure 5.23) recycling ratios decrease as well, meaning that of the lower precipitation and evaporation rates, proportionally even less recycles. The moisture fluxes show the same effects as the full year analysis. The direction is Westward (Figure 5.24), the moisture flux seems to be of larger magnitude on the West border of the case study area. This is again supported by the Eastward moisture flux, which is more Westward in the end-21st century (Figure 5.25b) than in the end-20th century scenario (Figure 5.25a) on the West side of Amazonia. The Northward flux (Figure 5.26) again shows more Southward moisture fluxes in the end-21st century scenario. This has however not resulted in more precipitation in any of the other results.

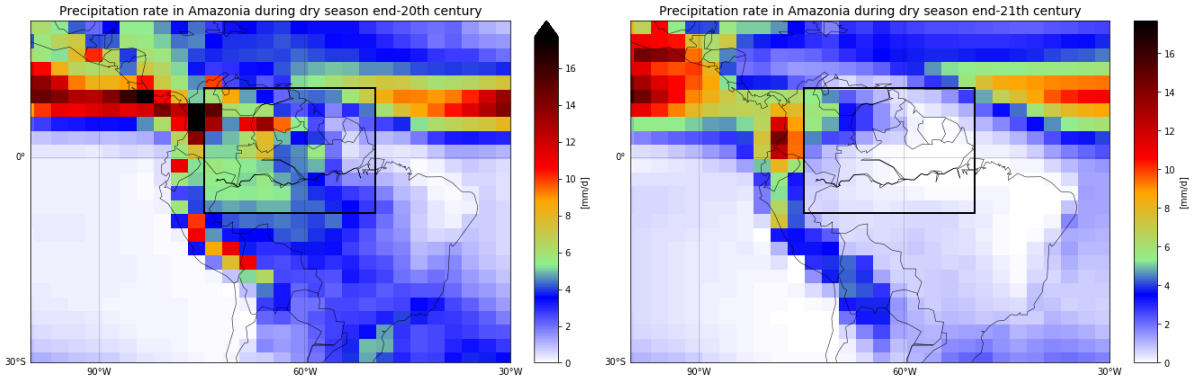

(a) (b)

Figure 5.18: The averaged daily precipitation rates in Amazonia for end-20th century (a) and end-21st century (b) during the dry season. The colors indicate the precipitation rate in mm d^{-1}, with red color indicating a higher rates and blue lower rates. The case study area is demarcated by the black rectangle.

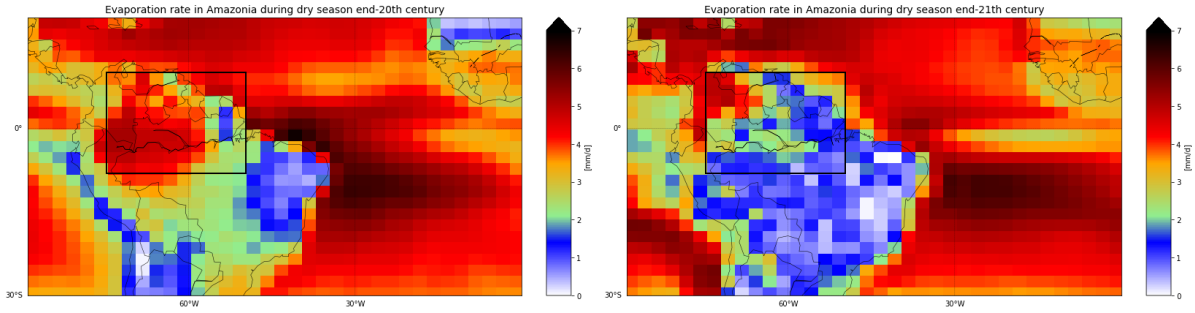

(a) (b)

Figure 5.19: The averaged daily evaporation rates in Amazonia for end-20th century (a) and end-21st century (b) during the dry season. The colors indicate the evaporation rate in mm d^{-1}, with red color indicating a higher rates and blue lower rates. The case study area is demarcated by the black rectangle.

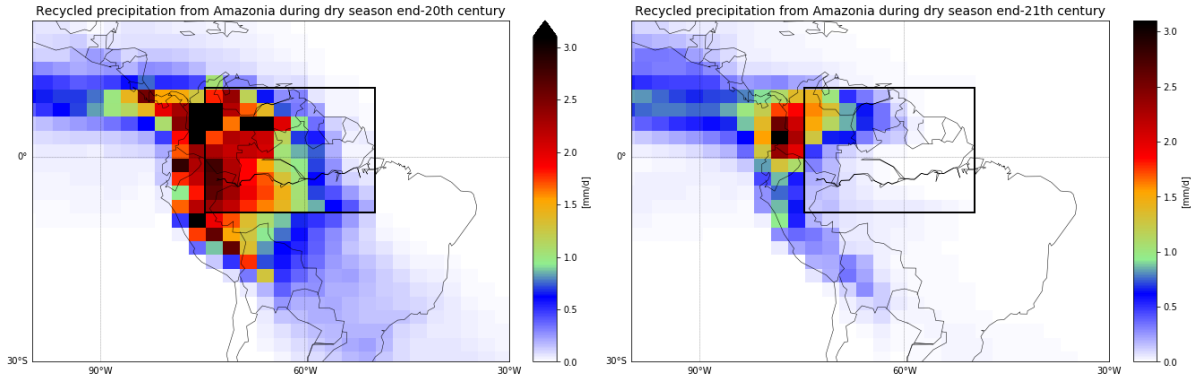

(a) (b)

Figure 5.20: The averaged daily rates that have recycled from Amazonian land for end-20th century (a) and end-21st century (b) during the dry season. The colors indicate the recycled precipitation rate in mm d^{-1}, with red color indicating a higher rates and blue lower rates. The case study area is demarcated by the black rectangle.

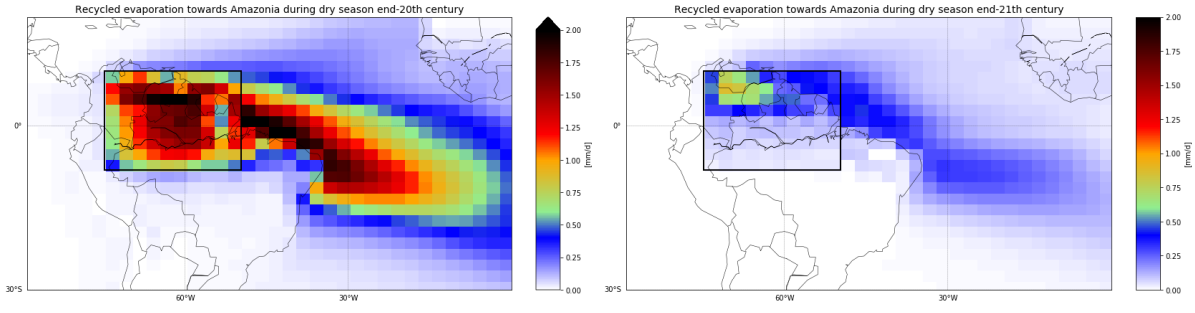

(a) (b)

Figure 5.21: The averaged daily rates of evaporation that will precipitate on Amazonian land for end-20th century (a) and end-21st century (b) during the dry season. The colors indicate the recyclable evaporation rate in mm d^{-1}, with red color indicating a higher rates and blue lower rates. The case study area is demarcated by the black rectangle.

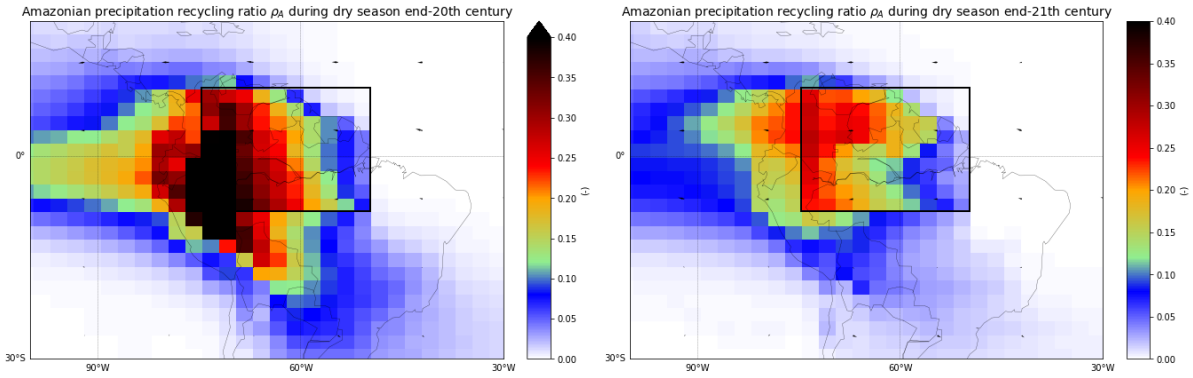

(a) (b)

Figure 5.22: The Amazonian precipitation recycling ratio for end-20th century (a) and end-21st century (b) during the dry season. The colors indicate the percentage of local precipitation in a specific grid cell that originates from the case study area (demarcated by the black rectangle), with red areas indicating a high percentage and blue low percentage. Arrows represent the direction and magnitude of the moisture fluxes.

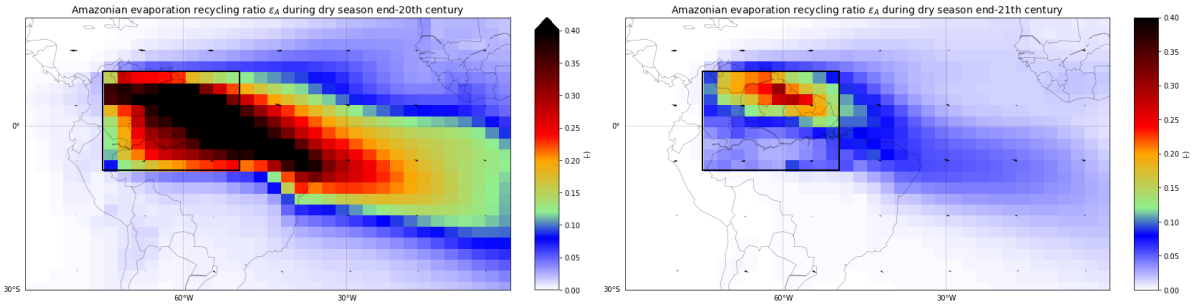

(a) (b)

Figure 5.23: The Amazonian evaporation recycling ratio for end-20th century (a) and end-21st century (b) during the dry season. The colors indicate the percentage of local evaporation in a specific grid cell that will return as precipitation in the case study area (demarcated by the black rectangle), with red areas indicating a high percentage and blue low percentage. Arrows represent the direction and magnitude of the moisture fluxes.

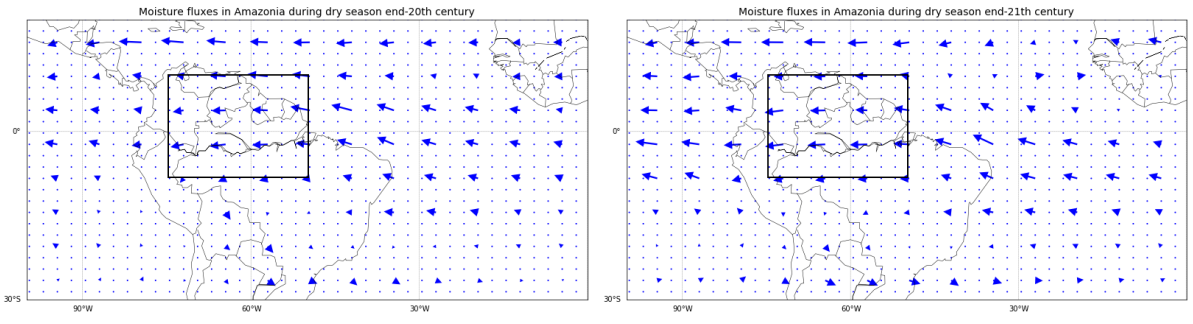

(a) (b)

Figure 5.24: The moisture fluxes for end-20th century (a) and end-21st century (b) during the dry season. The arrows indicate the direction and magnitude of the moisture flux in the the horizontal directions. The case study area is demarcated by the black rectangle.

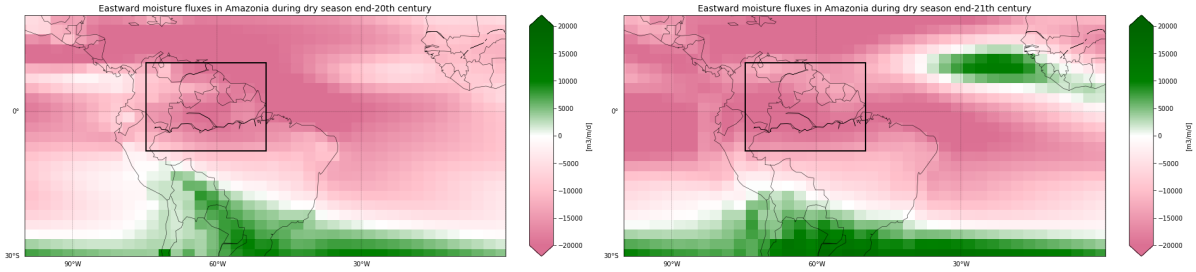

(a) (b)

Figure 5.25: The Eastward moisture flux for end-20th century (a) and end-21st century (b) during the dry season. The colors indicate the direction and magnitude of the moisture flux in the East-West plane. Green colors indicate an Eastward movement of moisture and pink colors indicate a Westward movement of moisture. The case study area is demarcated by the black rectangle.

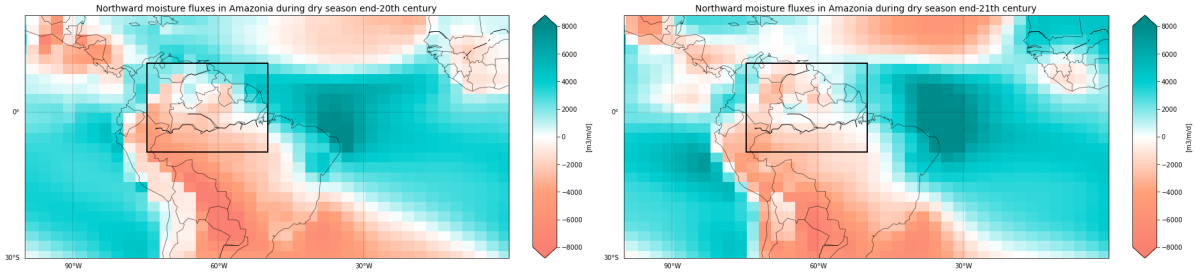

(a) (b)

Figure 5.26: The Northward moisture flux for end-20th century (a) and end-21st century (b) during the dry season. The colors indicate the direction and magnitude of the moisture flux in the North-South plane. Blue colors indicate an Northward movement of moisture and orange colors indicate a Southward movement of moisture. The case study area is demarcated by the black rectangle.

5.3. Case study area 2: Western Africa

Background information

The land cover type map of Western Africa is displayed in Figure 5.27. This region is dominated by (rainfed) cropland and (sparse) vegetation. In the North of the case study area lies the Southern border of the Sahara desert. Here the main land cover type is either bare soil or sparse vegetation. In the South are some regions with dense forests, closer to the equator where there is a more tropical climate. Some of this forest has already made way for croplands. The elevation map (Figure 5.28) shows that most of the case study area is located between a height of 200 and 500 meters. The population density map (Figure 5.29) shows that the highest population densities are in the East, to be specific in Nigeria. Some regions in this case study area have relatively high population densities as well, while other regions have very low densities. Western Africa is chosen as a case study because of the increase in precipitation seen on the difference plot in Figure 3.2 in Section 3.1.

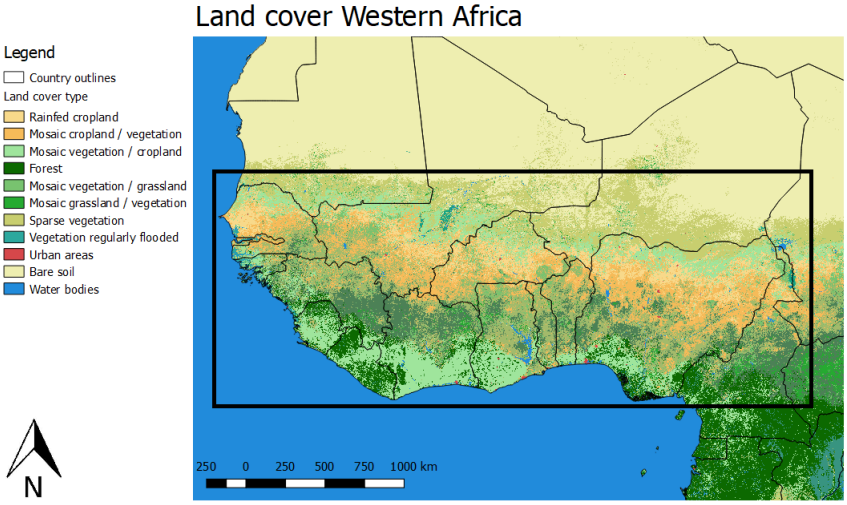

Figure 5.27: Land cover map for case study area 2: Western Africa. The map shows different land cover types, indicated with the colors on the left. The case study area is demarcated with the black outline (UCL, 2009; GADM, 2018).

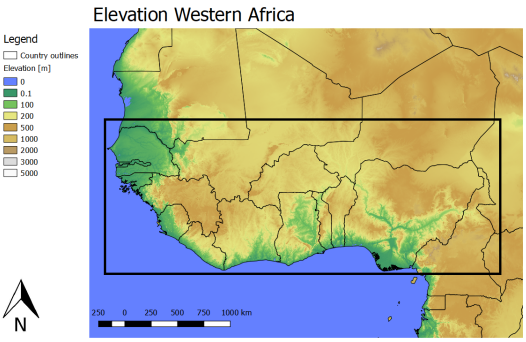

Figure 5.28: Elevation map for case study area 2: Western Africa. The map shows the elevation of the surface, indicated with the colors on the left. The case study area is demarcated with the black outline (USGS, 2010; GADM, 2018).

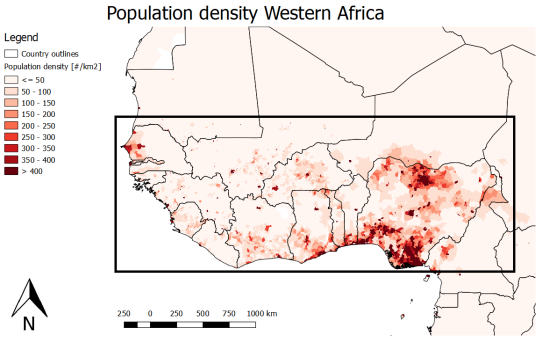

Figure 5.29: Population density map for case study area 2: Western Africa. The map shows the population density in inhabitants per km^2, scaled with the colors on the left. The case study area is demarcated with the black outline (SEDAC, 2015; GADM, 2018).

Seasonality

Figure 5.30 shows the mean daily precipitation in Western Africa as a plot over the year for the end-20th century scenario and the end-21st century scenario. The graphs show that in the future scenario the precipitation over the year follows the same pattern as in the past scenario from January to June and from October to December. However, the future scenario gives an elongated and magnified rain season from July until October. This increases the mean precipitation rate from 3.62 mm d^{-1} in the past scenario to 4.39 mm d^{-1} in the future

scenario.

Figure 5.31 presents the mean evaporation in Western Africa for the end-20th century scenario and the end-21st century scenario. The mean evaporation rate is 2.12 mm d^{-1} in the past scenario and 2.40 mm d^{-1} in the future scenario. This means that also the evaporation rate increases in the future scenario. However, the graphs show a slight decrease in January to April and an increase in the rest of the year. In which way the precipitation and evaporation rates are interlinked is studied further with the moisture tracking model, which will be explained in Section 5.3.1.

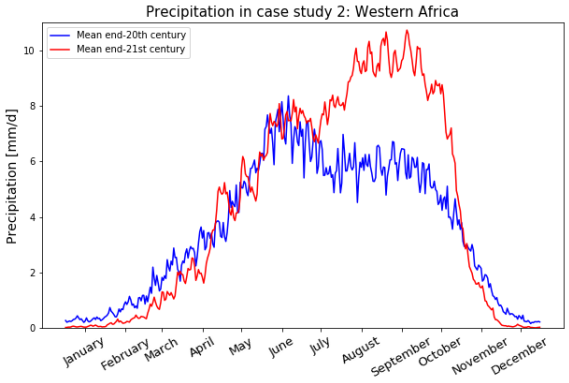

Figure 5.30: Mean land precipitation in the case study area of Western Africa. The blue line represents the end-20th century scenario and the red line represents the end-21st century scenario. The graph displays the rate in mm d^{-1}.

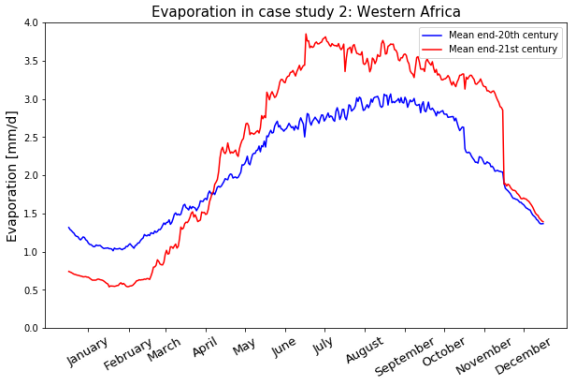

Figure 5.31: Mean land evaporation in the case study area of Western Africa. The blue line represents the end-20th century scenario and the red line represents the end-21st century scenario. The graph displays the rate in mm d^{-1}.

The display of distribution of the precipitation and evaporation data in Western Africa are determined with the use of box plots. For the precipitation rates, Figure 5.32a shows the box plot in the past scenario and Figure 5.32b the box plot in the future scenario, both corresponding to Figure 5.30. The elongated rain season from July to October in the future scenario seems to be fairly uncertain, given the high spread in precipitation rates throughout the years in these months, while the rain season in the past scenario had a relatively lower spread throughout those months.

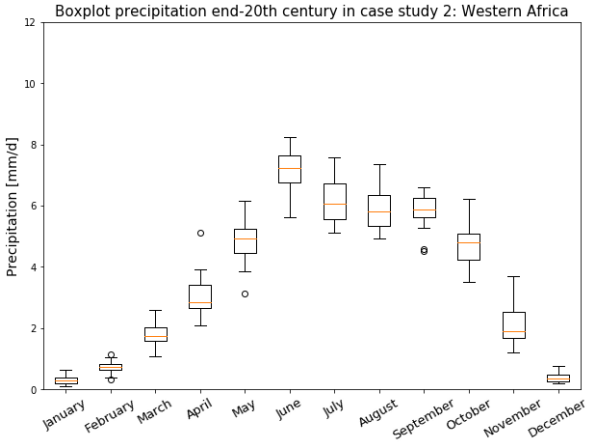

(a)

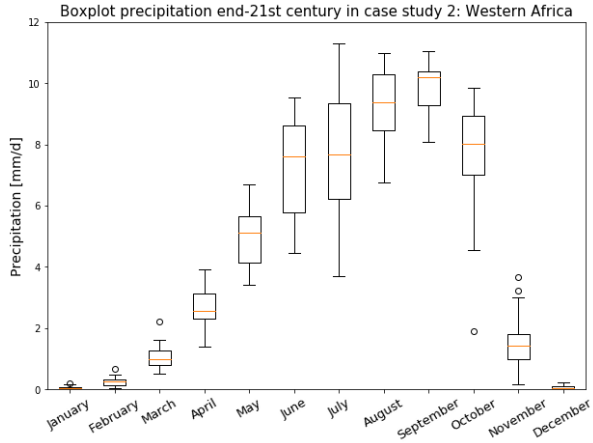

(b)

Figure 5.32: Box plots of land precipitation in the case study area of Western Africa for the end-20th century scenario (a) and end-21st century scenario (b). The box plots represent the statistical spread for each month within the year by using quartiles to show the distribution of the used data. The median precipitation rate per month is shown as the orange line, the box represents the data from the first quartile until the third quartile and the two whiskers have maximum and minimum of 1.5 times the interquartile range (from Q1 to Q3). The dots are the outliers.

The box plots for the evaporation rates corresponding to Figure 5.31 are presented in Figure 5.33a for the past scenario and Figure 5.33b for the future scenario. The past scenario's evaporation rates of each month have fairly low spread. In the future scenario the decrease in evaporation rates in January and February have

relatively low spread, while the increase in evaporation rates have slightly higher spread and thus more uncertainty, but are still reasonably reliable.

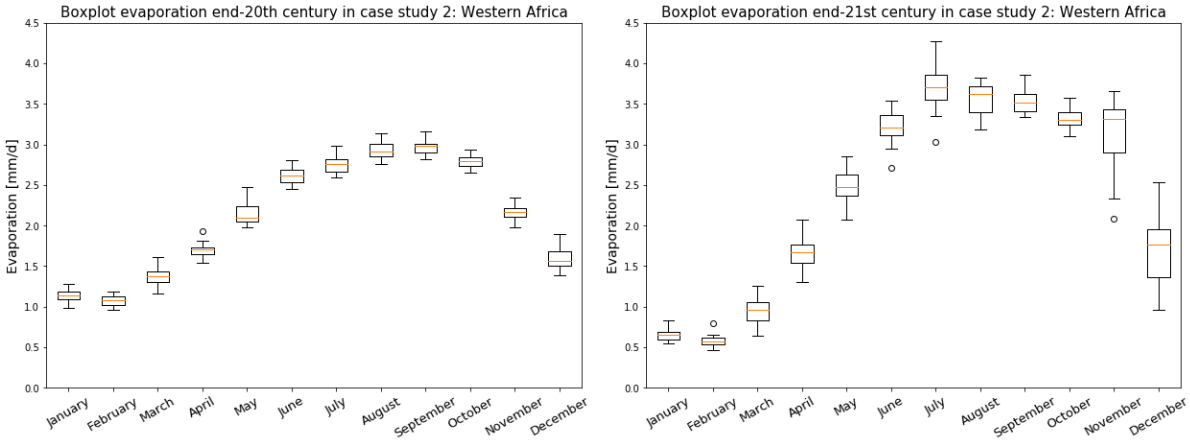

(a) (b)

Figure 5.33: Box plots of land evaporation in the case study area of Western Africa for the end-20th century scenario (a) and end-21st century scenario (b). The box plots represent the statistical spread for each month within the year by using quartiles to show the distribution of the used data. The median evaporation rate per month is shown as the orange line, the box represents the data from the first quartile until the third quartile and the two whiskers have maximum and minimum of 1.5 times the interquartile range (from Q1 to Q3). The dots are the outliers.

5.3.1. Moisture tracking for full year

	Precipitation [mm d^{-1}]	Evaporation [mm d^{-1}]	Recycled moisture [mm d^{-1}]	ρ_{WA}	ϵ_{WA}
end-20th century	3.62	2.12	0.91	0.25	0.43
end-21st century	4.39	2.40	1.00	0.23	0.42

Table 5.3: Precipitation (P), evaporation (E) and recycled moisture rates (in mm d^{-1}) within the case study area of Western Africa. The West-African precipitation (ρ_{WA}) and evaporation (ϵ_{WA}) recycling ratios are the ratios between either the precipitation or the evaporation rate and the recycled moisture rate, thus within the case study area as well.

In the case study area of Western Africa precipitation and evaporation rates will increase, as will the recycled moisture (see Figure 5.3). The recycled moisture however does not increase proportionally to either precipitation or to evaporation rate, meaning that the ratios ρ_{WA} and ϵ_{WA} slightly decrease. Looking at the plots, the precipitation rate in Western Africa increases mostly in the North (Figure 5.34). Evaporation rates (Figure 5.35) increase slightly in most regions, but do not change significantly. The recycled rates do show some changes. The recycled moisture from the region mostly precipitates within the case study area itself, as can be seen in Figure 5.36. Less moisture will end up as precipitation on the West side of the case study area in the end-21st century scenario than in the end-20th century scenario. The recycled evaporation, thus where the moisture comes from, changes more clearly. Figure 5.37b shows an increase in recycled evaporated moisture from the South of the region compared to Figure 5.37a. However, the outcomes of the West-African recycling ratios (Figure 5.38 and Figure 5.39) give misleading outputs. Since the evaporation and precipitation rates in the subtropics are relatively high and in the Sahara desert are relatively low, the ratio between recycled moisture and total precipitation or evaporation can be very high or low in one of these areas, while it is actually skewed because of the division by a very high or low number. Because of these dry and wet regions close to each other, it is clearer to look at the recycled precipitation and evaporation in absolute numbers for the Western Africa case study. Figure 5.40 shows that the main direction of the moisture fluxes in the case study area is Western, although in the end-21st century scenario it seems to have shifted to no horizontal direction at the Western border of the region. This is supported by looking at the Eastward moisture flux in Figure 5.41. Figure 5.42 explains the increase in precipitation towards the North border of the case study area, since in the end-21st century scenario (Figure 5.42b) there is a larger Northern moisture flux in the region, especially

towards the North side. The slight increase in precipitation and evaporation can not really be explained by looking at the full water year, this is why for Western Africa it is especially important to look at the wet season specifically, in Section 5.3.2.

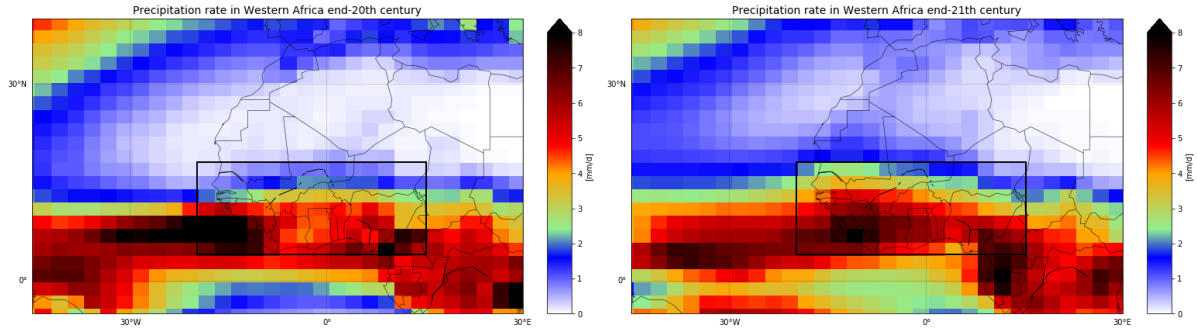

(a) (b)

Figure 5.34: The averaged daily precipitation rates in Western Africa for end-20th century (a) and end-21st century (b). The colors indicate the precipitation rate in mm d^{-1}, with red color indicating a higher rates and blue lower rates. The case study area is demarcated by the black rectangle.

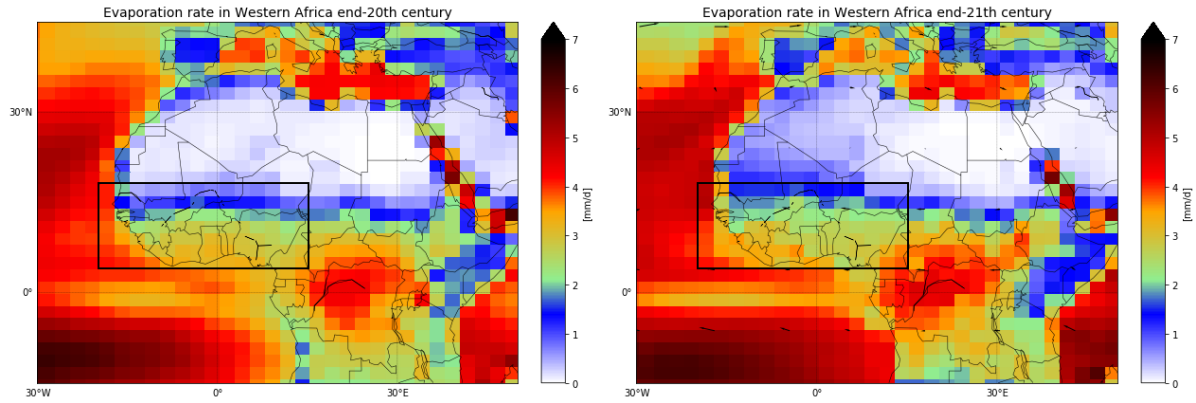

(a) (b)

Figure 5.35: The averaged daily evaporation rates in Western Africa for end-20th century (a) and end-21st century (b). The colors indicate the evaporation rate in mm d^{-1}, with red color indicating a higher rates and blue lower rates. The case study area is demarcated by the black rectangle.

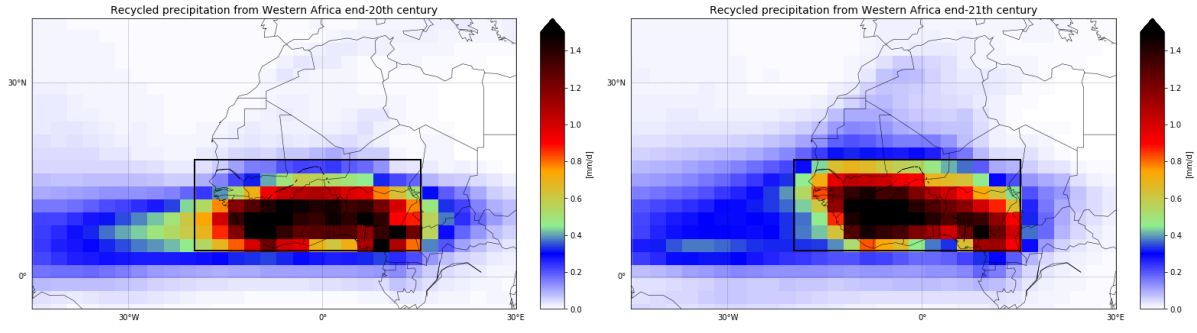

(a) (b)

Figure 5.36: The averaged daily rates that have recycled from West-African land for end-20th century (a) and end-21st century (b). The colors indicate the recycled precipitation rate in mm d^{-1}, with red color indicating a higher rates and blue lower rates. The case study area is demarcated by the black rectangle.

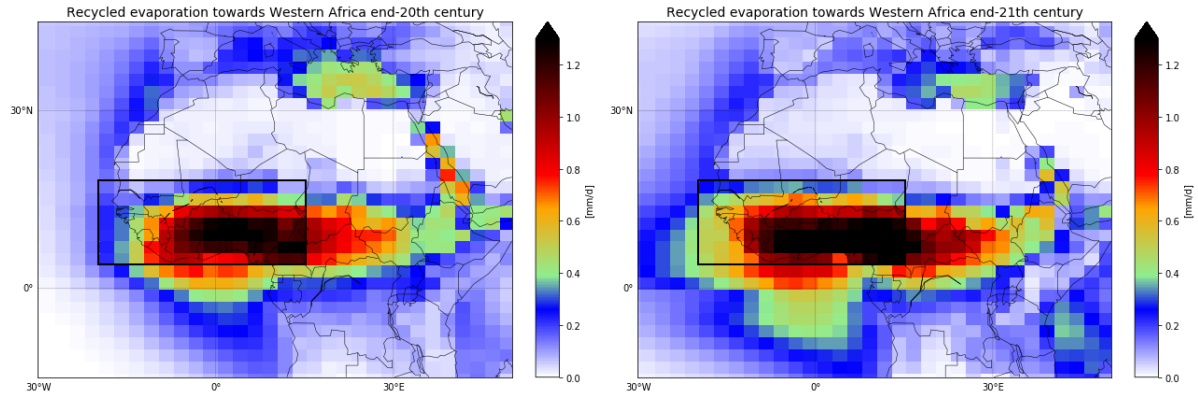

(a) (b)

Figure 5.37: The averaged daily rates of evaporation that will precipitate on West-African land for end-20th century (a) and end-21st century (b). The colors indicate the recyclable evaporation rate in mm d^{-1}, with red color indicating a higher rates and blue lower rates. The case study area is demarcated by the black rectangle.

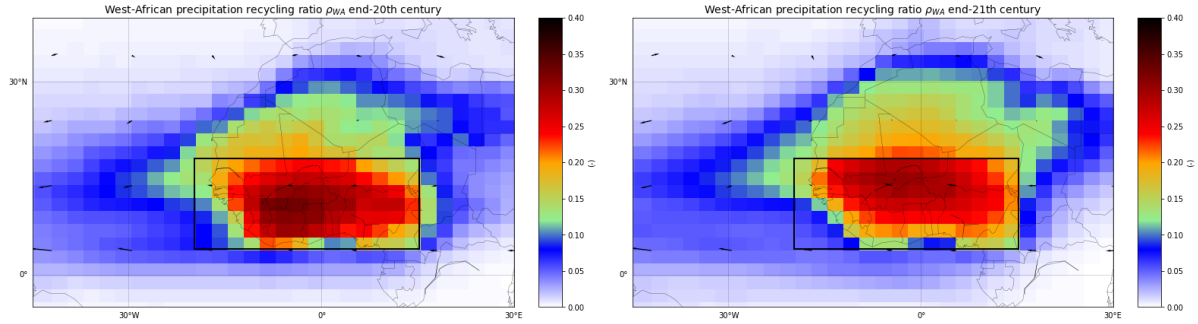

(a) (b)

Figure 5.38: The West-African precipitation recycling ratio for end-20th century (a) and end-21st century (b). The colors indicate the percentage of local precipitation in a specific grid cell that originates from the case study area (demarcated by the black rectangle), with red areas indicating a high percentage and blue low percentage. Arrows represent the direction and magnitude of the moisture fluxes.

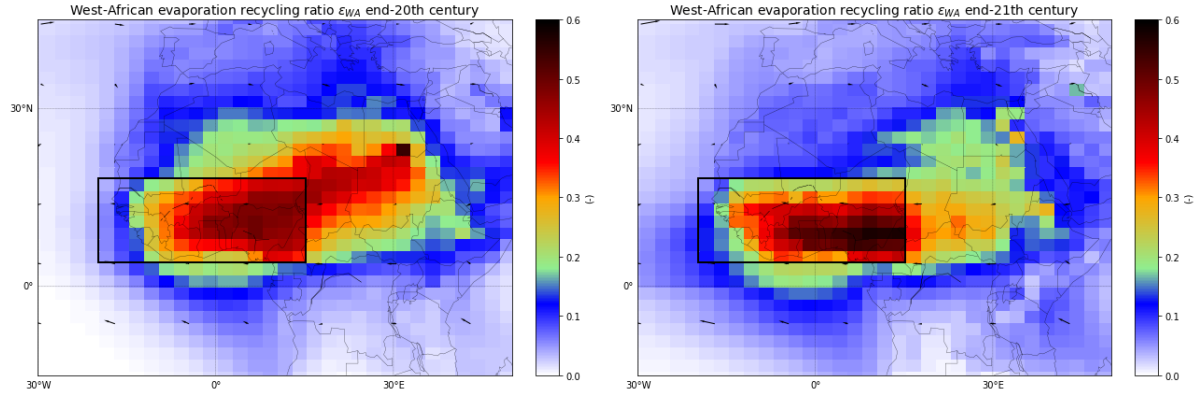

(a) (b)

Figure 5.39: The West-African evaporation recycling ratio for end-20th century (a) and end-21st century (b). The colors indicate the percentage of local evaporation in a specific grid cell that will return as precipitation in the case study area (demarcated by the black rectangle), with red areas indicating a high percentage and blue low percentage. Arrows represent the direction and magnitude of the moisture fluxes.

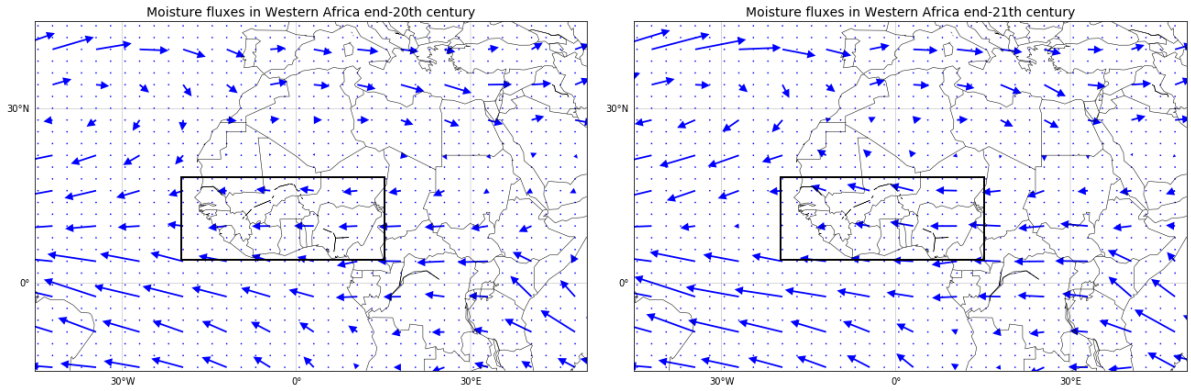

(a) (b)

Figure 5.40: The West-African moisture fluxes for end-20th century (a) and end-21st century (b). The arrows indicate the direction and magnitude of the moisture flux in the the horizontal directions. The case study area is demarcated by the black rectangle.

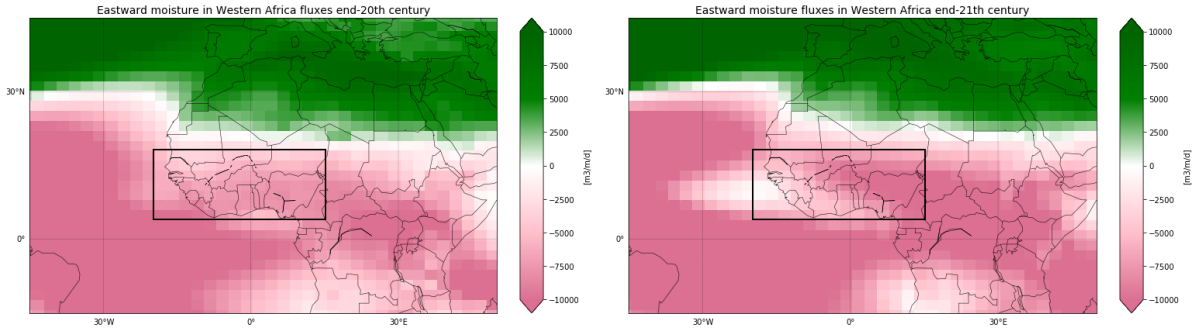

(a) (b)

Figure 5.41: The Eastward moisture flux in West Africa for end-20th century (a) and end-21st century (b). The colors indicate the direction and magnitude of the moisture flux in the East-West plane. Green colors indicate an Eastward movement of moisture and pink colors indicate a Westward movement of moisture. The case study area is demarcated by the black rectangle.

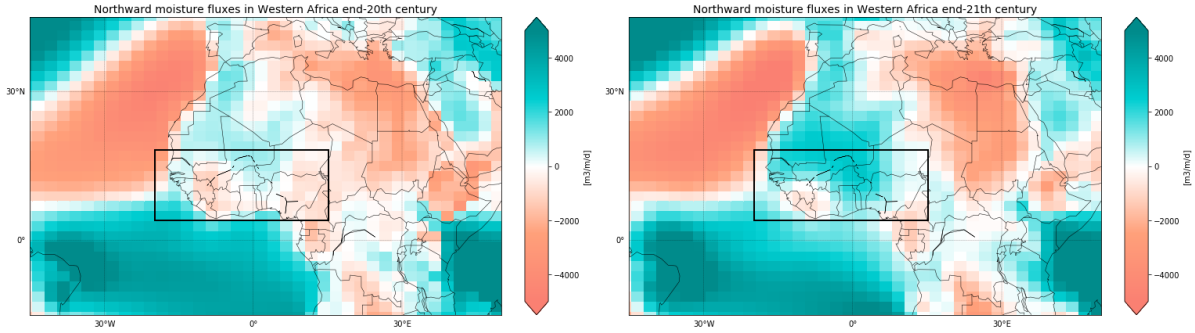

(a) (b)

Figure 5.42: The Northward moisture flux in West Africa for end-20th century (a) and end-21st century (b). The colors indicate the direction and magnitude of the moisture flux in the North-South plane. Blue colors indicate an Northward movement of moisture and orange colors indicate a Southward movement of moisture. The case study area is demarcated by the black rectangle.

5.3.2. Moisture tracking during wet season (July - October)

	Precipitation [mm d^{-1}]	Evaporation [mm d^{-1}]	Recycled moisture [mm d^{-1}]	ρ_{WA}	ϵ_{WA}
end-20th century	5.66	2.86	1.49	0.26	0.52
end-21st century	8.53	3.55	1.90	0.22	0.53

Table 5.4: Precipitation (P), evaporation (E) and recycled moisture rates (in mm d^{-1}) within the case study area of Western Africa during the wet season (July until October). The West-African precipitation (ρ_{WA}) and evaporation (ϵ_{WA}) recycling ratios are the ratios between either the precipitation or the evaporation rate and the recycled moisture rate, thus within the case study area as well.

The wet season in Western Africa is from July until October: in these months the end-21st century scenario shows a large increase in precipitation. During these months the mean precipitation increases from 5.66 to 8.53 mm d^{-1}, evaporation rates increase from 2.86 to 3.55 mm d^{-1}, recycled moisture within the region increases from 1.49 to 1.90 mm d^{-1}, the ρ_{WA} decreases and the ϵ_{WA} barely increases, as mentioned in Table 5.4. Even though the precipitation increases, the recycled moisture does not increase proportionally, which means most of the increase in precipitation comes from outside the case study area. The slight increase in ϵ_{WA} means that a higher percentage of the moisture evaporated from the case study area will again return as precipitation within the area. The plots however give much more understanding to why there is an increase in precipitation in Western Africa by just looking at the wet months as opposed to looking at the full year in Section 5.3.1. Precipitation rates increase almost everywhere within the case study area (Figure 5.43) and so do evaporation rates (Figure 5.44). The highest recycled precipitation rates are inside the case study area in the end-21st century (Figure 5.45b), as opposed to the end-20th century (Figure 5.45a), where only in the center of the area are regions that receive a lot of recycled moisture and some moisture will precipitate in the ocean West of the case study area. The most interesting is the change in recycled evaporation. In the end-21st century (Figure 5.46b) much evaporation from the oceans South and West of the Western Africa case study area will precipitate in the area, while in the end-20th century (Figure 5.46a) the amount of evaporation from these ocean regions did not contribute much to the precipitation within the case study area. In the tropical regions in Central Africa there is also an increase in recycled evaporation in the end-21st century scenario. The West-African precipitation and evaporation recycling ratios plots do not show an understandable effect because of the large differences in absolute precipitation and evaporation rates, as mentioned in Section 5.3.1. The moisture fluxes can explain the increased precipitation in Western Africa the best. Figure 5.49 shows that in the end-21st century scenario (Figure 5.49b) on the West border of the case study area the moisture flux has changed direction from Westward to Eastward. This is even more clear in Figure 5.50. Figure 5.51 shows an increase in Northward moisture flux in the end-21st century scenario. However, the Eastward fluxes in Figure 5.50 are more dominant than the Northward fluxes in Figure 5.51.

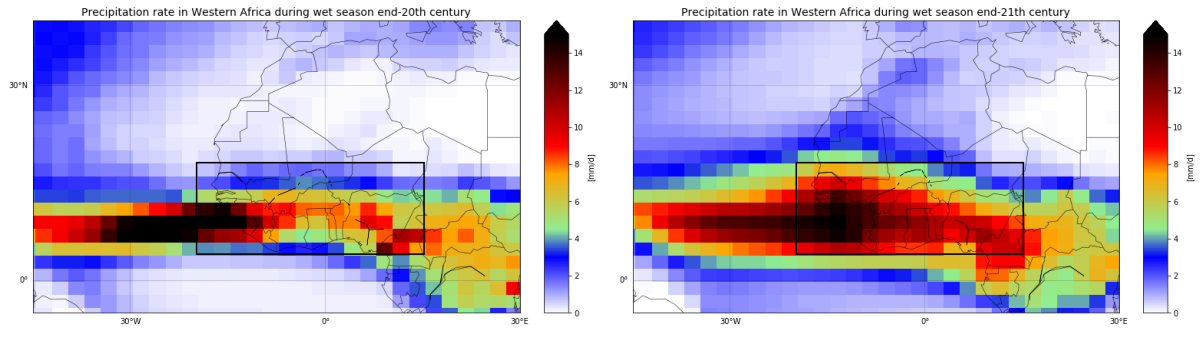

(a) (b)

Figure 5.43: The averaged daily precipitation rates in Western Africa for end-20th century (a) and end-21st century (b) during the wet season (July until October). The colors indicate the precipitation rate in mm d^{-1}, with red color indicating a higher rates and blue lower rates. The case study area is demarcated by the black rectangle.

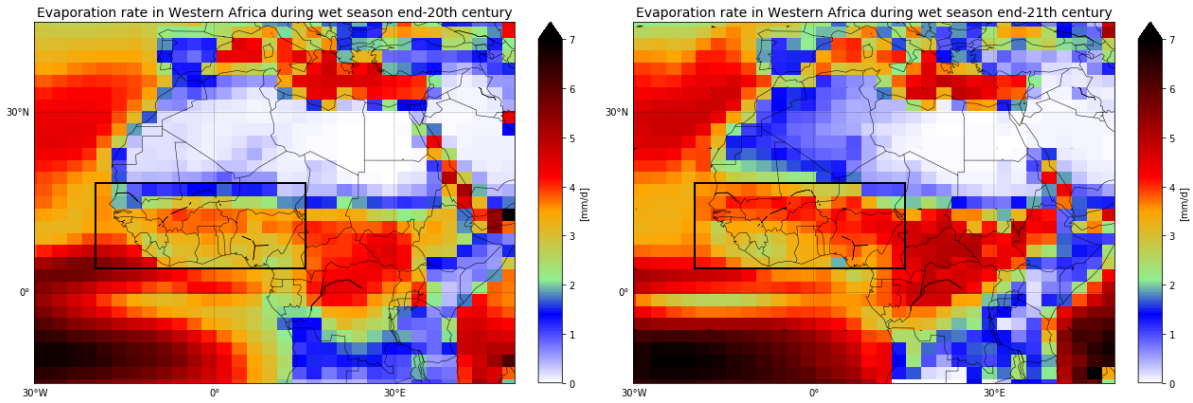

(a) (b)

Figure 5.44: The averaged daily evaporation rates in Western Africa for end-20th century (a) and end-21st century (b) during the wet season (July until October). The colors indicate the evaporation rate in mm d^{-1}, with red color indicating a higher rates and blue lower rates. The case study area is demarcated by the black rectangle.

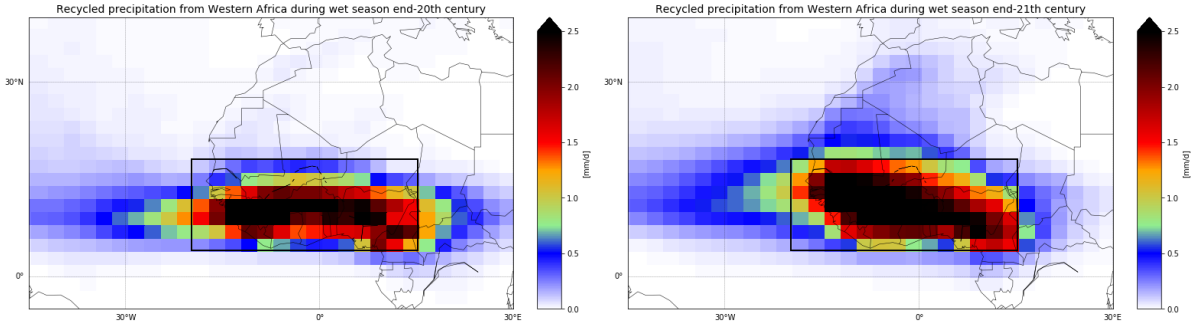

(a) (b)

Figure 5.45: The averaged daily rates that have recycled from West-African land for end-20th century (a) and end-21st century (b) during the wet season (July until October). The colors indicate the recycled precipitation rate in mm d^{-1}, with red color indicating a higher rates and blue lower rates. The case study area is demarcated by the black rectangle.

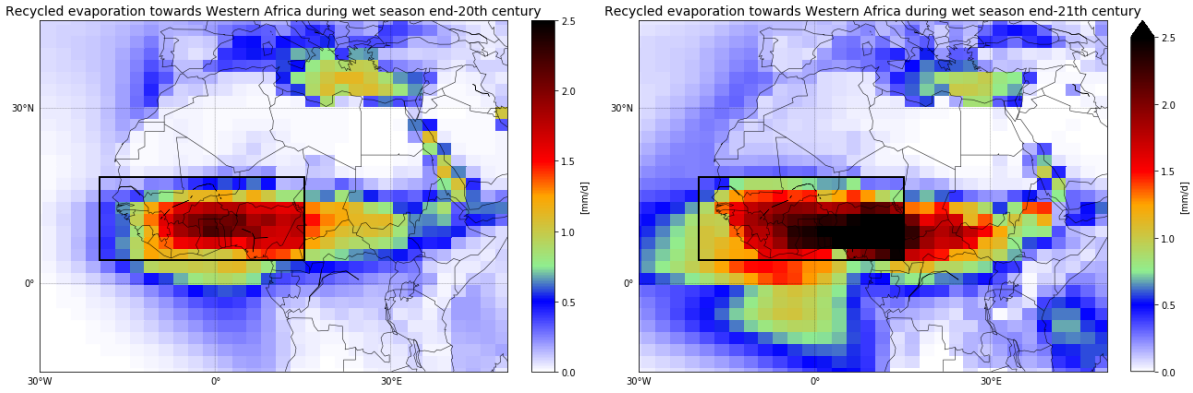

(a) (b)

Figure 5.46: The averaged daily rates of evaporation that will precipitate on West-African land for end-20th century (a) and end-21st century (b) during the wet season (July until October). The colors indicate the recyclable evaporation rate in mm d^{-1}, with red color indicating a higher rates and blue lower rates. The case study area is demarcated by the black rectangle.

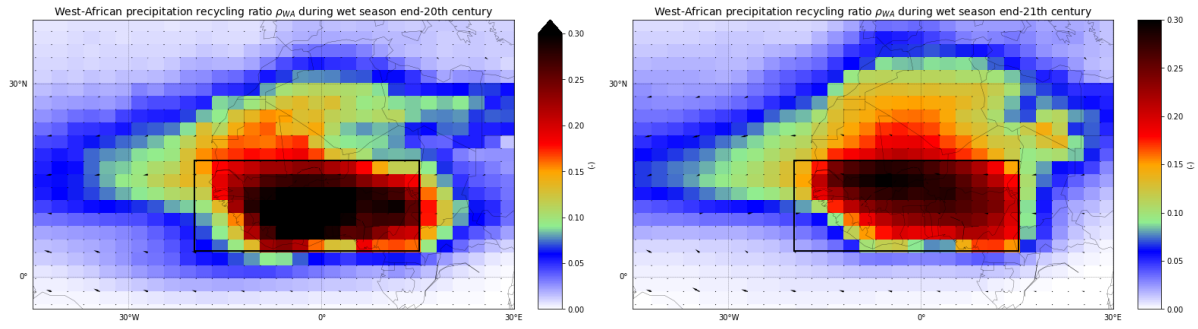

(a) (b)

Figure 5.47: The West-African precipitation recycling ratio for end-20th century (a) and end-21st century (b) during the wet season (July until October). The colors indicate the percentage of local precipitation in a specific grid cell that originates from the case study area (demarcated by the black rectangle), with red areas indicating a high percentage and blue low percentage. Arrows represent the direction and magnitude of the moisture fluxes.

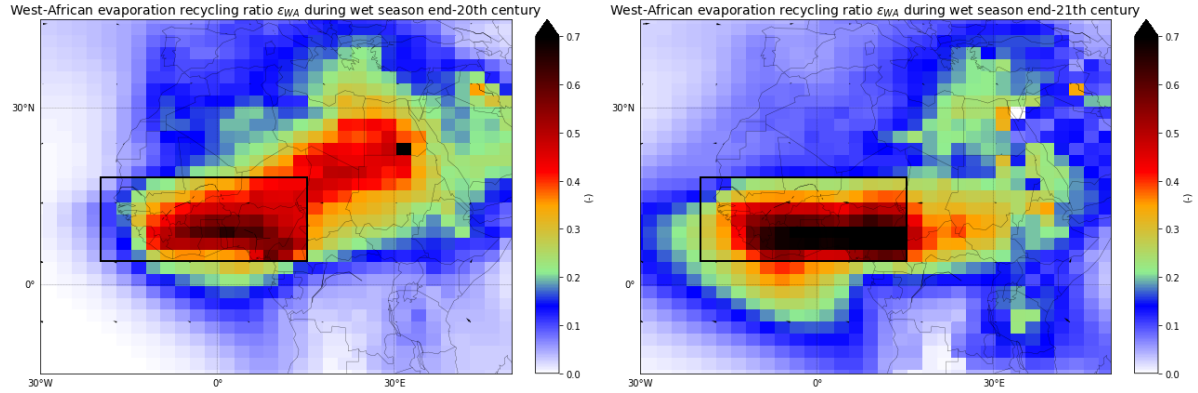

(a) (b)

Figure 5.48: The West-African evaporation recycling ratio for end-20th century (a) and end-21st century (b) during the wet season (July until October). The colors indicate the percentage of local evaporation in a specific grid cell that will return as precipitation in the case study area (demarcated by the black rectangle), with red areas indicating a high percentage and blue low percentage. Arrows represent the direction and magnitude of the moisture fluxes.

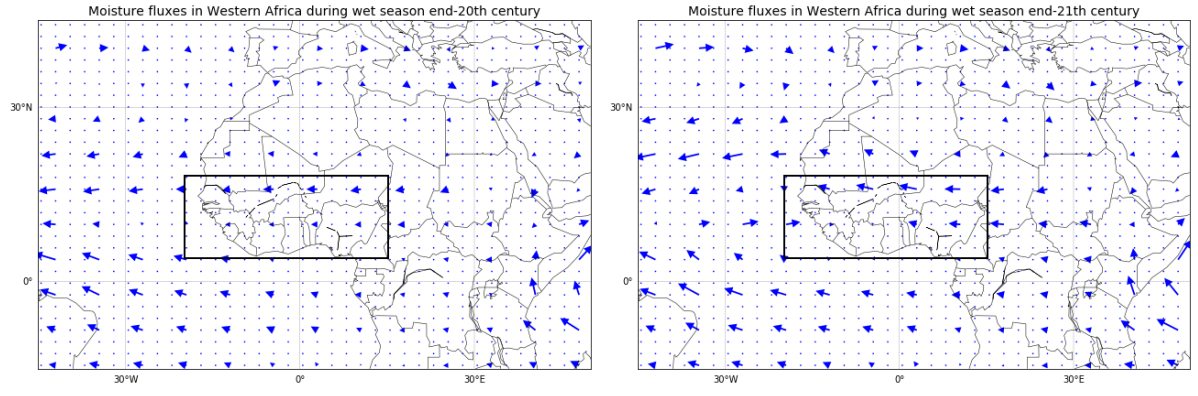

(a) (b)

Figure 5.49: The West-African moisture fluxes for end-20th century (a) and end-21st century (b) during the wet season (July until October). The arrows indicate the direction and magnitude of the moisture flux in the the horizontal directions. The case study area is demarcated by the black rectangle.

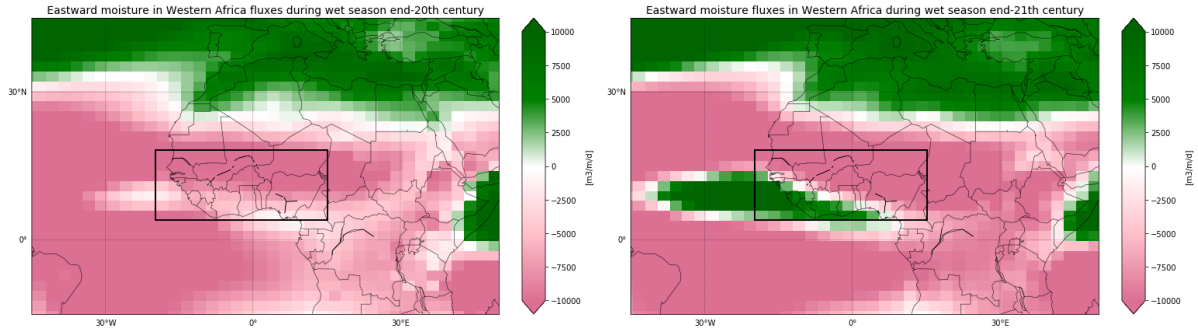

(a) (b)

Figure 5.50: The Eastward moisture flux in West Africa for end-20th century (a) and end-21st century (b) during the wet season (July until October). The colors indicate the direction and magnitude of the moisture flux in the East-West plane. Green colors indicate an Eastward movement of moisture and pink colors indicate a Westward movement of moisture. The case study area is demarcated by the black rectangle.

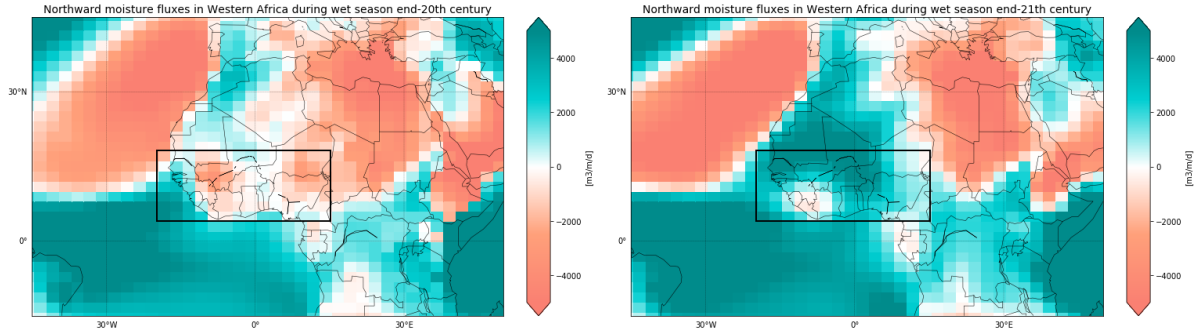

(a) (b)

Figure 5.51: The Northward moisture flux in West Africa for end-20th century (a) and end-21st century (b) during the wet season (July until October). The colors indicate the direction and magnitude of the moisture flux in the North-South plane. Blue colors indicate an Northward movement of moisture and orange colors indicate a Southward movement of moisture. The case study area is demarcated by the black rectangle.

Based on the impact analysis including background information, seasonality and the moisture tracking, the change in precipitation and evaporation in both case studies can now be explained. The lower precipitation and evaporation rates in Amazonia were already seen by just looking at the difference plots in Section 3.1. The seasonality analysis showed a drastic increase in seasonal variability and a distinct dry season in the end-21st century. This can be explained by the decrease in local evaporation due to land transitions (from deforestation). This leads to less precipitation over the case study area, even when surrounding oceans still evaporate at the same rate as in the end-20th century. The lower evaporation rate of the rain forest gives less moisture for clouds to form and precipitate. Moisture evaporates from the oceans on the East of Amazon region but moves over the region before it can precipitate, indicated by higher wind speed and larger moisture fluxes. The higher precipitation and partly higher, partly lower evaporation rates in Western Africa were indicated in Chapter 3. The seasonality analysis of Western Africa showed an magnified rain season in the end-21st century. This surplus in precipitation can be explained by an increase in moisture moving in from the oceans West and South of the case study area, because of changed moisture flux directions in the end-21st century as opposed to end-20th century. All in all this leads up to a mean precipitation rate during the wet season of 8.53 mm d^{-1}.

6

Discussion

The results of this research are based on the forecasts of two GFDL model experiments. Even though the GFDL is a well-known research institute, their model assumptions are made based on certain research. Climate research is done by many more institutes, therefore there are many more ways to model climate change.

The seasonality analysis of this research is relatively small. It was in fact found that there is an influence on precipitation seasonality when looking at a specific region. Marelle et al. (2018) concludes that future climate change could change the seasonal timing of precipitation events. The increased precipitation rates in Indonesia found in this research are also found by Ge et al. (2019), suggesting this is the result of enhanced convection in this region. In another region, other research has found contrasting results. In North America, where GFDL data shows increase in precipitation rates, Seager et al. (2007) shows that there is a broad consensus among climate models that this region will dry in the 21st century and that the transition to a drier climate should already be under way. Recent research from Ge et al. (2019) suggests that with climate change there will be more extremely wet days worldwide. Further research into worldwide seasonality changes with climate change will give a broader understanding to what will happen with precipitation patterns. Having more knowledge on shifts in precipitation seasonality with climate change will eventually give more information to base the moisture tracking on, leading to a possible different output.

The GFDL data showed two different patterns in Europe, where the Southern countries will experience less precipitation and the Northern countries will experience more precipitation. Moreover, the moisture tracking showed that Europe will receive more moisture from land, however, it is not found yet where this increase comes from. Europe is therefore a region of high interest for further research. Asia is another continent that is interesting to look further into. GFDL data shows that most of the Northern part shows increasing precipitation rates while the Middle East shows strong decreasing rates. Beurs et al. (2015) calls Central Asia a 'climate change hotspot', where there are strong spatial variations in weather patterns with climate change. Regional climate patterns will play a more important role, which means that only looking at global climate patterns does not provide enough information to project the impact of climate change locally.

During this research, zooming into smaller regions in every step, it became clear that land use has a large effect on the global water cycle. Most reports from the IPCC focuses mainly on the influence of greenhouse gas emissions and concentrations on temperature and precipitation. Whilst finalising this report, the latest IPCC report was published, that focuses on climate change, desertification, land degradation and sustainable land management (IPCC, 2019). The IPCC states that better land management could help in tackling climate change, but that it is not enough only looking at land management. Moisture tracking in this research shows that land management is a large part of combating climate change. The decrease in precipitation in Amazonia is mostly the effect of land management - since the Amazon forest will be logged under RCP8.5. The effects that happen because of climate change in Western Africa however are not caused by any land management changes. The increased West-African precipitation more so were an effect of increased oceanic evaporation near this region and an increase in moisture transport towards the region. This only has to do with increased temperatures caused by increased amounts of greenhouse gases in the atmosphere. Land management and conservation of forests is however a large part of the remedy against changing precipitation patterns with climate change.

7

Conclusion

Based on the output of the hydrological variables from GFDL data, surface air temperatures increase significantly both on land and on oceans. Land air temperatures increases more than ocean air temperatures. Increasing temperatures lead to significant increases in precipitation and evaporation rates over the oceans in the end-21st century. Over land these rates will show barely any change compared to the end-20th century. However, regionally there are significant changes. Firstly, there is a smaller spatial variability of mean precipitation and evaporation rates on land in the future. This means that the precipitation and the evaporation rate at the wettest place will lie closer to the precipitation and the evaporation rate at the driest place in the end-21st century compared to the end-20th century. Secondly, a 'DDWW paradigm' - where dry regions get drier and wet regions get wetter - is not supported by the GFDL data. In fact, some dry regions will get drier, but other dry regions will get wetter and the same counts for wet regions.

Global continental precipitation and evaporation recycling ratios do not show a significant change in the end-21st century compared to the end-20th century, because of different signs of change per continent that even out the globally averaged ratios. South America shows the biggest contrast to other continents, since precipitation as well as evaporation decrease considerably, with decreasing recycling in precipitation and evaporation in absolute as well as relative numbers. The three continents in the Northern Hemisphere - North America, Europe and Asia - show the opposite from South America. Here precipitation and evaporation rates increase, leading to more moisture available for recycling and thus higher moisture recycling rates. Africa and Oceania's increased precipitation is explained by the fact that these continents receive more from oceanic evaporation.

Zooming into the case study areas shows that regions specifically can be affected by seasonality in precipitation and evaporation rates. It became clear that Amazonia will get drier, with a distinct dry season from August until November. This can be explained by decreased evaporation from the case study area itself. Even though moisture still evaporates from the oceans East of the area, the clouds that this evaporation forms will not precipitate on Amazonia as much as it did in the end-20th century. Instead, the clouds do not fill up with moisture while travelling over Amazonia, causing the clouds to move over the region before they precipitate. Western Africa on the other hand showed an increase in precipitation rate, with a specific wet season from July until October. This increase in precipitation is explained by tracking moisture through the atmosphere. Increased oceanic evaporation South and West of Western Africa and a change in direction of moisture fluxes lead to a larger input of moisture from the oceans. Although this is the largest contributor to the increased precipitation in Western Africa, increased local moisture recycling contributed as well.

In conclusion, atmospheric moisture transport can explain changes that occur in precipitation patterns with climate change. Although globally there are no significant changes visible in precipitation patterns, zooming into smaller regions explains more about the changes that might happen in the future. With increasing air temperatures, evaporation will increase as long as there is enough moisture available. Regions will get wetter if their source areas are not yet constraint by their moisture limit. Oceanic regions will have enough moisture to evaporate, however, evaporation in land regions will rely on dense vegetation and water bodies. Regions will get drier if their source areas already are limited in moisture, or will be limited in the end-21st century. On top of that, when moisture evaporated from land is more limited in the future, it is likely that moisture travels over land without precipitating.

A

Theoretical background

The IPCC and its forecasts

The Intergovernmental Panel of Climate Change (IPCC) is an organization of governments that are members of the United Nations or WMO. The IPCC currently has 195 members. Thousands of people from all over the world contribute to the work of the IPCC. For the assessment reports, IPCC scientists volunteer their time to assess the thousands of scientific papers published each year to provide a comprehensive summary of what is known about the drivers of climate change, its impacts and future risks, and how adaptation and mitigation can reduce those risks. The IPCC does not conduct its own research. The IPCC has predicted that anthropogenic greenhouse gas emissions are extremely likely the dominant cause of the observed warming since mid-20th century. The IPCC has studied changes in the climate over the last few decades (IPCC, 2014a). The global surface temperature shows a warming trend over the 1880 to 2012 period and precipitation has increased in the mid-latitude land areas of the Northern Hemisphere since 1901. The IPCC expects that the climate will exhibit more changes in the coming decades.

The panel has established four different pathways to describe possible scenarios for the 21st century as a result of greenhouse gas emissions. These Representative Concentration Pathways (RCPs) contain concentration values for greenhouse gases, aerosols and chemically active gases. Next to these climate change related variables, land-use and land-cover change data is also included; meaning that the IPCC has made certain assumptions about land use change and greenhouse gas emissions in the future. For each RCP the values are different. The four RCPs have been named after the related radiative forcing that the respective pathway will lead to by 2100 relative to pre-industrial values. Thus, there is a prediction that there will be an increase in radiative forcing of 2.6 Wm^{-2}, 4.5 Wm^{-2}, 6 Wm^{-2} and 8.5 Wm^{-2} in the scenarios of RCP2.6, RCP4.5, RCP6 and RCP8.5, respectively. In order to understand climate change in the future, the RCPs have been used as an input for many climatic models. Several climate models have produced output based on these RCPs formulated by the IPCC. The latest climate models are combined in the Coupled Model Intercomparison Project Phase 5 (CMIP5). The experiments from the CMIP5 were conducted in order to answer questions that arose from the Fourth Assessment Report (AR4) of the IPCC (IPCC, 2007). The Fifth Assessment Report (AR5) of the IPCC summarises the information found from the CMIP5 experiments (IPCC, 2014a). Currently climate institutes are working on the Coupled Model Intercomparison Project Phase 6 (CMIP6) and early in 2020 the IPCC plans to deliver the Sixth Assessment Report (AR6).

In the AR5 the IPCC addresses the findings of the CMIP5 about observed changes and their causes, future climate change, as well as future pathways for adaptation. There are a few observations and causes that are worth mentioning from the AR5 in the context of the water cycle. Ocean surface salinity can provide evidence for changes in the global water cycle according to the IPCC. The IPCC has noticed that ocean regions with high salinity where evaporation dominates have become more saline, while regions of low salinity where precipitation dominates have become fresher. This indicates a intensification in the global water cycle (IPCC, 2014a). Furthermore, the IPCC states that it is likely that there are more land regions where there was an increase in extreme precipitation events than land regions where these events decreased. Heavy precipitation events could potentially lead to greater risks of flooding on a regional scale. The IPCC also confidently asserts that many human systems and some ecosystems are significantly vulnerable to climate variability, as can be seen from impacts from recent climate-related extremes, such as heat waves, droughts, floods, cyclones and wildfires (IPCC, 2014a). The panel states with high probability that anthropogenic influences have affected

the global water cycle since 1960 (IPCC, 2014a).

Besides the observations linked to climate change, there are also future climate change predictions. Focusing on the global water cycle, there are a few elements to consider. The IPCC foresees a change in precipitation patterns (IPCC, 2014a). It is expected that changes in precipitation will not be uniform. While some regions are likely to experience an increase in annual mean precipitation under RCP8.5, many other regions will probably experience a decrease in annual mean precipitation under the same scenario. To be precise, the IPCC expects an increase in annual mean precipitation in the high-latitudes, equatorial Pacific regions and many mid-latitude wet regions and a decrease in annual mean precipitation in many mid-latitude and subtropical dry regions. Secondly, the IPCC forecasts that extreme precipitation events will very likely become more intense and frequent in the mid-latitudes and over wet tropical regions. The estimated change in precipitation (1986-2005 to 2081-2100) from the IPCC shows the forecast for RCP2.6 and RCP8.5 (Figure A.1). In the scenario with RCP8.5 (on the right) there is a lot of agreement between the different models about the sign of change. In the scenario with RCP2.6 there are still changes, but most of them are within the range of natural variability of precipitation in this area. By looking at the map showed as a result of the change in precipitation in case of RCP8.5 (the right map in Figure A.1), it can be seen that there are a few areas where there is a relative extreme change in precipitation where at least 90% of the models agree upon.

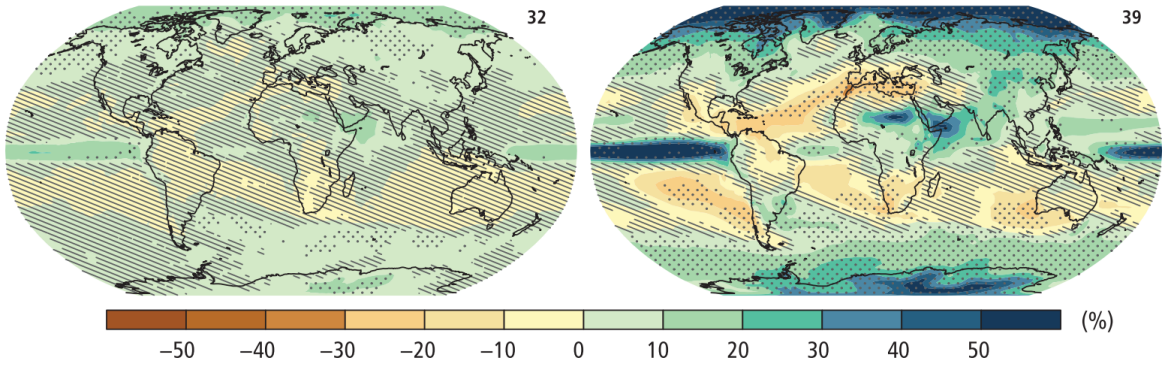

Figure A.1: Change in average precipitation (1986-2005 to 2081-2100) for RCP2.6 (left) and RCP8.5 (right) (IPCC, 2014a). Dots indicate where the estimated precipitation change is larger than one standard deviation in comparison to natural interannual variability and where at least 90% of models agree on the sign of change. Hatching indicates where the estimated change is less than one standard deviation.

Research on changing precipitation patterns

Water scarcity seems to be a more pressing problem in the next decades. Chang et al. (2018) found that even with active water conservation programs, increases in public water demand projected for 2045 could not be met from ground and surface water supplies while achieving current groundwater level and surface water flow regulations. Therefore it is important to study the effects on fresh water availability with climate change. The study of Bosilovich et al. (2005) finds that CO2 has an increasing effect on the water vapor in the atmosphere, which decreases the precipitation. However, this is only the case over oceans, because over land the feedback caused by the surface temperature changes increases the precipitation, since some regions show an increasing trend of continental precipitation, for example in central United States. The warming of the oceans in simulations of Bosilovich et al. 2005 causes higher levels of evaporation and precipitation. Only taking this into account would imply that the water cycle is intensifying. However, the warming of the air causes the total water vapor to increase, as supported by Trenberth (2011). Despite the increasing precipitation, the higher water vapor in the atmosphere increases residence time of water in the atmosphere as well. If the residence time increases, the global cycling rate is decreasing. Another view on the precipitation rates with climate change starts at the fact that the heat capacity of land is smaller than that of the oceans (Kumar et al., 2004). This implies that the adjustment of surface temperatures over land would be quicker than over the ocean. If this were true and there is no moisture constraint on land, this would mean that with increased global warming, there will be a quicker increase in evaporation over land than over the ocean (Kumar et al., 2004). Other research on the other hand concluded that currently available observations do not allow to definitively link changes in global-mean precipitation with changes in the radiative energy budget of the atmosphere (O'Gorman et al., 2012). This study emphasizes the uncertainties that arise for both the observed changes in radiative fluxes and precipitation, meaning that a more extensive and longer-term set of

observations is desirable.

The 'DDWW paradigm' - where dry regions dry out further, whereas wet regions become wetter as the climate warms - has been proposed as a simplified summary of many expected as well as observed changes in precipitation patterns over land (Greve et al., 2014). Held and Soden (2006) show that under certain assumptions about atmospheric behaviour, wet regions will get wetter and dry regions will get drier. However, other research shows that the fraction of land area that experiences a 'DDWW' pattern is approximately as large as the fraction of land area that experiences the opposite pattern, where dry areas will get wetter, and wet areas will get drier (Greve et al., 2014). Moreover, comparing the average annual precipitation between 1999-2008 (Figure A.2) to the expectations for changes in precipitation from the IPCC (Figure A.1), it can be seen that some dry regions will experience an increase in precipitation. However, the IPCC does state that "In many mid-latitude and subtropical dry regions, mean precipitation will likely decrease, while in many mid-latitude wet regions, mean precipitation will likely increase under the RCP8.5 scenario." (IPCC, 2014a). This does not necessarily imply that all dry regions dry out futher and all wet regions will get wetter, but it also does not deny the DDWW paradigm.

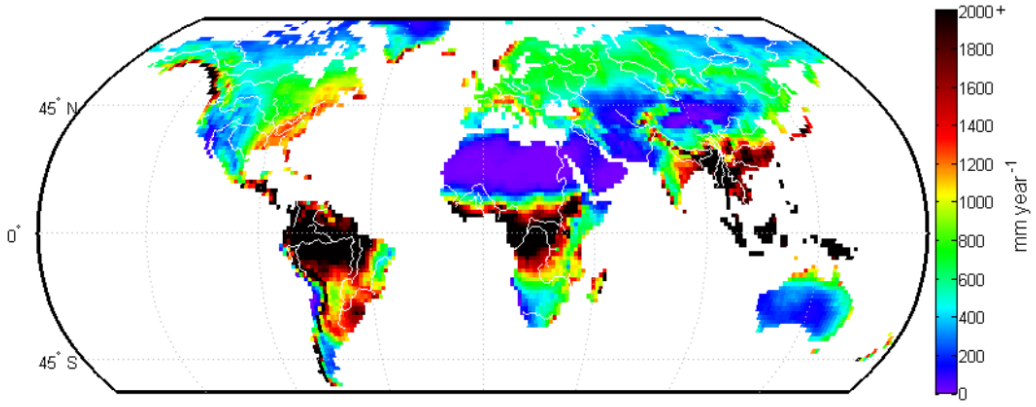

Figure A.2: Annual average precipitation (1999-2008) in mm y^{-1}. The plot shows areas with low rates as purple to blue, areas with moderate rates as green to yellow and areas with high rates as red to black. (van der Ent, 2014)

Research on moisture recycling

Precipitation is often seen as an external forcing. However, all moisture that precipitates, has evaporated somewhere from the Earth's surface, either from land or from the oceans. Continental moisture recycling is the phenomenon of terrestrial evaporation upwind travelling through the atmosphere and returning as terrestrial precipitation downwind (Keys et al., 2014). Research into moisture recycling shows that a large fraction of terrestrial precipitation finds its origin as evaporation from land surfaces (Dirmeyer and Brubaker, 2007). For example, the global decrease in continental precipitation is mostly related to regional decreases in tropical land areas (Bosilovich et al., 2005). Changes in land use and human interactions with water resources can affect the amount of moisture available as a source for terrestrial evaporation (van der Ent, 2014). For example, deforestation decreases evaporation and the construction of water reservoirs increases evaporation. Because of moisture recycling, water can cross catchment and continental boundaries through the atmosphere. Therefore land-use changes upwind affect the situation downwind, in terms of precipitation rates and runoff (Wang-Erlandsson et al., 2018). This is happening because vegetation affects precipitation patterns by mediating moisture, energy and trace-gas fluxes between the surface and atmosphere (Spracklen et al., 2012). By replacing forests by meadows or crops, evaporation from soil and vegetation decreases, leading to reduced atmospheric humidity and potentially decreasing precipitation locally or in other regions. Climate models predict that large-scale tropical deforestation causes reduced regional precipitation, although the magnitude of the effect is model and resolution dependent (Spracklen et al., 2012). However, deforestation has also been linked to increased precipitation locally but observational studies have been unable to explore the impact of large-scale deforestation. More than 60% of tropical land surface produce twice as much precipitation in air passing over the dense forests than over sparse vegetation (Spracklen et al., 2012).

Modelling moisture recycling

In order to research the hydrological cycle and the origin of precipitation the WAM-2layers model is used (van der Ent, 2014). The WAM-2layers model tracks moisture through the atmosphere. This provides information to study moisture recycling. The model identifies two parameters; the continental precipitation recycling ratio (ρ_c) and the continental evaporation recycling ratio (ϵ_c). The continental precipitation recycling ratio ρ is defined as the amount of precipitation that originates from terrestrial evaporation over the total amount of precipitation. The continental evaporation recycling ratio ϵ is defined as the amount of evaporation that returns as terrestrial precipitation over the total amount of evaporation. These two parameters together can indicate which areas are sinks - where there is high ρ_c - and from which source this precipitation originates - where there is high ϵ_c (Van Der Ent et al., 2010). Research from van der Ent (2014) presents both ratios with atmospheric data from 1999-2008. The annual average ρ and ϵ are presented in Figure A.3 and Figure A.4, respectively.

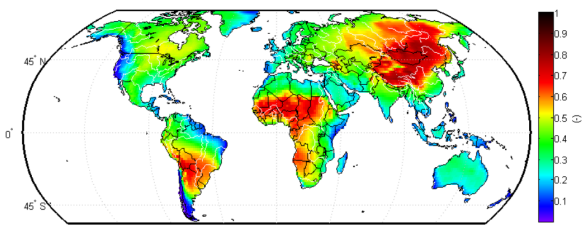

Figure A.3: Continental precipitation recycling ratio ρ_c (1999-2008), defined as the ratio between the precipitation at a certain location that originated as evaporation from land surface and the total precipitation at that location. Red colors indicate that a relatively large amount of the precipitation originates from land and blue colors indicate that a relatively small amount of precipitation originates from land, thus in blue areas most precipitation originates from the ocean. (van der Ent, 2014)

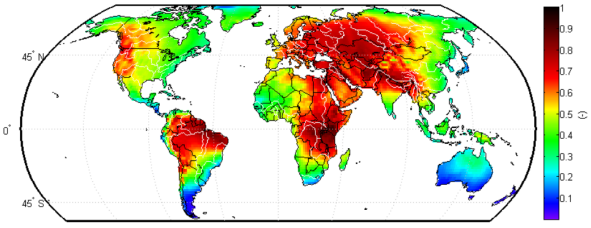

Figure A.4: Continental evaporation recycling ratio ϵ (1999-2008), defined as the ratio between the evaporation at a certain location that will return as precipitation on land and the total evaporation at that location. Red colors indicate that a relatively large amount of the evaporation will precipitate on land and blue colors indicate that a relatively small amount of evaporation will precipitate on land, thus in blue areas most evaporation will precipitate on the oceans. (van der Ent, 2014)

From these two figures the large scale motions of moisture through the atmosphere can already be identified. Areas where there is high ϵ_c - the red areas in Figure A.4 - are major sources for continental precipitation. Areas where there is high ρ_c - the red areas in Figure A.3 - are major sinks for continental evaporation. Broadly it can be said that water moves through the atmosphere from the red areas in Figure A.3 to the red areas in Figure A.4. In the Northern Hemisphere this is from East to West and in the Southern Hemisphere from West to East. This information together with the expected change in precipitation can illustrate which regions are the most sensitive to changes in temperature and land use. Namely, regions with high ρ_c, depend on certain terrestrial regions as a source for precipitation. When climate change occurs there might be an increase or decrease in evaporation at these moisture providing regions and thus either a positive or a negative change in precipitation on the receiving end. The moisture tracking model can be used to provide explanation to why there is a change in precipitation pattern due to climate change.

Results from van der Ent (2014) show that in the years 1999-2008 there was more moisture recycling in summer than in winter. Not only the overall continental moisture feedback is a more dominant process in summer than in winter, this also plays a larger role on a local scale. The effect of land-use change on moisture recycling is also very different during wet and dry seasons and during summer and winter. This indicates that seasonality is an important factor to take into account (van der Ent, 2014).

Problem analysis
The RCP trajectories contain information of greenhouse gas emissions and atmospheric concentrations, air pollutant emissions and land-use changes. RCP8.5 gives input for the GFDL model runs. The GFDL model generates projections with output for several variables, including the surface air temperature and the average daily precipitation rates. These two variables are not independent. On the contrary, the amount of precipitation has an indirect causal relation with the variables within the RCPs and is more directly linked to the surface temperature. In Figure A.5, the main causal relations within the modelling environment are displayed. This diagram shows the main variables that are focused on in this research. Many variables that are also interlinked with the displayed variables are left out the diagram, because these are not the variables of interest.

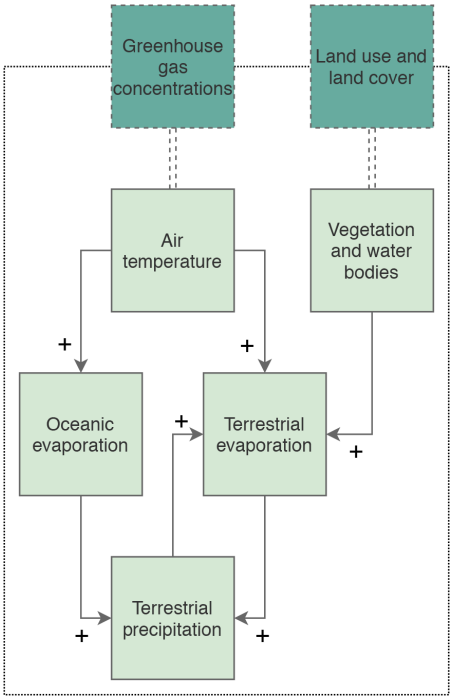

Figure A.5: Causal relation diagram. The darker colored boxes indicate external factors, the lighter boxes are factor influenced within the scope of the research and thus lie within the system boundary. Double dotted lines indicate that the external factor has an effect on the factor, the arrows indicate a causal relation, either negative (-) or positive (+). This diagram is intended as a tool for explanation and is a simplified version of reality.

The RCPs contain values for greenhouse gas concentrations and land use changes, which influences air temperature and the amount of vegetation and water bodies on land. Higher air temperature would increase the energy present to evaporate moisture, and thus increase both oceanic and terrestrial evaporation. It can be assumed that the ocean does not have a moisture constraint. Terrestrial evaporation however, is constrained by the available moisture, since moisture on land is limited. Consecutively, the moisture that is available on land is influenced by the land use in terms of vegetation type and amount of water bodies, such as lakes. Land-use change can either increase or decrease the available moisture, by for example deforestation or building reservoirs. Vegetation and water bodies in general increase the available moisture. More evaporation from both an oceanic and a terrestrial source will increase terrestrial precipitation.

The factor of interest from the diagram in Figure A.5 is the terrestrial precipitation. Finding out where the origin of the precipitation is in the expected increase or decrease of precipitation with the climate change forecast from the IPCC, might provide a clearer explanation to why there is an effect on terrestrial precipitation in the first place. The origin of terrestrial precipitation is either as oceanic or terrestrial evaporation. The reason for spatial changes in precipitation or regions that become dryer or wetter are currently not understood either. Understanding the global water cycle is relevant for future studies, because it can explain many future climate scenarios. Moisture tracking could contribute to an answer for this, because it provides information about the ratio between oceanic and terrestrial evaporation as a source for terrestrial precipitation.

Based on the fact that it is not yet understood why certain changes in precipitation happen with climate change, it can be concluded that finding out where the increase or decrease in precipitation finds its origin

can explain a lot about the effects from climate change on the global water cycle. The goal of this research is to gain more insights about the causes of either positive or negative changes in precipitation due to climate change. In order to achieve this goal, the following research question needs to be answered:

To what extent can atmospheric moisture transport explain changes in precipitation with climate change?

This research question consists of two parts. The first part is a global study. The outcome of the global study will define what regions the second part will focus on. This second part is a regional study that gives the opportunity for a study focused more on seasonality. The step-by-step plan for the global phase is the following:

1. What are the global spatial changes in precipitation, evaporation and air temperature between the end-20th century (1986-2005) and the end-21st century (2081-2100)?
2. What is the globally averaged yearly precipitation, evaporation and air temperature in both the end-20th century (1986-2005) and the end-21st century (2081-2100)?
3. What is the continental precipitation recycling ratio ρ_c for the end-20th century (1986-2005) and the end-21st century (2081-2100)?
4. What is the continental evaporation recycling ratio ϵ_c for the end-20th century (1986-2005) and the end-21st century (2081-2100)?

   Following these steps for the global phase will lead to the identification of the case study areas, that have the following step-by-step plan, for the regional phase:

5. What are the yearly temporal patterns in precipitation, evaporation and temperature for the end-20th century (1986-2005) and the end-21st century (2081-2100) in the two case study areas?
6. What is the continental precipitation recycling ratio ρ_c for the end-20th century (1986-2005) and the end-21st century (2081-2100) for the case study areas? Where do these regions depend on? What is the precipitationshed of these regions?
7. What are the current characteristics of the study areas (population, land use, ecosystems) and how are they affected by the changes?

Research scope
The focus of the research lies on the effect of climate change on precipitation patterns and tracks atmospheric moisture transport to provide an explanation of this effect. This project focuses on two specific case studies, which demarcates the geographic scope of this research. The study regards terrestrial precipitation, evaporation and temperature and explores the ratio between the source of oceanic and terrestrial precipitation as well as the ratio between the destination of oceanic and terrestrial evaporation. The project only focuses on two 20-year time series, namely 1986-2005, the end-20th century scenario and 2081-2100, the end-21st century scenario.

B

Methodological foundation

Precipitation
Precipitation is an important hydrological variable and will be analysed in depth before using it in the WAM-2layers.

P	Precipitation	mm d^{-1}

The GFDL data provides precipitation in kg $m^{-2}s^{-1}$, this needs to be rewritten to m^3d^{-1}. This is done with the following equation:

$$P_{WAM2} = P_{GFDL} * \rho * A * \frac{t}{t} \tag{B.1}$$

Where:

P_{WAM2}	Precipitation in WAM-2layers	m^3d^{-1}
P_{GFDL}	Precipitation in GFDL data	kg m^{-2}
ρ	Density of water	1000 kg m^{-3}
A	Surface area of grid cell	m^2
$\frac{t}{t}$	Correcting for time units	86400 s d^{-1}

Evaporation
Similarly to precipitation, evaporation is an important variable for describing the hydrological circumstances. Evaporation will be analysed before it will be used to model moisture recycling.

E	Evaporation	mm d^{-1}

Evaporation is initially given as latent heat flux in the GFDL data. It needs to be calculated in $m^{-3}d^{-1}$.

$$E_{WAM2} = \frac{H}{\rho\lambda} * A * \frac{t}{t} \tag{B.2}$$

Where:

E_{WAM2}	Evaporation in WAM-2layers	m^3d^{-1}
H	Surface upward latent heat flux	W m^{-2}
ρ	Density of water	1000 kg m^3
λ	Heat of vaporisation	J kg^{-1}
A	Surface area of grid cell	m^2
$\frac{t}{t}$	Correcting for time units	86400 s d^{-1}

Surface air temperature
Even though the surface air temperature is not necessary to model moisture recycling, it provides important

background information. This variable is thus included in the derivation of the hydrological variables.

Surface pressure
To calculate the surface pressure, the temperature and geopotential height over multiple levels is needed. The surface pressure can be calculated using the vertical pressure variation:

$$z_s = \frac{T_0}{L}((\frac{P_s}{P_0})^{-\frac{LR}{g}} - 1) \tag{B.3}$$

This can be rewritten into:

$$p_s = p_0(\frac{z_s L}{T_0} + 1)^{-\frac{g}{LR}} \tag{B.4}$$

Where:

p_s	Surface pressure	Pa
p_0	Pressure at reference level	Pa
z_s	Surface height in respect to reference level	m
T_0	Air temperature at reference level	K
L	Atmospheric lapse rate	-6.5 10^{-3} K m^{-1}
R	Gas constant	287.053 J kg^{-1} K^{-1}
g	Gravitational acceleration	9.81 m s^{-2}

This method uses a reference point, which is in this case the pressure level where the temperature and geopotential height are known. The reference pressure level is the pressure levels nearest to the surface and above the surface. The difference in height between the surface and the pressure level is calculated with the surface height and the geopotential height of the pressure level. Subsequently, with equation B.4 the surface pressure can be calculated.

Air pressure at the boundary layer
With the surface pressure the boundary level can be determined. The pressure at the boundary layer is determined by van der Ent 2014, where wind above the boundary layer travels in another direction than the wind below the boundary layer.

$$p_{boundary} = 7438.803 + 0.728786 p_s \tag{B.5}$$

Where:

$p_{boundary}$	Pressure at boundary layer	Pa
p_s	Surface pressure	Pa

Wind
The horizontal wind patterns are available in the GFDL data for the northward wind speed - where a positive sign means a movement of wind towards the North and negative means a movement towards the South - and the eastward wind speed - where a positive sign means a movement of wind towards the East and negative means a movement towards the West. Both the northward and the eastward wind data are available for multiple levels and at the surface. If a pressure level is located under the surface level (coming from the previously calculated surface pressure), this will be corrected for the wind levels.

u_a	Eastward wind	m s^{-1}
v_a	Northward wind	m s^{-1}

Specific humidity
The GFDL data for specific humidity is available over multiple layers as well as for the surface. Similarly to the wind data, if a pressure level is located under the surface level (coming from the previously calculated surface pressure), this will be corrected for the specific humidity levels.

q_s	Specific humidity	kg kg^{-1}

The static parameters:

- Land sea mask
  The land sea mask describes whether a certain grid cell is classified as land (more than 50% land) or sea (less than 50% land). This mask is needed to determine if moisture originates from land or sea and whether it precipitates on land or sea.
- Surface height
  The surface height is the height of the surface of the Earth for each grid cell. In this research it is assumed that the surface height is a static parameter.

C

Extra model output

Hydrological parameters

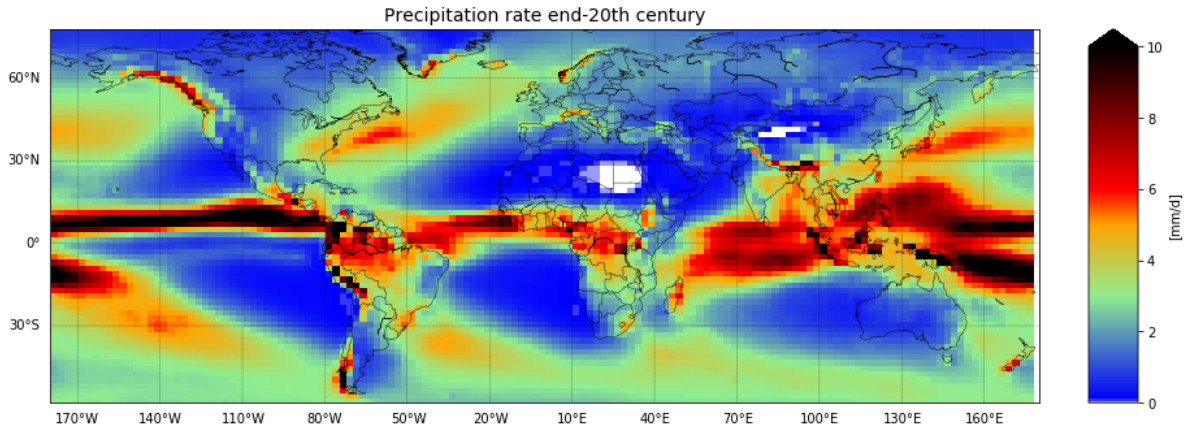

(a)

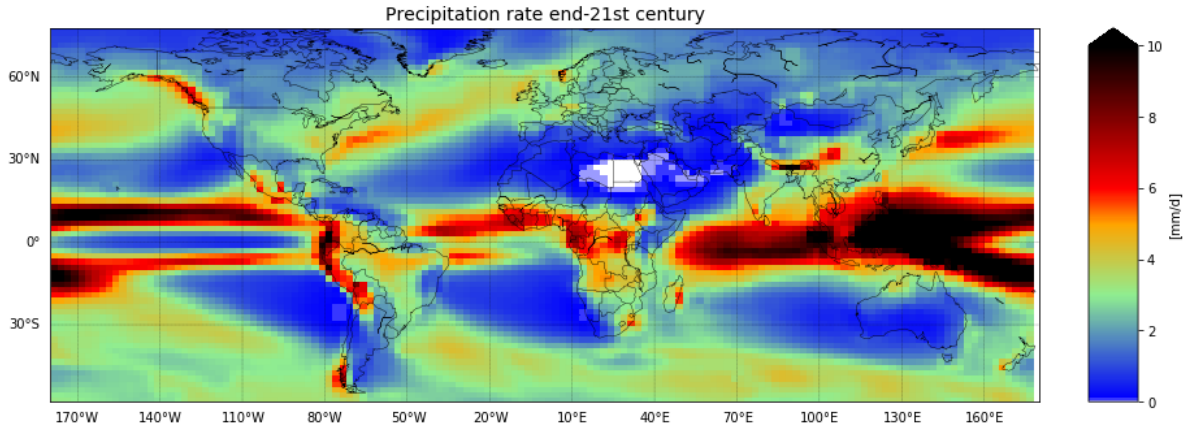

(b)

Figure C.1: Global precipitation rates including the oceans for end-20th century (a) and end-21st century (b), in mm d^{-1}. The plots show areas with low rates as blue, areas with moderate rates as green to yellow and areas with high rates as red to black. White areas represent regions with precipitation rates close to zero.

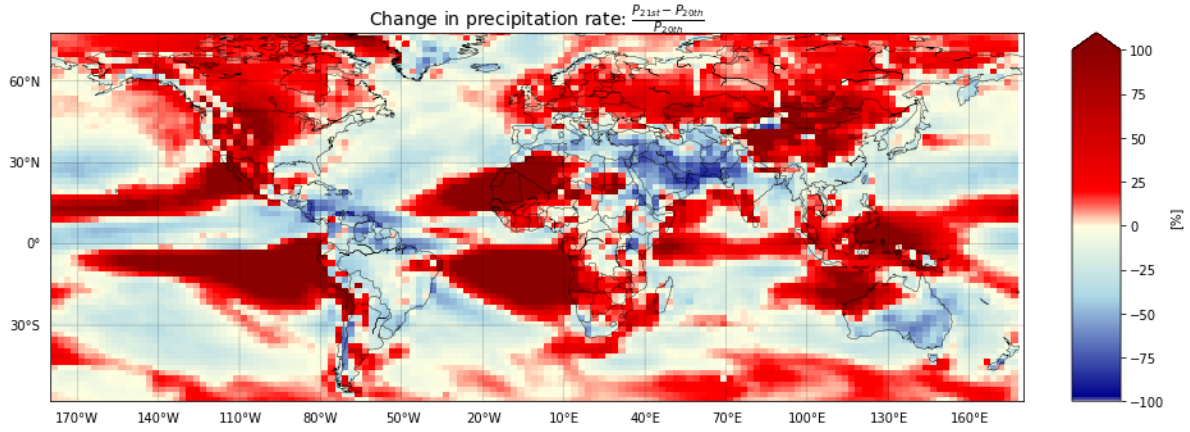

Figure C.2: Global average change in daily precipitation in percentage change relative to the past scenario including the oceans. Red regions refer to an increase in precipitation and blue regions refer to a decrease in precipitation.

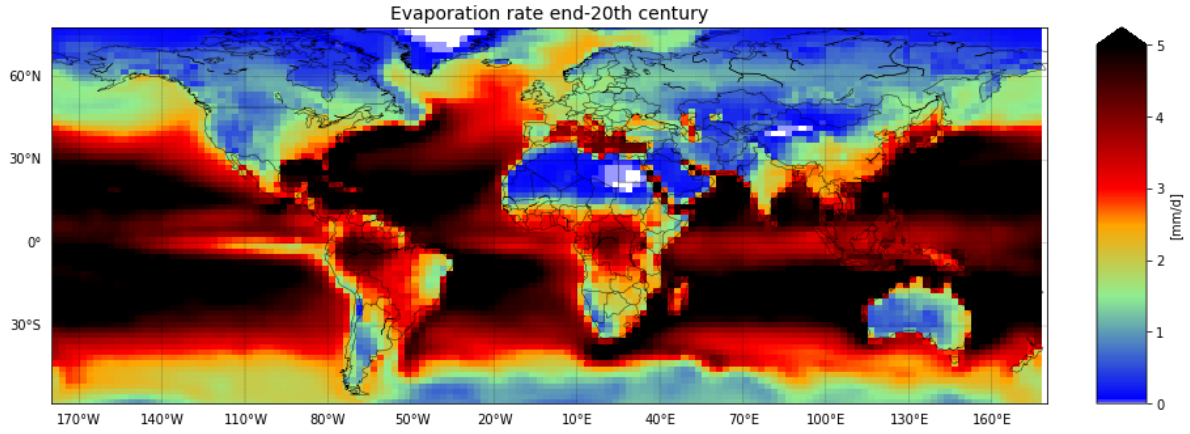

(a)

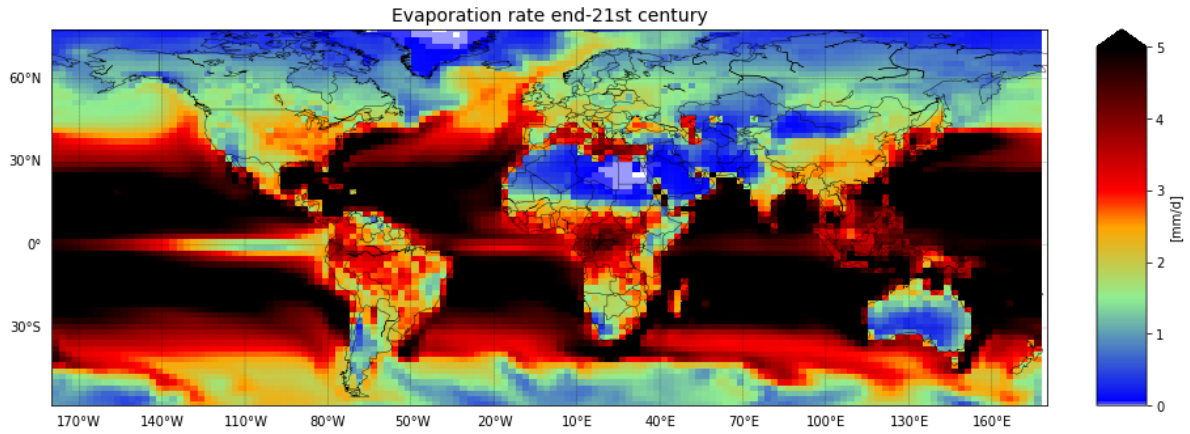

(b)

Figure C.3: Global evaporation rates including the oceans for end-20th century (a) and end-21st century (b), in mm d^{-1}. The plots show areas with low rates as blue, areas with moderate rates as green to yellow and areas with high rates as red to black. White areas represent regions with evaporation rates close to zero.

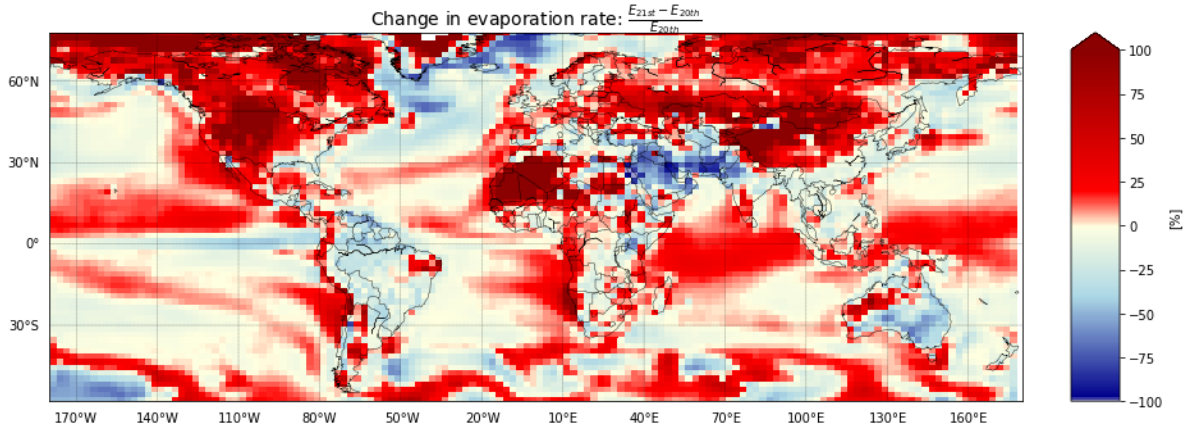

Figure C.4: Global average change in daily evaporation in percentage change relative to the past scenario including the oceans. Red regions refer to an increase in evaporation and blue regions refer to a decrease in evaporation.

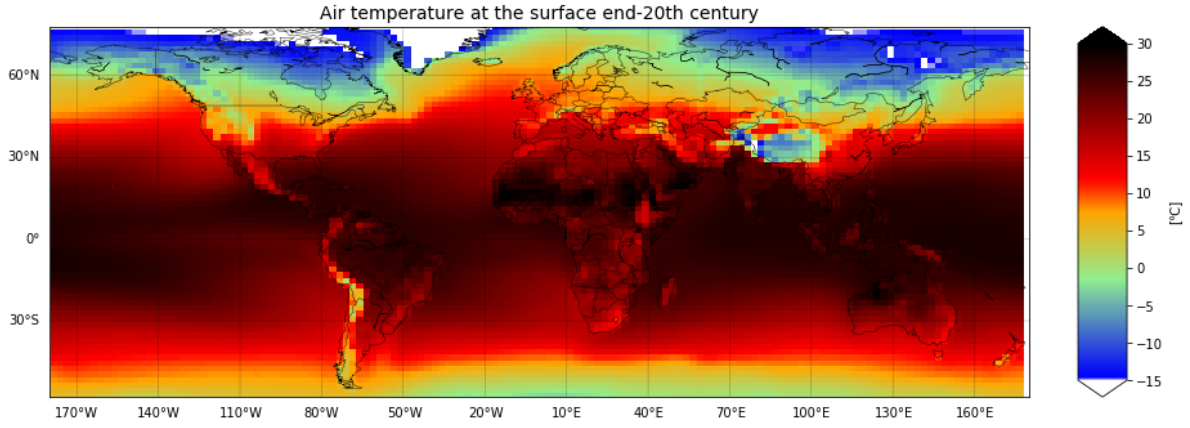

(a)

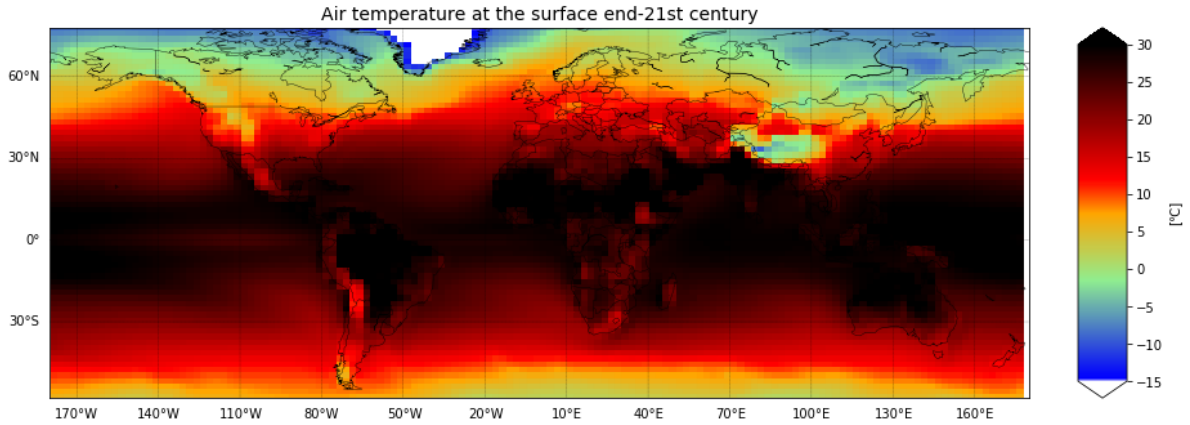

(b)

Figure C.5: Global surface air temperature including the oceans for end-20th century (a) and end-21st century (b), in °C. Blue colors indicate the lowest temperatures, green to yellow colors indicate moderate temperatures and red to black indicate the highest temperatures.

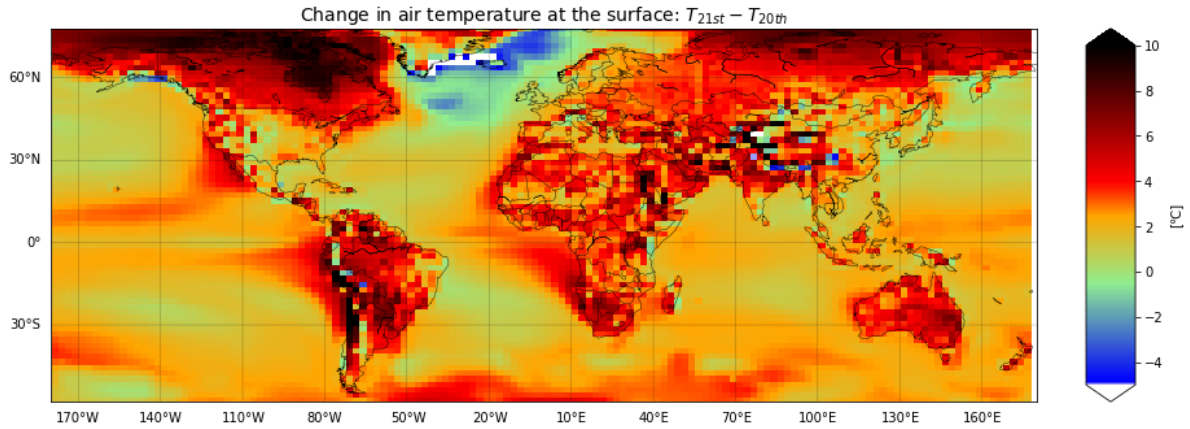

Figure C.6: Global absolute change in daily surface air temperature of the future scenario as respect to the past scenario (end-21st century minus end-20th century) in °C including the oceans, with green indicating no change, blue indicating lower temperatures in the future and yellow to red to black indicating an increase in temperature in the future.

Moisture recycling

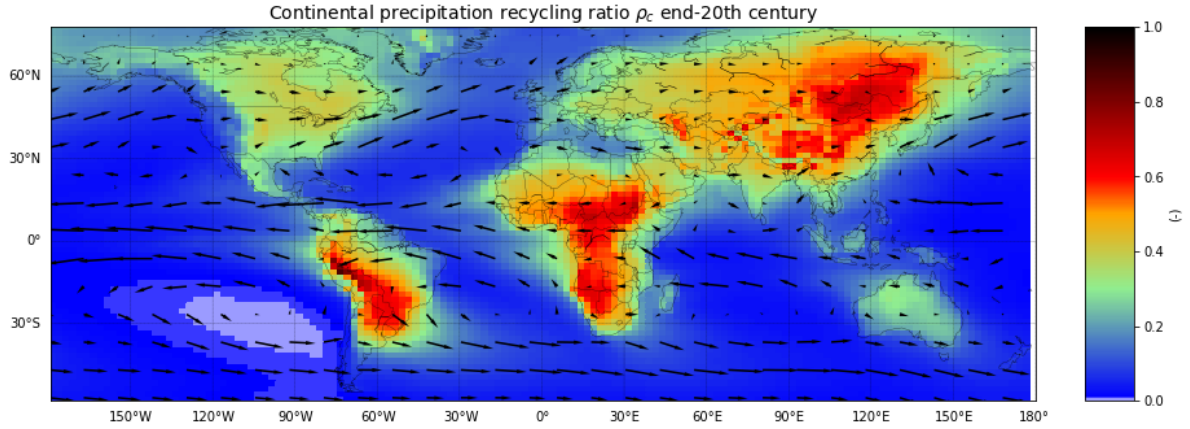

(a)

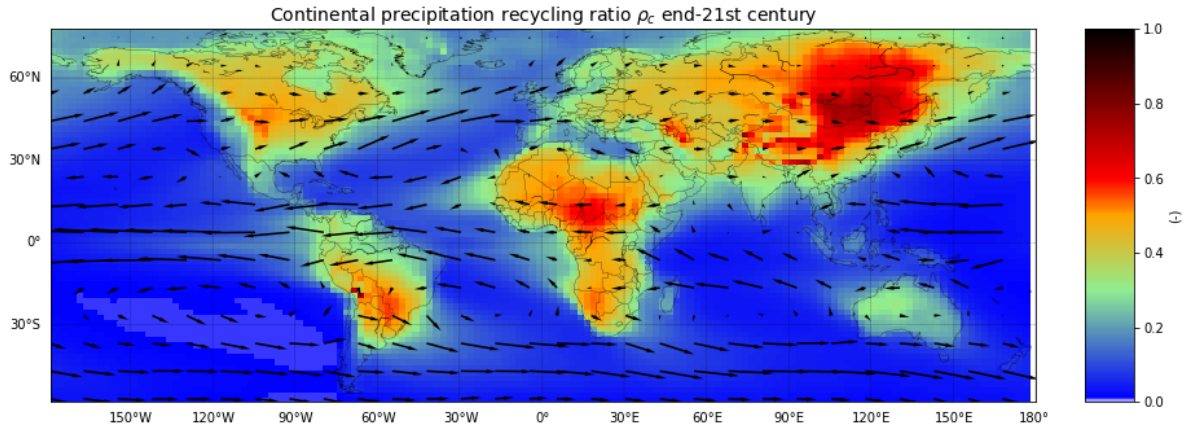

(b)

Figure C.7: Continental precipitation recycling ratio including the oceans for end-20th century (a) and end-21st century (b), defined as the ratio between the precipitation in a specific grid cell that originated as evaporation from land surface and the total precipitation in that grid cell. Red colors indicate that a relatively large amount of the precipitation originates from land and blue colors indicate that a relatively small amount of precipitation originates from land, thus in blue areas most precipitation originates from the ocean. Arrows represent the direction and magnitude of the moisture fluxes.

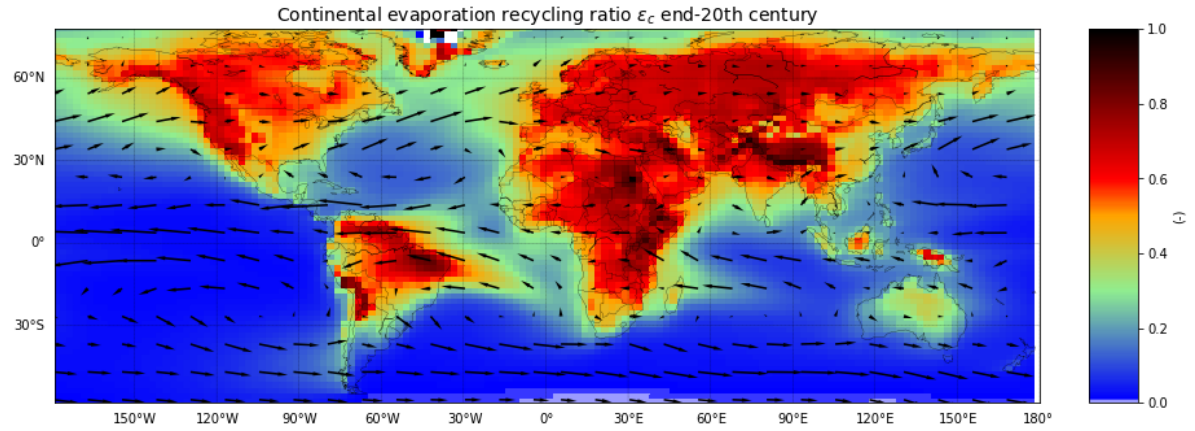

(a)

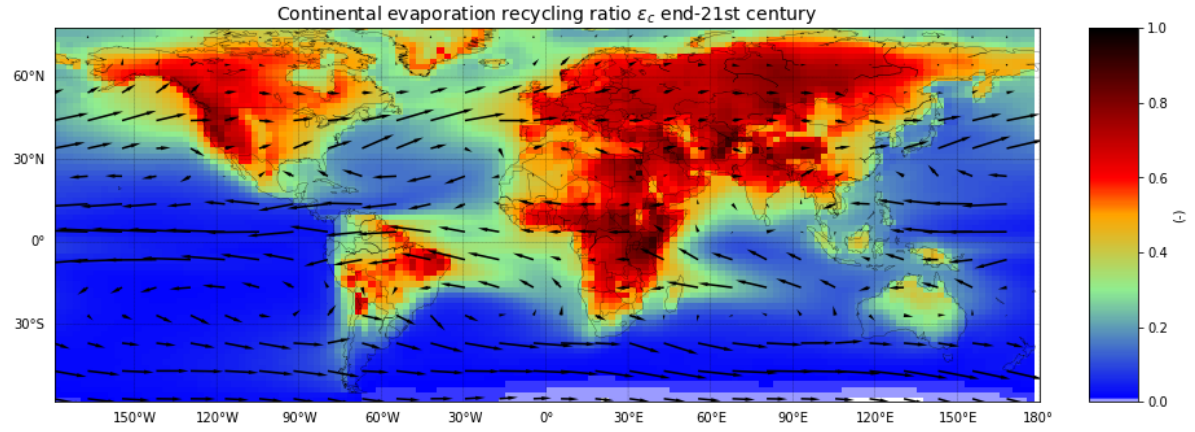

(b)

Figure C.8: Continental evaporation recycling ratio including the oceans for end-20th century (a) and end-21st century (b), defined as the ratio between the evaporation in a specific grid cell that will return as precipitation on land and the total evaporation in that grid cell. Red colors indicate that a relatively large amount of the evaporation will precipitate on land and blue colors indicate that a relatively small amount of evaporation will precipitate on land, thus in blue areas most evaporation will precipitate on the oceans. Arrows represent the direction and magnitude of the moisture fluxes.

Moisture fluxes

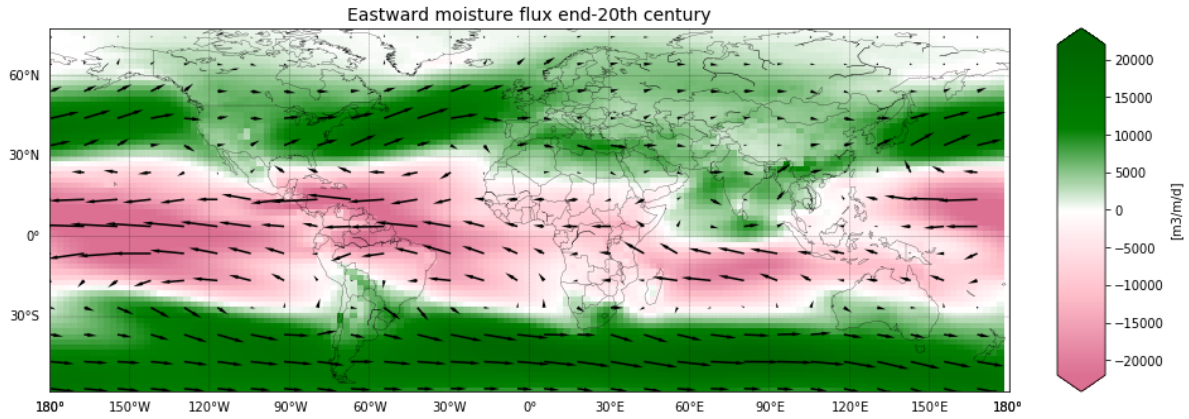

(a)

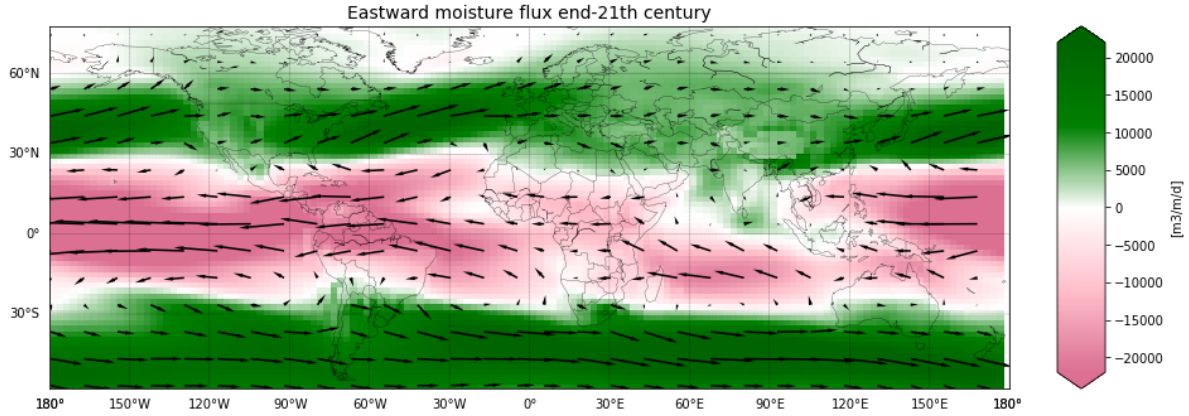

(b)

Figure C.9: Global eastward moisture fluxes including the oceans for end-20th century (a) and end-21st century (b). The colors indicate the direction and magnitude of the moisture flux in the East-West plane. Green colors indicate an Eastward movement of moisture and pink colors indicate a Westward movement of moisture. The case study area is demarcated by the black rectangle.

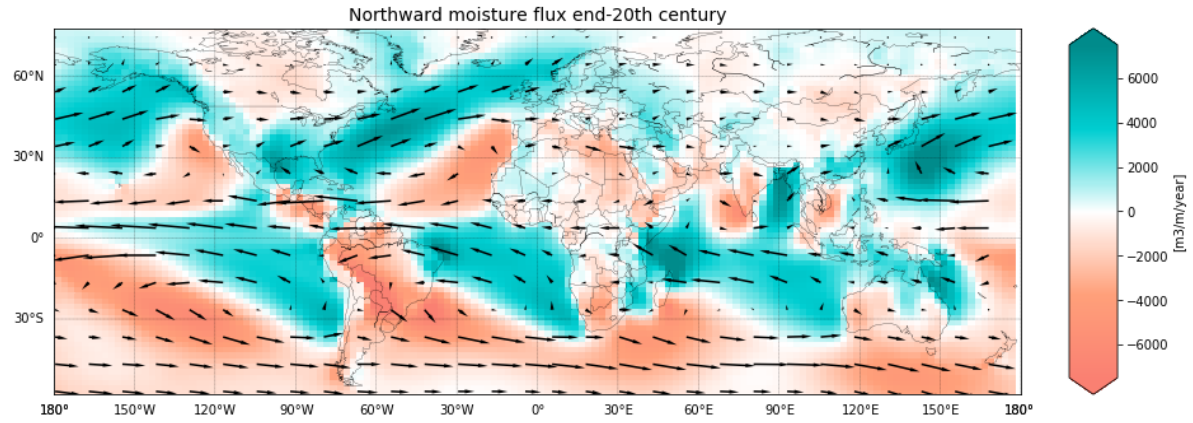

(a)

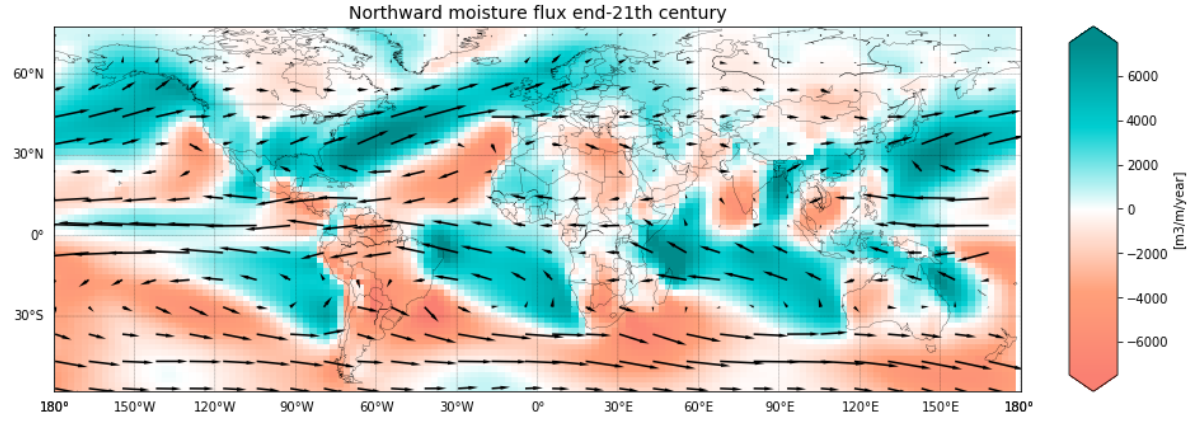

(b)

Figure C.10: Global northward moisture fluxes including the oceans for end-20th century (a) and end-21st century (b). The colors indicate the direction and magnitude of the moisture flux in the North-South plane. Blue colors indicate an Northward movement of moisture and orange colors indicate a Southward movement of moisture. The case study area is demarcated by the black rectangle.

Bibliography

Allen, M. R. and Ingram, W. J.: Constraints on future changes in climate and the hydrologic cycle, Nature, 419, https://doi.org/10.1038/nature01092, 2002.

Anderson-Teixeira, K. J., Snyder, P. K., Twine, T. E., Cuadra, S. V., Costa, M. H., and Delucia, E. H.: Climate-regulation services of natural and agricultural ecoregions of the Americas, Nature Climate Change, 2, 177–181, https://doi.org/10.1038/nclimate1346, URL http://dx.doi.org/10.1038/nclimate1346, 2012.

Beurs, K. M. D., Henebry, G. M., Owsley, B. C., and Sokolik, I. N.: Large scale climate oscillation impacts on temperature , precipitation and land surface phenology in Central Asia Large scale climate oscillation impacts on temperature , precipitation and land surface phenology in Central Asia, 2015.

Bosilovich, M. G., Schubert, S. D., Walker, G. K., Bosilovich, M. G., Schubert, S. D., and Walker, G. K.: Global Changes of the Water Cycle Intensity, Journal of Climate, 18, 1591–1608, https://doi.org/10.1175/JCLI3357.1, URL http://journals.ametsoc.org/doi/abs/10.1175/JCLI3357.1, 2005.

Chang, S., Graham, W., Geurink, J., Wanakule, N., and Asefa, T.: Evaluation of impact of climate change and anthropogenic change on regional hydrology, Hydrology and Earth System Sciences Discussions, pp. 1–43, https://doi.org/10.5194/hess-2018-91, URL https://www.hydrol-earth-syst-sci-discuss.net/hess-2018-91/, 2018.

Dirmeyer, P. A. and Brubaker, K. L.: Characterization of the Global Hydrologic Cycle from a Back-Trajectory Analysis of Atmospheric Water Vapor, Journal of Hydrometeorology, 8, 20–37, https://doi.org/10.1175/JHM557.1, URL http://journals.ametsoc.org/doi/abs/10.1175/JHM557.1, 2007.

FAO: Food and Argiculture Organization of the United Nations, Hydrological basins in South America (Derived from hydrosheds), URL http://www.fao.org/geonetwork/srv/en/main.home, 2009.

GADM: Database of Global Administrative Areas, shapefile level 0, v3.6, URL https://gadm.org/download_world.html, 2018.

Ge, F., Zhu, S., Peng, T., Zhao, Y., Sielmann, F., Fraedrich, K., and Zhi, X.: Risks of precipitation extremes over Southeast Asia : does 1 . 5 ° C or 2 ° C global warming make a difference ? Risks of precipitation extremes over Southeast Asia : does 1 . 5 ° C or 2 ° C global warming make a difference ?, 2019.

Greve, P., Orlowsky, B., Mueller, B., Sheffield, J., Reichstein, M., and Seneviratne, S. I.: Global assessment of trends in wetting and drying over land, Nature Geoscience, 7, 716–721, https://doi.org/10.1038/NGEO2247, 2014.

Held, I. M. and Soden, B. J.: Robust responses of the hydrologic cycle to global warming, J. Clim., 19, 5686–5699, https://doi.org/10.1175/JCLI3990.1, URL http://dx.doi.org/10.1175/JCLI3990.1, 2006.

Huber, M. and Knutti, R.: Anthropogenic and natural warming inferred from changes in Earth ' s energy balance, Nature Geoscience, 5, 31–36, https://doi.org/10.1038/ngeo1327, URL http://dx.doi.org/10.1038/ngeo1327, 2011.

Hurtt, G. C., Chini, L. P., Frolking, S., Betts, R. A., Feddema, J., and Fischer, G.: Harmonization of land-use scenarios for the period 1500 – 2100 : 600 years of global gridded annual land-use transitions , wood harvest , and resulting secondary lands, pp. 117–161, https://doi.org/10.1007/s10584-011-0153-2, 2011.

IPCC: Climate Change 2007 Synthesis Report, Intergovernmental Panel on Climate Change [Core Writing Team IPCC], https://doi.org/10.1256/004316502320517344, 2007.

IPCC: Climate Change 2014: Synthesis Report., Contribution of Working Groups I, II and III to the Fifth Assessment Report of the Intergovernmental Panel on Climate Change, https://doi.org/10.1017/CBO9781107415324, 2014a.

IPCC: Climate Change 2014 Synthesis Report Summary Chapter for Policymakers, Ipcc, p. 31, https://doi.org/10.1017/CBO9781107415324, 2014b.

IPCC: Climate Change and Land, Ipcc, URL https://www.ipcc.ch/2019/08/08/land-is-a-critical-resource{_}srccl/, 2019.

Keys, P. W., Barnes, E. A., Van Der Ent, R. J., and Gordon, L. J.: Variability of moisture recycling using a precipitationshed framework, Hydrology and Earth System Sciences, 18, 3937–3950, https://doi.org/10.5194/hess-18-3937-2014, 2014.

Kumar, A., Yang, F., Goddard, L., and Schubert, S.: Differing Trends in the Tropical Surface Temperatures and Precipitation over Land and Oceans, Journal of Climate, pp. 653–664, URL https://doi.org/10.1175/1520-0442(2004)017{%}3C0653:DTITTS{%}3E2.0.CO;2, 2004.

Marelle, L., Myhre, G., Samset, B. H., Hodnebrog, Ø., and Sillmann, J.: The Changing Seasonality of Extreme Daily Precipitation, https://doi.org/10.1029/2018GL079567, 2018.

Marengo, J. A. and Espinoza, J. C.: Extreme seasonal droughts and floods in Amazonia : causes ,, 1050, 1033–1050, https://doi.org/10.1002/joc.4420, 2016.

Meinshausen, M., Smith, S. J., Calvin, K., Daniel, J. S., Kainuma, M. L., Lamarque, J., Matsumoto, K., Montzka, S. A., Raper, S. C., Riahi, K., Thomson, A., Velders, G. J., and van Vuuren, D. P.: The RCP greenhouse gas concentrations and their extensions from 1765 to 2300, Climatic Change, 109, 213–241, https://doi.org/10.1007/s10584-011-0156-z, 2011.

N. Diffenbaugh, C. F.: Changes in Ecologically Critical Terrestrial Climate Conditions, Science, 341, 486–493, 2013.

O'Gorman, P. A., Allan, R. P., Byrne, M. P., and Previdi, M.: Energetic Constraints on Precipitation Under Climate Change, Surveys in Geophysics, 33, 585–608, https://doi.org/10.1007/s10712-011-9159-6, 2012.

Seager, R., Ting, M., Held, I., Kushnir, Y., Lu, J., Vecchi, G., Huang, H., Harnik, N., Leetmaa, A., Lau, N., Li, C., Velez, J., and Naik, N.: Model Projections of an Imminent Transition to a More Arid Climate in Southwestern North America, 1475, 1181–1185, 2007.

SEDAC: Socioeconomic Data and Applications Center, Gridded Population of the World (GPW), Population Density, v4.11, URL https://sedac.ciesin.columbia.edu/data/set/gpw-v4-population\protect\discretionary{\char\hyphenchar\font}{}{}density\protect\discretionary{\char\hyphenchar\font}{}{}rev11, 2015.

Smil, V.: Energy Transitions: Global and National Perspectives (Second expanded and updated edition), URL http://vaclavsmil.com/2016/12/14/energy-transitions-global-and-national-perspectives-second-expanded-and-updated-edition/, 2016.

Spracklen, D. V., Arnold, S. R., and Taylor, C. M.: Observations of increased tropical rainfall preceded by air passage over forests, Nature, 489, 282–285, https://doi.org/10.1038/nature11390, URL http://dx.doi.org/10.1038/nature11390, 2012.

Trenberth, K. E.: Changes in precipitation with climate change, Climate Research, 47, 123–138, https://doi.org/10.3354/cr00953, 2011.

Tuinenburg, O. A., Hutjes, R. W. A., and Kabat, P.: The fate of evaporated water from the Ganges basin, Journal of Geophysical Research Atmospheres, 117, 1–17, https://doi.org/10.1029/2011JD016221, 2012.

UCL: Université catholique de Louvain, Geoportail, Geomatics Earth and Life institude, Globcover 2009 (v2.3), URL http://maps.elie.ucl.ac.be/geoportail/, 2009.

USGS: United States Geological Survey: Earth Explorer, Digital Elevation Map, GMTED2010 W060 to W090, S10 to S30, URL https://earthexplorer.usgs.gov/, 2010.

van der Ent, R. J.: A new view on the hydrological cycle over continents, https://doi.org/10.4233/uuid:0ab824ee-6956-4cc3-b530-3245ab4f32be, 2014.

Van Der Ent, R. J. and Tuinenburg, O. A.: The residence time of water in the atmosphere revisited, Hydrology and Earth System Sciences, 21, 779–790, https://doi.org/10.5194/hess-21-779-2017, 2017.

Van Der Ent, R. J., Savenije, H. H., Schaefli, B., and Steele-Dunne, S. C.: Origin and fate of atmospheric moisture over continents, Water Resources Research, 46, 1–12, https://doi.org/10.1029/2010WR009127, 2010.

Vano, J. A. and Lettenmaier, D. P.: A sensitivity-based approach to evaluating future changes in Colorado River discharge, pp. 621–634, https://doi.org/10.1007/s10584-013-1023-x, 2014.

Vuuren, D. P. V., Edmonds, J., Kainuma, M., Riahi, K., Nakicenovic, N., Smith, S. J., and Rose, S. K.: The representative concentration pathways : an overview, pp. 5–31, https://doi.org/10.1007/s10584-011-0148-z, 2011.

Wang-Erlandsson, L., Fetzer, I., Keys, P. W., Van Der Ent, R. J., Savenije, H. H., and Gordon, L. J.: Remote land use impacts on river flows through atmospheric teleconnections, Hydrology and Earth System Sciences, 22, 4311–4328, https://doi.org/10.5194/hess-22-4311-2018, 2018.

Weng, W., Luedeke, M., Zemp, D., Lakes, T., and Kropp, J.: Aerial and surface rivers: Downwind impacts on water availability from land use changes in Amazonia, Hydrology and Earth System Sciences, 22, 911–927, https://doi.org/10.5194/hess-22-911-2018, 2018.